CATALYTIC CONVERSION OF GLYCEROL TO PROPYLENE GLYCOL: SYNTHESIS AND TECHNOLOGY ASSESSMENT

A Dissertation presented to the Faculty of the Graduate School

University of Missouri- Columbia

In Partial Fulfillment

of the Requirements for the Degree

Doctor of Philosophy

---

by

CHUANG-WEI CHIU

Dr. Galen J. Suppes, Dissertation Supervisor

DECEMBER 2006

The undersigned, appointed by the Dean of the Graduate School, have examined the dissertation entitled

CATALYTIC CONVERSION OF GLYCEROL TO PROPYLENE GLYCOL: SYNTHESIS AND TECHNOLOGY ASSESSMENT

Presented by Chuang-Wei Chiu

a candidate for the degree of Doctor of Philosophy

and hereby certify that in their opinion it is worthy of acceptance.

_____

Dr. Galen J. Suppes

_____

Dr. Thomas R. Marrero

_____

Dr. Eric J. Doskocil

_____

Dr. Qingsong Yu

_____

Dr. Fu-hung Hsieh

_____

Dr. Leon G. Schumacher

ACKNOWLEDGEMENTS

I would like to express my gratitude and respect to my advisor, Dr. Galen J. Suppes, for his unfailing assistance, guidance and patience; which made it possible for me to complete this research project.

I also wish to express my sincere appreciation to other members of his dissertation committee Drs. Thomas R. Marrero, Eric J. Doskocil, Qingsong Yu, Fu-hung Hsieh, and Leon G. Schumacher for their valuable suggestions and critical reviews of the dissertation.

Appreciation is extended to Drs. Rusty Sutterlin and Mohanprasad Dasari for provided me the guidance of an experienced researcher throughout my experimental work. I would like to thank the research team for their constant help and support. I also thank the faculty and staff of the Department of Chemical Engineering for their friendship during my academic years.

Finally, I wish to express my deepest gratitude to my parents for their understanding patience and many sacrifices throughout this work. Their endless support and love gave me the courage to carry out my dream.

TABLE OF CONTENTS

LIST OF TABLES

LIST OF FIGURES

CHAPTER 1

1. INTRODUCTION

1.1 Glycerol By-product from Biodiesel Production

Biodiesel is a generic term that refers to mixed Fatty Acid Methyl Esters (FAME). Mixed FAMEs, obtained from biogenic fats and oils, are recognized as a viable alternative fuel for compression ignition (diesel) engines. Biodiesel is defined as "a substitute or an additive to diesel fuel that is derived from the oils and fats of plants and animals".[1] There has been a considerable interest in developing biodiesel as an alternative fuel in recent years because it is a renewable fuel that is non-toxic, biodegradable and environmentally benign[2, 3, 4, 5, 6].

Worldwide biodiesel production is approaching a billion gallons per year. The U.S. production of biodiesel is 30-40 million gallons, which is expected to grow at a rate of 50-80% per year, with a projected 400 million gallons of production by the year 2012. For every 9 kilograms of biodiesel produced, about 1 kilogram of a crude glycerol by-product is formed. With the annual world biodiesel production expected to increase to over a billion gallons by the end of this decade, the projected amount of the process's crude glycerol by-product will increase to over 100 million gallons per year. The major drawback on biodiesel commercialization is its high cost when compared to diesel. The production cost for biodiesel range from $0.65- $1.50 per gallon[6]. Today, establishing a technology to utilize this new source of glycerol for biodiesel cost reduction is one

of the priorities on the minds of biodiesel producers.

1.2 New Use of Glycerol

Chemically glycerol is a tri-basic alcohol and more correctly named 1,2,3-propanetriol. Most of the larger biodiesel producers purify and refine this crude glycerol by several steps including vacuum distillation for sale in the commodity glycerol market. Many smaller plants simply discard the glycerol by-product as a waste. A primary reason for discarding the glycerol is because refining the crude glycerol which contains residual catalysts, water and other organic impurities is too complex and expensive to handle for small scale producers in their available limited facilities. Hence, 50% of the total crude glycerol by-product that is generated is disposed of and only the remaining is sold at a very minimal price.

Today, with plenty of glycerol available to the world market, prices and U.S. exports have declined. Prices in the glycerol market will continue to drop with an over saturated market and new supplies of glycerol coming into the market from the burgeoning biodiesel industry. The price of glycerol is already (2005) about half the price of past averages in Europe where biodiesel production exceeds 400 million gallons per year. Increased biodiesel production is expected to further suppress glycerol prices. In addition, glycerol can be a platform chemical that serves as an important biorefinery feedstock, and so, conversion of glycerol to other commodity chemicals is desirable.

Converting glycerol to propylene glycol is one of the potential solutions to this problem. Propylene glycol demand is not only twice that of glycerol demand,

but also the opportunity exists to market propylene glycol in the antifreeze market as an alternative to ethylene glycol. This technology also could be used in biodiesel production plants to increase profitability. The preferred technology would be to convert crude natural glycerol with high selectivity to propylene glycol at moderate temperatures and pressures.

1.3 Applications of Propylene Glycol

Propylene glycol ($CH_3CHOHCH_2OH$), also named as 1,2 propanediol, is a three carbon diol with two hydroxyl groups on the 1 and 2 carbon. It is a major commodity chemical that some typical uses of propylene glycol are in unsaturated polyester resins, functional fluids (antifreeze, de-icing, and heat transfer), pharmaceuticals, foods, cosmetics, liquid detergents, tobacco humectants, flavors and fragrances, personal care, paints and animal feed. There are approximately 1.3 billion pounds of propylene glycol produced each year in the U.S. The pie chart shown in Figure 1.1 shows the breakout of the many uses of propylene glycol. As shown 23% or approximately 300 million pounds of the market is devoted to functional fluids such as antifreeze and deicers.

Unlike ethylene glycol, propylene glycol is not toxic when ingested. Currently, the commercial route to produce propylene glycol is by the hydration of propylene oxide derived from propylene by either the chlorohydrin process or the hydroperoxide process. In the antifreeze market, propylene glycol produced from glycerol would be a sustainable, domestically-produced and non-toxic alternative

to ethylene glycol.

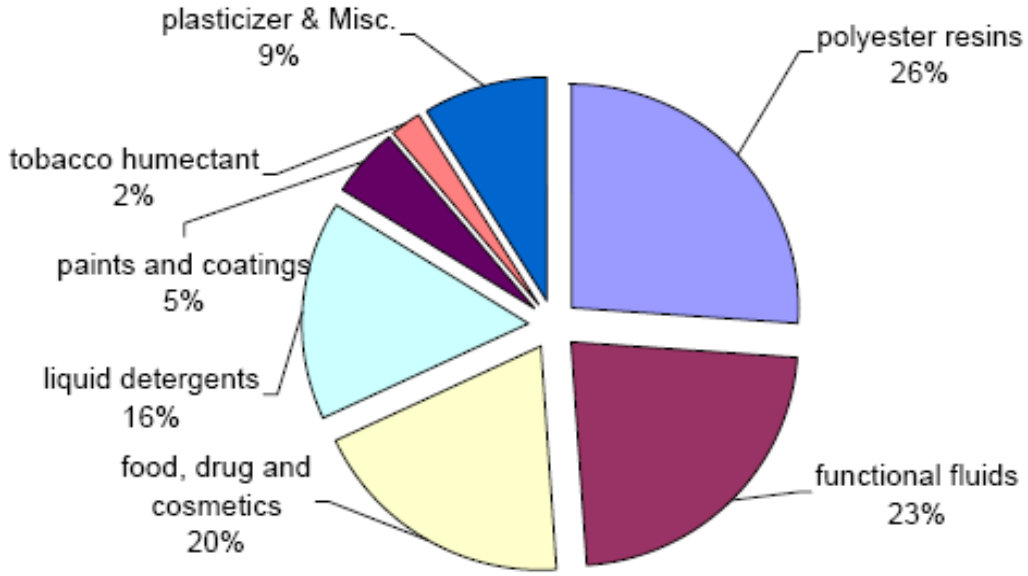

Figure 1.1. Breakout of propylene glycol use.

1.4 Improved Process for Converting Glycerol to Propylene Glycol

The hydrogenolysis of glycerol to propylene glycol has been long known. Conventional processing of glycerol to propylene glycol uses metallic catalysts and hydrogen as reported in several United States patents[7, 8, 9, 10]. These research efforts reported the satisfactory results of converting glycerol to form propylene glycol. However, there are concerns related to commercial viability, for example, high temperatures and high pressures, low production efficiency from using diluted solutions of glycerol, low selectivity to propylene glycol, and

high selectivity to ethylene glycol and other by-products. Higher process pressures translate to higher capital costs.

The benefits of highly selective conversion to propylene glycol go beyond reducing the cost of glycerol feed stock. Patent literature typically reports producing mixtures containing at least 1 part of ethylene glycol (or other glycol) for every 3 parts of propylene glycol. These large amounts of by-product dictate that additional distillation capacity must be added to the process to purify the propylene glycol to market specifications. Separation of propylene glycol and ethylene glycol is costly and difficult because of the close proximity of their boiling points. This additional separation process increases capital costs and decreases the process profitability.

In earlier work the novel reaction mechanism for converting glycerol to propylene glycol via a reactive intermediate was purposed as shown in Figure 1.2[11]. Relatively pure acetol was isolated from dehydration of glycerol as the transient intermediate indicates that the reaction process for producing propylene glycerol with high yield and selectivity can be done in two steps[12]. The first step on this proposed reaction mechanism is an irreversible reaction of glycerol to acetol. The second step of the reaction (acetol to propylene glycol) is expected to be equilibrium limited. The technology has been developed to the point of commercial viability for converting glycerol to propylene glycol based on copper-chromite catalysis and a two-step synthesis involving the novel reactive-distillation and acetol hydrogenation[13]. The preferred method for this reaction includes a vapor-phase reaction over a copper-chromite catalyst in a packed bed

reactor. In the presence of hydrogen, the vapor phase reaction approach allows glycerol to be converted to propylene glycol in a single reactor.

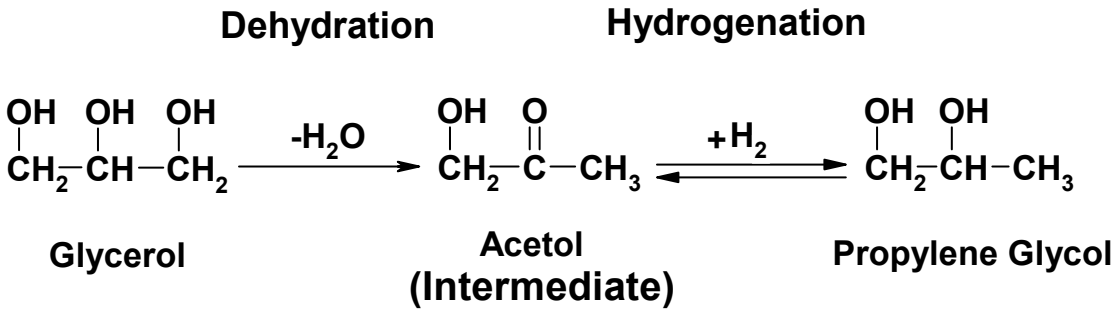

Figure 1.2. Proposed reaction mechanism for conversion of glycerol to propylene glycol.

1.5 Research Objectives

This dissertation is focused on developing a method that is applicable to the industrial-scale production of propylene glycol from glycerol with considerably high conversions and yields. The primary goal of this study is to convert glycerol to propylene glycol at lower temperatures and pressures than the multiple processes reported in the patent literature. A secondary goal is to attain high selectivity to propylene glycol with little selectivity towards ethylene glycol and other by-products.

This dissertation is written as a series of 9 chapters. The research can be broadly divided into 7 topics. Preceding each topic is a brief introduction describing the background, scope and objective of this research. Each paper has its own introduction, methods, materials, results and discussion, and

conclusions as well as figures and tables. For the clarity of presentation, the organization of this dissertation is presented in chronological order.

In chapter 2, the removal of sodium from glycerol solutions by crystallization/precipitation of hydroxyapatite (HAP) through the co-addition of lime [$Ca(OH)_2$] and phosphoric acid is evaluated as a means to remove soluble catalyst from the glycerol by-product of biodiesel production. The suitability of the resulting product is evaluated as a hydrogenolysis feedstock for producing propylene glycol. The continuous removal of phosphate by a lime packed column method is also evaluated for process scale-up considerations.

In chapter 3, dehydration of glycerol is performed in the presence of various metallic catalysts including alumina, magnesium, ruthenium, nickel, platinum, palladium, copper, raney nickel, and copper-chromite catalysts to obtain acetol in a single stage reactive distillation unit under mild conditions. The effects of operation mode, catalyst selection, glycerol feed flow rate, catalyst loading and initial water content are studied to arrive at optimum conditions. The acetol from this reaction readily hydrogenates to form propylene glycol providing an alternative route for converting glycerol to propylene glycol.

Chapter 4 describes the investigations carried out on the vapor phase hydrogenolysis of glycerol to propylene glycol over a copper-chromite catalyst in a continuous packed bed flow reactor. The effects of reaction method (liquid-phase versus vapor-phase mode), vapor-phase reaction with gas purge, reaction temperature, catalyst loading, and hydrogen purge rate are studied to arrive at optimum conditions. The production scheme that has application for production

of propylene glycol from crude glycerol containing various soluble salts is also discussed.

Chapter 5 focuses on reaction selectivity and unknown by-product formation. Propylene glycol and seven of the most prominent unknown by-products are chosen to carry out the study where the trends are studied in relation to propylene glycol production and reaction operating conditions.

The process scalability and pilot-scale testing are presented in chapter 6. Two types of packed bed reactors, the shell-and-tube packed-bed reactor and the tube-cooled packed-bed reactor, are employed to discuss their merits and drawbacks for production of propylene glycol from glycerol.

In chapter 7, the relative volatilities of seven unknown by-products calculated from experimental separation data are presented. The FUG shortcut method and rigorous model used for modeling this multicomponent distillation process are also discussed.

The objective of chapter 8 is to study the kinetics of converting glycerol to propylene glycol for process design, control and optimization. Another important corollary to this chapter is to attempt to control the chemical equilibrium—varying the conditions under which the reaction occurs can vary the amounts of intermediate (acetol) and final product (propylene glycol) present at equilibrium.

Finally, chapter 9 describes conclusions, recommendations, and several suggested future directions for additional research. The results will improve our understanding of the catalytic conversion of glycerol to propylene glycol.

CHAPTER 2

2. REMOVAL OF RESIDUAL CATALYST FROM SIMULATED BIODIESEL'S CRUDE GLYCEROL FOR GLYCEROL HYDROGENOLYSIS TO PROPYLENE GLYCOL

This research paper was published as:

Removal of Residual Catalyst from Simulated Biodiesel's Crude Glycerol for Glycerol Hydrogenolysis to Propylene Glycol,

Chuang-Wei Chiu, Mohanprasad A. Dasari, Willam R. Sutterlin, Galen J. Suppes*, *Industrial & Engineering Chemistry Research* (2006), 45(2), 791-795.

2.1 Abstract

The removal of sodium from glycerol solutions by crystallization/precipitation of hydroxyapatite (HAP)through the co-addition of lime [$Ca(OH)_2$] and phosphoric acid was evaluated as a means to remove soluble catalyst from the glycerol byproduct of biodiesel production. Phosphate ions precipitated as hydroxyapatite upon reacting with calcium and hydroxide ions. Seed crystals and pH impacted crystallization.

The yield decreased due to the polymerization of glycerol at high pH values ($pH \geq 11$). The continuous removal of phosphate by a lime packed column method was also evaluated for process scale-up considerations. Higher temperatures favored the phosphate removal efficiency with higher temperatures raising the pH and the supersaturation region of the respective effluents to the desired level for HAP crystallization/precipitation.

The suitability of the resulting product was evaluated as a hydrogenolysis feedstock for producing propylene glycol. The yield of propylene glycol increased with increasing filtrate pH.

Keywords: sodium, phosphate, glycerol, crystallization/precipitation, hydroxyapatite, lime, hydrogenolysis, propylene glycol, pH, packed column

2.2 Introduction

With the annual world production of biodiesel expected to increase to over four billion liters by the end of this decade, the projected amount of the crude glycerol byproduct of the process will increase to over 400 million liters per year. For larger biodiesel facilities that refine and sell glycerol, the increased glycerol supply has resulted in lower glycerol prices. Many smaller plants simply discard the glycerol byproduct as a waste. A primary reason for discarding the glycerol is the 5-15% (water-free basis) of soluble salts that can be costly to remove.

The traditional method of removing salts from crude glycerol is to evaporate the glycerol from nonvolatile salts in a flash-separation process. While flash-separation processes are effective, they present capital, maintenance, and utility costs. The purpose of this paper is to evaluate alternative salt removal methods and to evaluate the compatibility of these removal methods with converting the glycerin to propylene glycol over a copper-chromite catalyst.

In the production of biodiesel, a catalyst is used to promote transesterification, producing methyl esters (biodiesel) and a glycerol byproduct along with soaps from residual free fatty acids and water. The catalysts are typically base catalysts such as sodium hydroxide or other alkali metal hydroxides[14, 2, 3, 5]. A biodiesel plant that utilizes base catalysis can be described as a succession of different sections and is presented in Figure 2.1. At high conversions, the biodiesel and glycerol phases are immiscible. Most unreacted catalysts and soaps (base-neutralized fatty acids) are preferentially distributed into the glycerol phase[4].

After reaction, the biodiesel is typically decanted from the glycerol phase. For the biodiesel's crude glycerol byproduct, the treatment phase generally involves neutralization and recycling of the unreacted methanol, either of which could occur before or after decanting the biodiesel from the glycerol. Hydrochloric and sulfuric acids are commonly used to neutralize the catalyst after reaction to reduce the amount of soaps (potassium or sodium salts of free fatty acids) that adversely impact separation and represent a loss of yield.

Larger biodiesel facilities often refine the glycerol for sale in the commodity glycerol market. However, the price of glycerol is already (in 2005) about half the price of past averages in Europe, where biodiesel production exceeds 1600 million liters per year. Increased biodiesel production is expected to further suppress glycerol prices, and so, conversion of glycerol to other value-added consumer products is desirable. The hydrogenolysis of biodiesel's crude glycerol to propylene glycol is one process being evaluated to increase the profitability of biodiesel production.

2.2.1 Hydrogenolysis Catalysts

Propylene glycol can be produced by hydrogenating glycerol only with a highly selective hydrogenolysis catalyst. In general, the alcohol groups are more stable against hydrogenolysis than carbon π-bonds and do not readily react at normal hydrogenating conditions. In a previous study, the authors showed that copper-containing catalysts of different composition are potentially good catalysts for this purpose[11]. These catalysts exhibit poor hydrogenolytic activity toward C-

C bonds and efficient activity for C-O bond hydro-dehydrogenation.[15, 16] However, these catalysts are very sensitive to typical catalyst poisons such as S, Cl, and P.[17]

The salts found in biodiesel's crude glycerol typically act as hydrogenolysis catalyst poisons, causing deactivation. The primary objective of the research described in this paper was to identify cost-effective methods (alternative to refining) to neutralize or remove the catalyst and/or salts from biodiesel's crude glycerol in a manner that does not lead to hydrogenolysis catalyst deactivation.

The chlorides can be removed with a chloride absorbent. The sulfates can be eliminated by addition of barium hydroxide to form insoluble barium sulfate. While it is technically feasible to remove chlorides and sulfates, it is economically prohibitive. Phosphates are possibly the easiest and most economical anions to remove from solution and were the emphasis of the current study.

2.2.2 Phosphate Crystallization and Precipitation

Considerable worldwide research has been undertaken on phosphate removal technologies. The technical feasibility of phosphate crystallization and precipitation as a unitary process for wastewater treatment has been demonstrated by Zoltek;[18] Hirasawa, Shimada and Osanai;[19] Joko[20] and Van Dijk and Braakensiek[21]. This same approach should also be effective for removing phosphate salts from the biodiesel's crude glycerol in the existing biodiesel

facilities.

Crystallization can be categorized into two processes: nucleation and growth. For precipitation, both nucleation and growth take place simultaneously where there are only small concentrations of seed crystals; this is also referred to as spontaneous or homogeneous crystallization.[22] Crystallization/precipitation of hydroxyapatite (HAP), $Ca_5(PO_4)_3OH$, in an aqueous solution is fundamental to this phosphate removal method and is summarized by equation 1. The relative insolubility of HAP is due to its thermodynamic stability at pH's above 6.8.[23]

$$3HPO_4^{2-} + 5Ca^{2+} + 4OH^- \rightarrow Ca_5(PO_4)_3OH + 3H_2O \quad (1)$$

Kaneko et al.[24] reported the special affinity that crystals have for phosphate. The result is explained by a chemical reaction between the phosphate ions and the surface of the seed materials. This crystallization/precipitation of HAP on a seed crystal is commonly influenced by the nature of the seed crystal, the phosphate concentration, the calcium ion concentration, and the pH value. Research work was conducted to remove the phosphate anions from an aqueous glycerol solution by a crystallization/precipitation reaction with calcium ions as the seed crystal material coexisting in the solution. Several types of HAP salts will form that incorporate sodium, and so, this is an effective means to remove both the phosphorus and the sodium from the system.

To determine the optimal operation parameters for effective phosphate removal from aqueous glycerol solutions for subsequent hydrogenolysis of

glycerol to propylene glycol, sets of 50 g of phosphate-containing glycerol solutions were contacted with lime [$Ca(OH)_2$] by a batch-stirred reactor and a continuous packed column. The neutralized glycerol solutions were subjected to an autoclave reactor to perform the glycerol hydrogenolysis reaction using a copper-chromite catalyst at a hydrogen pressure of 200 psi and a temperature of 200 ^{o}C.

In the broader sense, apatite salts are a category of calcium-phosphate salts known to have low solubility. In this paper, we hypothesized that calcium-sodium-phosphate salts can be formed that have low solubilities and processabilities. In this study, sodium hydroxide was neutralized with phosphoric acid in aqueous glycerol solutions by the crystallization/precipitation of HAP using lime. The susceptibility of the glycerol was then evaluated in a hydrogenolysis reaction.

2.3 Experimental Section

2.3.1 Materials

Glycerol (99.9%), sodium hydroxide pellets, calcium hydroxide, and phosphoric acid (85%) were purchased from Fisher Scientific Co. (Fairlawn, NJ). Sodium monobasic phosphate (98%), sodium dibasic phosphate (98%), copper-chromite catalyst, and lime had an approximately mean particle size of 100 mesh and were purchased from Sigma-Aldrich (Milwaukee, WI). High purity grade hydrogen was obtained from Praxair.

2.3.2 Experimental Procedures

An 80% glycerol solution with 20% water was mixed with 4% sodium hydroxide in a glass flask for about 30 min at 50 ^{o}C. An 85% phosphoric acid solution was added to the mixture to neutralize it until a pH of 5.5 was reached. The phosphate-containing glycerol solution was contacted with excess lime through batch reactions and lime-packed columns in order remove the phosphate through crystallization/precipitation.

The batch crystallization/precipitation experiments were carried out in 200 mL glass flasks. Varying amounts of lime were added to a 50 g phosphate-containing glycerol solution as the seeding material and to adjust the pH of the glycerol solution. The change in pH with time was monitored with a pH meter. Glycerol solutions were maintained above constant pH values by the addition of lime, and the addition volume was recorded. The solution was continuously stirred at a constant speed of 250 rpm with a magnetic stirrer at a constant temperature of 50 ^{o}C. After stirring for predetermined times, the solution was vacuum-filtered.

Column removal experiments were carried out in a stainless steel column (i.d. 30 mm, length 150mm) equipped with an external heating tape for the heating system. The column packed with 15 g of lime was connected to a peristaltic high-performance liquid chromatography (HPLC) pump. The 50 g phosphate-containing glycerol solution was pumped in a downward direction through the column. The temperature of the column was controlled by the CAMILE 2000 control and data acquisition system using TG 4.0 software. The

residence time was adjusted by proper control of the flow rate.

After the glycerol solutions were treated through the batch or column methods, they were placed into the autoclave for the subsequent hydrogenolysis of glycerol to form propylene glycol. All reactions were carried out in a stainless steel multi-autoclave reactor capable of performing eight reactions simultaneously. Each reactor has a capacity of 150 mL and is equipped with a stirrer, a heater, and a sample port. The temperatures of the reactors were controlled by the CAMILE 2000 control and data acquisition system using TG 4.0 software. The reactors were flushed several times with nitrogen followed by hydrogen. Then, the system was pressurized with hydrogen to the necessary pressure and heated to the desired reaction temperature. The speed of the stirrer was set to be constant at 100 rpm throughout the reaction. The copper-chromite catalyst used in this study was reduced prior to the reaction by passing a stream of hydrogen over the catalyst bed at 300 ^{o}C for 4 h.

2.3.3 Analytical Methods

Reaction product samples were taken after 24 h of reaction time, cooled to room temperature, and centrifuged using an IEC (Somerville, MA) Centra CL3R centrifuge to remove the catalyst. These samples were analyzed with a Hewlett-Packard 6890 (Wilmington, DE) gas chromatograph equipped with a flame ionization detector. Hewlett-Packard Chemstation software was used to collect and analyze the data. A Restek Corp (Bellefonte, PA) MXT® WAX 70624 gas chromatography (GC) column (30m x 250 μm x 0.5μm) was used for separation.

A solution of *n*-butanol with a known amount of internal standard was prepared a priori and used for analysis. The samples were prepared for analysis by adding 0.1 mL of product sample to 1 mL of stock solution in a 2 mL glass vial. A 2 μL portion of the sample was injected into the column. The oven temperature program consisted of the following segments: start at 45 °C (0 min), ramp at 0.2 °C /min to 46 °C (0 min), and ramp at 30 °C /min to 220 °C (2.5 min). Using the standard calibration curves that were prepared for all the components, the integrated areas were converted to weight percentages for each component present in the sample.

For each data point, the theoretical yield of propylene glycol was calculated. The theoretical yield is defined as the ratio of the number of moles of propylene glycol produced to the theoretical number of moles of propylene glycol that would be produced at 100% conversion. Conversion of glycerol is defined as the ratio of the number of moles of glycerol consumed in the reaction to the total moles of glycerol initially present.

2.4 Results and Discussion

2.4.1 Reaction Profiles of Hydrogenolysis of Glycerol to Propylene Glycol

Earlier work in our group has demonstrated that copper or copper-based catalysts exhibit higher selectivity toward propylene glycol with little or no selectivity toward ethylene glycol and other degradation byproducts[11]. Figure 2.2 shows the reaction profiles of glycerol conversion and the yield of propylene

glycol with time at a temperature of 200 °C and 200 psi hydrogen pressure for the copper-chromite catalyst using an 80% glycerol solution. It can be seen that an equilibrium glycerol conversion of 54.8% was reached at 24 h with a total theoretical yield of 46.6%. Figure 2 also provides a baseline for the copper-chromite catalyst in the absence of all salts.

2.4.2 Effect of Residual Salts on Glycerol Hydrogenolysis

To evaluate the effect of residual salts from the biodiesel process on the glycerol hydrogenolysis reaction, reactions were carried out by simulating crude glycerol by the addition of sodium hydroxide, phosphoric acid, sodium phosphates (Na_2HPO_4 and NaH_2PO_4), and lime. Table 2.1 provides the summary of the conversions of the 80% glycerol solution with different salts at 200 °C and 200 psi hydrogen pressure using the copper-chromite catalyst. As expected, trace amounts of phosphate ions in the glycerol solution negatively affected the hydrogenolysis reactivity of the copper-chromite catalyst. There was no conversion observed with the addition of small amounts of sodium phosphates and phosphoric acid. This indicates that phosphates react with or irreversibly adsorb onto active sites to deactivate the catalyst. The presence of sodium hydroxide decreased the yield of propylene glycol due to the formation of degradation reaction products resulting in the polymerization of glycerol at high pH values. The data in Table 2.1 also show that the addition of lime, owing to its low solubility in glycerol solution, may also reduce the hydrogenolysis activity of copper-chromite due to catalyst site blockage with physical adsorption of the

insoluble calcium component.

Lime was selected for the phosphate removal material because it contains water-soluble calcium which reacts with the phosphate ion to form insoluble crystalline calcium phosphates, mainly HAP, and also because it can be a seeding crystal material due to its fine particle size. Experiments were performed in the batch mode to evaluate phosphate removal for the phosphate-containing glycerol solution with 1 wt % straight phosphoric acid by the addition of lime, as shown in Table 2.2. Lime effectively neutralizes the phosphoric acid, as shown by an increased yield of propylene glycol to 37.6% in the absence of sodium salts. These data indicate that phosphoric acid and lime can be used to improve the viability of crude glycerol as a hydrogenolysis feedstock.

2.4.3 Removal of Phosphate in Batch Reactors

The effects of the filtrate pH and the lime addition on the HAP crystallization/precipitation system were investigated by determining the yield of propylene glycol on hydrogenolysis of glycerol.

2.4.3.1 Effect of Filtrate pH

Figure 2.3 shows the effect of the pH value on the HAP crystallization/precipitation system for phosphate removal. The yield of propylene glycol is plotted as a function of the batch reaction time with different pH values of 7.5, 9, and 10. Both the yield and the reaction rate increased with increasing pH.

The yield of propylene glycol from glycerol hydrogenolysis is increased with increasing pH of the HAP crystallization/precipitation system from 14.3% at pH 7.5 to 32.2% at pH 10.5 after 120 min. An explanation for these trends is that the HAP continues to poison the catalyst—eventually poisoning all active sites. Higher pH's drive the precipitation of the HAP at the expense of increasing soluble base concentrations—apparently the soluble base (being low due to the low solubility of $Ca(OH)_2$) is less detrimental than the soluble anions of HAP.

2.4.3.2 Effect of Lime Addition

Table 2.3 summarizes the glycerol hydrogenolysis results of propylene glycol formation with different amounts of lime addition in the batch HAP crystallization/precipitation system. The amounts of lime added to obtain the indicated pH levels of mixtures containing 50g of the phosphate-containing glycerol solution in the batch HAP crystallization/precipitation system after 120 min of mixing are also provided.

In general, a higher yield of propylene glycol can be obtained at a higher dosing of lime since the phosphate removal through HAP precipitation is enhanced with a high calcium concentration and a raised pH level.[25] However, the yield of propylene glycol increased until 29.45 g (pH 10.5) of lime was added and began to decrease as the dosing was increased further. This decrease in the yield of propylene glycol with calcium hydroxide dosing over 30 g ($pH \geq 11$) is due to glycerol polymerization at high pH values.[26]

2.4.4 Removal of Phosphate by a Packed-Column Method

Due to the low solubility of lime, it is possible to remove phosphate from solution by passing the solution through a column packed with lime. In these experiments, the effects of the residence time and the column temperature were determined.

In these studies, the glycerol was passed through a column containing sodium hydroxide that had been neutralized with phosphoric acid. The objective was to form HAP in the column which would then precipitate from solution. Hydrogenolysis was then performed on the column effluent to evaluate how effectively the more soluble sodium phosphate salts had been removed.

2.4.4.1 Effect of Residence Time

In Figure 2.4, the yield of propylene glycol is plotted as a function of glycerol that had flowed through the column at different flow rates to induce different residence times for the precipitation process. The column temperature was 180 ^{o}C, and the hydrogenolysis conditions are the same as those previously used.

A gradual increase in the yield of propylene glycol was observed as the column residence time increased to 10 min asymptotically approaching a yield of 28%. This maximum yield is similar to that obtained for the batch results of Figure 2.3.

2.4.4.2 Effect of Column Temperature

The temperature of 180 ^{o}C, as used for the data reported in Figure 2.4,

was determined by a series of screening studies through the column. In these screening studies, the glycerol solutions were passed through a heated column at temperatures of 50, 100, 120, 150, 170, and 180 ^{o}C. Glycerol hydrogenolysis reactions were preformed with the effluent glycerol solutions to identify the impact of temperature on the crystallization/precipitation of HAP in the column. Table 2.4 shows the hydrogenolysis results of the effluent glycerol solutions through the column at different temperatures. The yield of propylene glycol increased with increasing column temperature. A 26.9% yield of propylene glycol was obtained when the phosphate-containing glycerol solution flowed through a 180 ^{o}C column.

These results indicate that high phosphate removal efficiency can be obtained from a column with the removal efficiency highly dependent on the precipitation temperature. High temperatures increase the solubility of lime and possibly the rate of solution, resulting in higher pH values.

The formation of HAP in aqueous solutions takes place following the development of supersaturation. Also, the crystallization of HAP should occur in the metastable supersaturated region of HAP.[27] Kaneko et al.[24] described the operating conditions that should be set up in the metastable supersaturated region close to the super solubility curve in order to induce phosphate crystallization on the seed crystal. However, increasing temperature contributes to the solution supersaturation development and to a metastable supersaturated region, because the sparingly soluble HAP has a reverse solubility. In other words, a driving force that provides a pH and solution supersaturation adjustment

is created by high temperature operation to crystallize the phosphate on the lime bed.

2.4.5 Efficiency Factor Comparison

The following expression (equation 2) was used to quantify the efficiency of lime consumption for phosphate removal as an easy comparison of the experiments.

$$X = \frac{Yield\ of\ \ propylene\ glycol}{Lime\ consumption} \qquad (2)$$

The efficiency factor *X* was calculated from the batch and column results with a high value of *X* indicating more effective use of the lime. At a pH value of 9 in the batch and column experiments, an *X* value of 1.03 was obtained at a residence time of 15 min and 150 ^{o}C in the column experiment compared to 1.77 with 120 min in the batch experiment. The *X* value gradually increased as the column temperature increased (see Table 2.4). A maximum *X* value of 1.79 was achieved at the column temperature of 180 ^{o}C.

The column precipitation method exhibited an advantage over batch precipitation with respect to the efficiency of lime utilization. In the batch experiments (Table 2.3), *X* increased initially with increasing pH but, then, reached a maximum as the pH was increased further. The decrease of *X* from pH 9 to 10.5 is due to the relatively higher amount of lime that is needed to

maintain a desired pH value in the high alkalinity region. A low value *X* of 0.56 at pH 11 in the batch study is due to glycerol polymerizing to polyglycerol during the glycerol hydrogenolysis.

2.5 Conclusions

Sodium was removed from glycerol by first neutralizing the mixture with phosphoric acid and then precipitating an insoluble salt by contacting the mixture with lime to form hydroxyapatite (HAP). Lime performed several roles in this separation, including supplying the calcium ions, controlling pH, and nucleating crystals.

The success of the glycerol cleanup was measured by the ability to hydrogenate the product over a copper-chromite catalyst to propylene glycol. In the batch experiments with a constant temperature, increasing the pH value from 7.5 to 10.5 improved hydrogenolysis yields by a separation method including HAP crystallization/precipitation. However, at pH values $\geq$ 11, the excess base promoted polymerization.

The effectiveness of separation over a packed column of lime was a strong function of temperature. A temperature of 180 °C provided a balance of separation rates and sufficiently low degradation of the glycerol. This study demonstrated the viability of using the crystallization/precipitation of HAP method for removal of the residual catalysts from the biodiesel's crude glycerol as a means to improve the quality of glycerol as a hydrogenolysis reagent.

2.6 Acknowledgments

This material is based upon work supported by the National Science Foundation under Grant No. 0318781 and The Missouri Soybean Merchandising Council.

Table 2.1. Effect of the Contaminants from the Biodiesel Process on the Formation of Propylene Glycol from Glycerol

contaminant	pH	% yield
none	-	46.6%
1 wt. % H_3PO_4	1.25	0
2 wt. % NaH_2PO_4	4.2	0
1 wt. % NaH_2PO_4	4.2	3.3
1 wt. % Na_2HPO_4	8.9	3.9
1 wt. % NaOH	12.5	14.4
1 wt. % $Ca(OH)_2$	11.5	18.3

All the reactions were performed using an 80% glycerol solution at 200 °C and 200 psi hydrogen pressure for 24 h.

Table 2.2. Summary of the Glycerol Hydrogenolysis Results with the Addition of $Ca(OH)_2$ in the Phosphate-Containing Glycerol Solution Prepared by 1 wt. % Phosphate Acid

$Ca(OH)_2$ (g)	filtrate pH	% yield
0	1.25	0
1.37	5	15.3
1.5	7	24.5
1.64	10.5	37.6

All phosphate removal experiments were performed in the batch method. All glycerol hydrogenolysis reactions were performed using an 80% glycerol solution at 200 °C and 200 psi hydrogen pressure for 24 h.

Table 2.3. Summary of the Glycerol Hydrogenolysis Results with Different Amounts of $Ca(OH)_2$ Addition in the Batch HAP Crystallization/Precipitation System

$Ca(OH)_2$ (g)	filtrate pH	% yield	*X*
0	5.5	0	0.00
4.88	6.5	4.9	1.00
8.39	7.5	14.3	1.70
15.04	9	26.6	1.77
29.45	10.5	32.2	1.09
39.23	11	22.1	0.56

All glycerol hydrogenolysis reactions were performed using an 80% glycerol solution at 200 °C and 200 psi hydrogen pressure for 24 h.

The efficiency factor (*X*) is the ratio of grams of propylene glycol produced per gram of lime used in preparing the reagent.

Table 2.4. Summary of Glycerol Hydrogenolysis Results of the Effluent Glycerol Solutions That Passed through the Column with 15 min Residence time at Different Temperatures

column temp (^{o}C)	effluent glycerol pH	% yield	X
50	5.98	3.9	0.26
100	6.9	10.6	0.71
120	7.65	11.5	0.77
150	8.86	15.5	1.03
170	10.01	23	1.53
180	10.57	26.9	1.79

All glycerol hydrogenolysis reactions were performed using an 80% glycerol solution at 200 °C and 200 psi hydrogen pressure for 24 h.

The efficiency factor (*X*) is the ratio of grams of propylene glycol produced per gram of lime used in preparing the reagent.

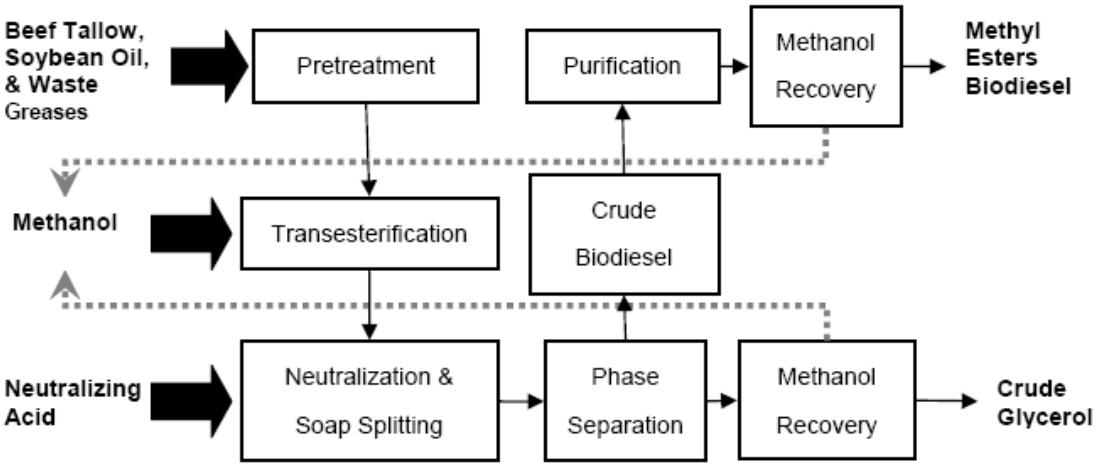

Figure 2.1. Example block flow diagram of biodiesel production.

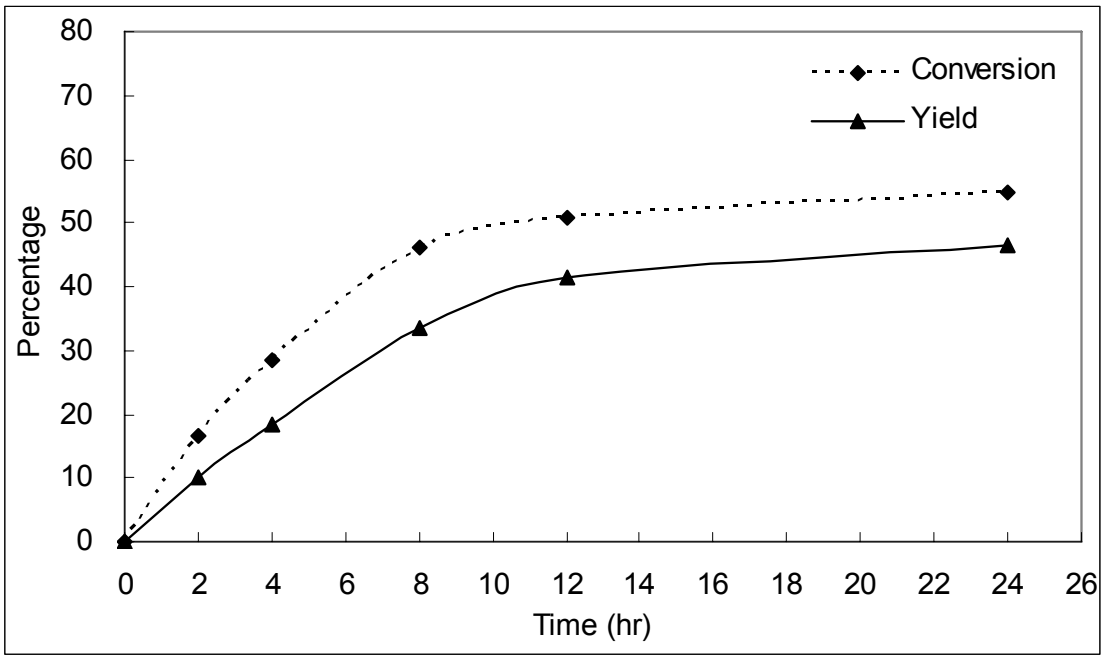

Figure 2.2. Reaction profiles of glycerol conversion and yield of propylene glycol for copper-chromite catalyst at 200 °C and 200 psi hydrogen pressure.

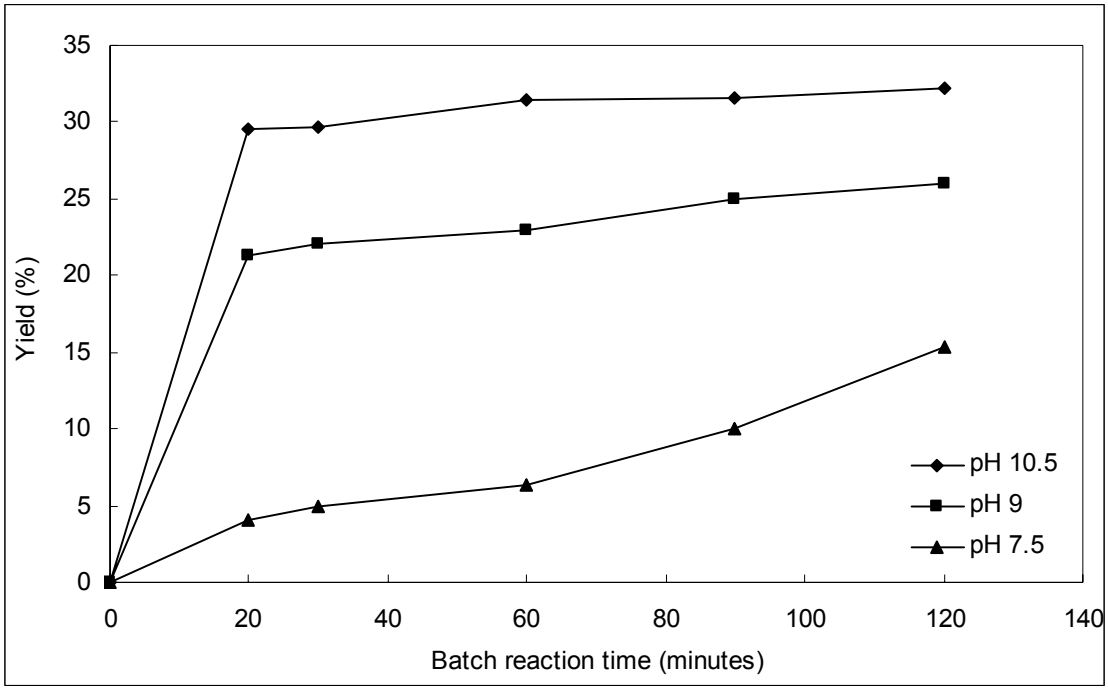

Figure 2.3. Summary of the glycerol hydrogenolysis results with different pH values in the batch HAP crystallization/precipitation system. All glycerol hydrogenolysis reactions were performed using an 80% glycerol solution at 200 °C and 200 psi hydrogen pressure for 24 h.

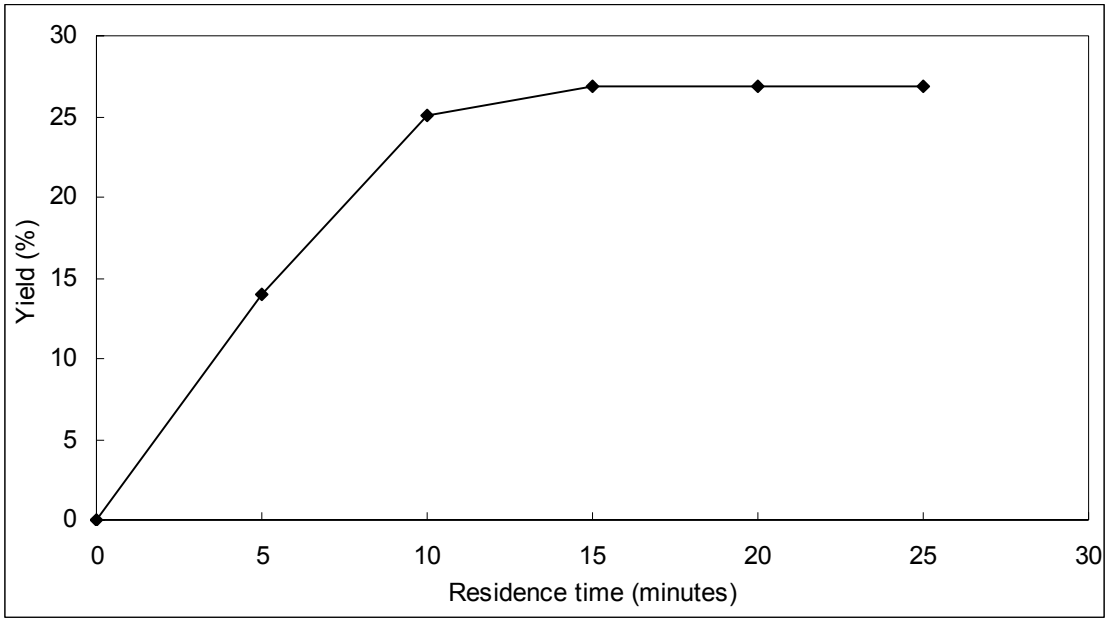

Figure 2.4. Summary of the glycerol hydrogenolysis results of the effluent glycerol solutions that passed through the column with different residence times at a constant column temperature of 180 °C. All glycerol hydrogenolysis reactions were performed using an 80% glycerol solution at 200 °C and 200 psi hydrogen pressure for 24 h.

CHAPTER 3

3. DEHYDRATION OF GLYCEROL TO ACETOL VIA CATALYTIC REACTIVE DISTILLATION

This research paper was published as:

Dehydration of Glycerol to Acetol via Catalytic Reactive Distillation, Chuang-Wei Chiu, Mohanprasad A. Dasari, Willam R. Sutterlin, Galen J. Suppes*, *AIChE Journal* (2006), 52(10), 3543-3548.

3.1 Abstract

Dehydration of glycerol was performed in the presence of various metallic catalysts including alumina, magnesium, ruthenium, nickel, platinum, palladium, copper, raney nickel, and copper-chromite catalysts to obtain acetol in a single stage reactive distillation unit under mild conditions. The effects of operation mode, catalyst selection, glycerol feed flow rate, catalyst loading and initial water content were studied to arrive at optimum conditions.

High acetol selectivity levels ($>$ 90%) were achieved using copper-chromite catalyst and operating in semi-batch reactive distillation mode. A small amount of water content in glycerol feedstock was found to reduce the tendency for residue to form therein extending catalyst life. The acetol from this reaction readily hydrogenates to form propylene glycol providing an alternative route for converting glycerol to propylene glycol.

Keywords: dehydration, glycerol, acetol, copper-chromite, reactive distillation, residue, propylene glycol.

3.2 Introduction

Use of fatty acid methyl esters (FAME) derived from vegetable oils and animal fats as diesel fuel extenders known as biodiesel has received considerable attention in recent years[2, 3, 4, 5]. The U.S. production of biodiesel is 120-160 million liters, which is expected to grow at a rate of 50-80% per year, with a projected 1.6 billion liters of production by the year 2012. A major drawback of biodiesel is its high cost when compared to diesel—the production costs for biodiesel range from $0.17- $0.40 per liter[28].

For every 9 kilograms of biodiesel produced, about 1 kilogram of a crude glycerol by-product is formed. Most of the larger biodiesel producers refine the glycerol for sale in the commodity glycerol market. However, the price of glycerol is already (2005) about half the price of past averages in Europe where biodiesel production exceeds 1.6 billion liters per year. Increased biodiesel production is expected to further suppress glycerol prices, and so, conversion of glycerol to other consumer products is desirable.

Propylene glycol is a major commodity chemical with an annual production of over 450 million kilograms in the United States[29] and sells for $1.56 to over $2.20 per kilogram with a 4% growth in the market size annually[30]. If crude glycerol could be used to produce propylene glycol, this technology could increase the profitability of biodiesel production plants and thereby reduce the costs of producing biodiesel.

The commercial petroleum-based propylene glycol is produced by either the chlorohydrin process or the hydroperoxide process that hydrates propylene

oxide to propylene glycol[31, 32]. Conventional processing of glycerol to propylene glycol uses metallic catalysts and hydrogen as reported in several United States patents[7, 8, 9, 10]. These research efforts report the successful hydrogenation of glycerol to form propylene glycol. However, none of the processes that can suitablely commercialize the resultant reaction products due to some common drawbacks of existing technologies, for example, high temperatures and high pressures, low production efficiency from using diluted solutions of glycerol, and low selectivity towards propylene glycerol.

In earlier work we proposed the novel reaction mechanism for converting glycerol to propylene glycol via a reactive intermediate as shown in Figure 3.1[11]. Relatively pure hydroxyacetone (acetol) is isolated from dehydration of glycerol as the transient intermediate indicates that the reaction process for producing propylene glycerol with high selectivity can be done in two steps. In the broader sense, the present process may potentially advance the art and overcome those problems outlined above by the novel reaction mechanism to convert glycerol to acetol, and then acetol is hydrogenated in a further reaction step to produce propylene glycol.

In the absence of hydrogen, glycerol can be dehydrated to acetol via a reactive-distillation technique. Acetol is considerably more volatile than glycerol. Reaction product vapors (acetol and water) are simultaneously removed or separated from the reaction mixture as they are formed during the step of heating. The possibility of degrading acetol by continuing exposure to the reaction conditions is commensurately decreased by virtue of this removal. In addition,

the acetol is inherently removed from the catalysts to provide relatively clean acetol. Since removal of products allows the equilibrium to be shifted far to the forward direction and high acetol yields to be achieved under relatively mild operation conditions, this reactive distillation technique is particularly advantageous for reactions which are equilibrium limited.

Several prior works have been published on reactive distillation by Gaikar and Sharma (1989)[33] and Doherty and Buzad (1992)[34]. Reactive distillation technique is now commercially exploited for the manufacture of methyl tert-butyl ether (MTBE), ethyl tert-butyl ether (ETBE), and tert-amylmethyl ether, which are used as octane number enhancers[35]. Reactive distillation is also used for esterificaiton of acetic acid with alcohols like methanol and ethanol, and hydrolysis reactions of esters like methyl acetate.

There are only a limited number of publications documenting schemes for converting glycerol to acetol and none of these are based on reactive distillation. The present study focused on demonstrating the feasibility of producing acetol by dehydration of glycerol using heterogeneous metallic catalysts in a single stage reactive distillation unit. Performance of operating in batch and semi-batch mode and effect of various reaction parameters were investigated.

3.3 Experimental Section

3.3.1 Materials

Glycerol (99.9%) and n-butanol were purchased from Sigma-Aldrich (Milwaukee, WI). Methanol (HPLC grade) was purchased from Fisher Scientific

Co. (Fairlawn, NJ). Table 1 gives the description of various catalysts used in this study and their suppliers. All catalysts used in this study were used in the condition in which they arrived.

3.3.2 Experimental Setup

3.3.2.1 Batch Reactive Distillation

The experiments on batch reactive distillation were carried out in a fully agitated glass reactor of capacity 1.25 x 10^{-4} m^3. A magnetic stirrer at an agitation speed of 100 rpm was used to create a slurry reaction mixture. A condenser was attached to the top of glass reactor through which chilled water was circulated. The glass reactor was immersed in a constant temperature oil batch, the temperature of which was maintained within ±1 ^oC of the desired temperature. In the glass reactor the catalyst was first heated to the reaction temperature of 240 °C, and then the amount of glycerol solution was charged immediately to the reactor. Complete addition of the glycerol solution was taken as zero time for the reaction. All experiments were conducted at a reduced pressure of 98 kPa (slight vacuum) by using an aspirator.

3.3.2.2 Semi-batch Reactive Distillation

The same reactive distillation setup was used as described in the section of batch reactive distillation. Experiments were carried out in a continuous mode of operation in the reactive distillation setup as shown in Figure 3.2. Glycerol solution was continuously introduced at the bottom of the glass reactor with different feed flow rates by a peristaltic pump. All experiments were conducted at

a reduced pressure of 98 kPa (slight vacuum) by using an aspirator.

3.3.3 Analytical Methods

In the batch mode, the completion of reaction was considered when additional condensate ceased to collect. In the semi-batch mode, a digestion of the mixture was induced by stopping the feed and allowing the reaction to proceed for about 30 min to an hour at the end of the reaction—during this digestion the volume of the reaction mixture decreased and the residue became more apparent. The residues in the glass reactor were weighed. The liquid samples in the distillate were weighed and analyzed with a Hewlett-Packard 6890 (Wilmington, DE) gas chromatograph equipped with a flame ionization detector. Hewlett-Packard Chemstation software was used to collect and analyze the data. A Restek Corp (Bellefonte, PA) MXT® WAX 70624 GC column (30m x 250 μm x 0.5μm) was used for separation.

For preparation of the GC samples, a solution of n-butanol with a known amount of internal standard was prepared a priori and used for analysis. The samples were prepared for analysis by adding 100 μL of product sample to 1000 μL of stock solution into a 2mL glass vial. Two microliters of the sample was injected into the column. The oven temperature program consisted of: start at 45 °C (0 min), ramp at 0.2 °C /min to 46 °C (0 min), ramp at 30 °C /min to 220 °C (2.5 min). Using the standard calibration curves that were prepared for all the components, the integrated areas were converted to weight percentages for each component present in the sample.

For each data point, conversion of glycerol and selectivity of acetol were calculated. Conversion of glycerol is defined as the ratio of number of moles of glycerol consumed in the reaction to the total moles of glycerol initially present. Selectivity is defined as the ratio of the number of moles of product formation to the moles of glycerol consumed in the reaction, taking into account the stoichiometric coefficient.

For the semi-batch mode, the terms “conversion” and “selectivity” defined by the following expressions were used to present the performance of reactive distillation.

$$Conversion = \frac{Molar\ \ flow\ rate\ of\ \ glycerol\ reacted}{Feed\ molar\ \ flow\ rate\ of\ \ glycerol} \times 100\% \qquad (1)$$

$$Selectivity = \frac{Molar\ \ flow\ rate\ of\ \ acetol\ in\ distillate}{Molar\ \ flow\ rate\ of\ \ glycerol\ reacted} \times 100\% \qquad (2)$$

3.4 Results and Discussion

3.4.1 Catalyst Screening and Selection

Reactivities of heterogeneous catalysts, including alumina, magnesium, ruthenium, nickel, platinum, palladium, copper, raney nickel and copper-chromite were tested in the batch mode of reactive distillation at a reaction temperature of 240 °C and a reduced pressure of 98 kPa. Table 3.1 shows the performance comparison of these catalysts and their suppliers. Conventional dehydration catalysts like alumina were not effective for dehydrating glycerol to acetol since

these catalysts with high acidic sites favor the dehydration of glycerol to acrolein[36]. Ruthenium catalysts showed low selectivities and high residue to initial glycerol ratios, greater than 30%, due to the polymerization (condensation) of hydrocarbon free radicals leading to further deactivation of catalyst. Low selectivities and low residue to initial glycerol ratios were observed in nickel and palladium based catalysts since they tend to be too active which results in excess reaction (degradation) of glycerol to form lower molecular alcohols and gases.

On the other hand, copper or copper-based catalysts are superior to the other catalysts studied here in both acetol selectivity and residue formation. The superiority is enhanced by mixing copper with chromite. A high acetol selectivity of 86.62% was obtained by using copper-chromite mixed oxide catalyst. Copper increases the intrinsic catalyst activity; however, copper favors sinterization leading to catalysts with low surface areas. Chromium acts as a stabilizer to preventing sintering (reduce the sintering rate) and thus maintains catalysts in high activity[37]. Copper-chromite catalyst was selected for further studies.

3.4.2 Batch versus Semi-batch Processing

Glycerol was reacted in presence of copper-chromite catalyst to form acetol in each of batch and semi-batch process modes. Relatively pure acetol was isolated from glycerol in absence of hydrogen at a reaction temperature of 240 °C and a reduced pressure of 98 kPa. The theoretical maximum 100% yield of glycerol dehydration would be achieved if 50 g of glycerol would form a

maximum of 40.2 g of acetol.

In batch mode, glycerol and catalyst were loaded into the reactor at the start of the reaction. In semi-batch mode, the reactor was changed with catalyst and glycerol was continuously fed into the reactor at a uniform rate of 33.33 g/h over a period of about 1.25 hours. It was observed that propylene glycol was produced even in the absence of hydrogen. Since the only source of hydrogen for reacting with acetol or glycerol to form propylene glycol was from another acetol or glycerol molecule, it was hypothesized that the absence of free hydrogen in the system led to scavenging of hydrogen from the glycerol and that this scavenging led to undesired by-products and loss in selectivity. Either process mode produced a residue which was a dark solid coated on the catalyst that was not soluble in water. Table 3.2 shows the semi-batch reactive-distillation exhibits higher yield and selectivity, and lower residue formation than batch due to the semi-batch operation has a higher catalyst loading to glycerol ratio in the reaction.

3.4.3 Effect of Glycerol Feed Flow Rate

Reactions were performed to study the effect of glycerol feed flow rate on semi-batch operation mode with 2.5% copper-chromite catalyst loading. It can be seen in Table 3.3 that increasing the flow rate decreases acetol selectivity and increases the residue to initial-glycerol ratio. As the amount of catalyst is fixed, an increase of the glycerol feed flow rate results in an accumulation of fed glycerol in the reaction mixture, hence reduces the catalyst loading to glycerol

ratio during the reaction. This decrease in the catalyst loading to glycerol ratio results in lower acetol selectivity and higher residue formation reinforcing the afore-conclusion in the section of comparison of batch and semi-batch operation modes. It was also observed that decreasing the flow rate from 33.33 g/h decreases the conversion of glycerol because the glycerol could be easily vaporized and appear in the distillate as an unconverted glycerol.

3.4.4 Effect of Catalyst Loading

For copper-chromite catalyst, it was generally observed that as reaction proceeded, the reaction rate tended to decrease and the amount of residue increased. During the digestion time induced at the end of semi-batch reaction, the volume of the reaction mixture decreased and the residue became more apparent. It indicates that the activity of copper-chromite catalyst is lost before the reaction goes to completion.

In order to find the minimum catalyst loading required to achieve necessary conversion, lowering catalyst loadings from 5% to 0.83% was evaluated to determine the impact of catalyst loading on conversion of glycerol to acetol and residue formation. Reactions were carried out by reacting various amounts of glycerol: 25g (5%), 50g (2.5%), 75g (1.67%), 100g (1.25%), 150g (0.83%) to 1.25g of copper-chromite catalyst in semi-batch reactive distillation mode. Table 3.4 summarizes the conversion results. These data illustrate that the formation of residue increased with increasing throughput of glycerol over the catalyst. Also, the acetol selectivity decreased with increasing throughput of

glycerol over a fixed catalyst loading in the reactor due to residue increasing with reaction time leading to further deactivation of catalyst.

3.4.5 Effect of Initial Water Content

Reactions were performed to study the effect of initial water content on the overall reaction. Glycerol was reacted in the presence of 2.5% copper-chromite catalyst to form acetol in a semi-batch reactive distillation method. Water was added to the glycerol to evaluate if water would decrease the accumulation of the water-insoluble residue. Table 3.5 summarizes the conversion results. As the initial water in the reaction increases, the residue to initial glycerol ratio decreased. The initial water content reduces the residue formation by stripping of the acetol along with water vapors from the reaction mixture before it can degrade/polymerize to form residue—water boils and provides the near-ideal diffusion of acetol in the reaction.

In addition, those reactions with initial water content have higher acetol selectivities compared with the reaction without initial water. For glycerol solutions with water concentration $>5\%$, a decrease in the glycerol conversion was observed due to the entrained glycerol presented in distillate. It demonstrates that high yields of acetol can be achieved and formation of residue can be controlled by using a small amount of water in glycerol.

3.4.6 Catalyst Stability—Ability to Reuse Catalyst

The residue was taken as a solid form at room temperature and a slurry

form at the reaction temperature during the long period of reaction time. The solid was soft and tacky in nature and readily dissolved in methanol to form slurry. Reactions were carried out to find the stability of the copper-chromite catalyst. After each run the catalyst was washed with methanol until the wash was clear and then the catalyst was dried in a furnace at 80 °C to remove the methanol for the subsequent runs. The physical appearance of this catalyst after washing was similar to that of the new catalyst. The data of Figure 3.3 demonstrate the copper-chromite catalyst can be used repeatedly. The conversion of glycerol and the selectivity of acetol were slightly decreased over repeated usage.

Methanol wash is effective to remove the residue, allowing the catalyst to be reused multiple times. However, it was observed that residue started foaming on the catalyst at 30 minute after total glycerol was fed (during the digestion time). Once the reaction mixture started foaming, a methanol wash was not effective for removing the residue from the catalyst. If the reaction was stopped prior to commencement of foaming, the methanol was effective for removing the residue from the catalyst. When catalyst loading less than 2.5%, the reaction mixture started foaming while the glycerol was still being fed into the reactor, hence, the catalyst could not be recovered at end of the reaction.

3.5 Conclusions

Acetol was successfully isolated from dehydration of glycerol as the transient intermediate for producing propylene glycerol. This catalytic process provided an alternative route for the production of propylene glycol from

renewable resources. In this study, selective dehydration of glycerol to acetol has been demonstrated using copper-chromite catalyst under mild conditions. Reactive distillation technology was employed to shift the equilibrium towards the right and achieve high yields. High acetol selectivity levels ($>$90%) have been achieved using copper-chromite catalyst in semi-batch reactive distillation. This reactive distillation technology provides for higher yields than is otherwise possible for producing acetol from glycerol feedstock. In parametric studies, the optimum conditions were delineated to attain maximum acetol selectivity as well as high levels of glycerol conversion.

3.6 Acknowledgements

This material is based upon work supported by the National Science Foundation under Grant No. 0318781 and The Missouri Soybean Merchandising Council.

Table 3.1. Summary of conversion of glycerol, selectivity of acetol and residue to initial glycerol ratio from glycerol over various metal catalysts

Supplier	Description	Conversion (%)	Selectivity (%)	Residue: Initial-Glycerol Ratio (%)
	Mg/Alumina	0	0	-
	Mg/Chromium	0	0	-
Johnson Matthey	5% Ru/C	89.18	31.72	36.54
Johnson Matthey	5% Ru/Alumina	88.24	33.81	34.14
Degussa	5% Pd/C	87.12	4.68	12.33
Degussa	5% Pt/C	0	0	-
PMC Chemicals	10% Pd/C	86.98	3.32	10.51
PMC Chemicals	20% Pd/C	85.14	2.69	9.87
Sud-Chemie	Alumina	0	0	-
Sud-Chemie	Copper	85.19	51.54	15.03
Sud-Chemie	Copper-chromite	86.62	80.17	13.37
Grace Davision	Raney Nickel	82.40	30.38	7.99
Johnson Matthey	Ni/C	79.47	52.97	6.81
Alfa-Aesar	Ni/Silica-Alumina	89.37	57.29	3.33

All reactions were performed in batch reactive distillation at 240 ^{o}C and 98 kPa (vac).

Table 3.2. Comparison of batch reactive distillation and semi-batch (continuous) reactive distillation on formation of acetol from glycerol

Mass balance details on batch reactive distillation using 5% copper-chromite catalyst loading. Initial loading of glycerol, 42.48; glycerol in distillate, 3.64; residue, 5.68; and amount of glycerol reacted, 38.84 all in grams. The glycerol reacted as described below.

	Reacted Glycerol (g)	**Best possible (g)**	**Distillate (g)**
Glycerol	38.84	0	3.64
Acetol	0	31.24	23.73
Propylene glycol	0	0	1.67
Water	0	7.6	6.99

Mass balance details on semi-batch reactive distillation using 5% copper-chromite catalyst loading. Initial loading of glycerol, 54.29; glycerol in distillate, 4.91; residue, 3.80; and amount of glycerol reacted, 49.38 all in grams. The glycerol reacted as described below.

	Reacted Glycerol (g)	**Best possible (g)**	**Distillate (g)**
Glycerol	49.38	0	4.91
Acetol	0	39.71	35.99
Propylene glycol	0	0	1.65
Water	0	9.66	5.79

Mass balance details on semi-batch reactive distillation using 2.5% copper-chromite catalyst loading. Initial loading of glycerol, 52.8; Glycerol in Distillate, 3.85; Residue, 4.91; and Amount of glycerol reacted, 48.95 all in grams. The glycerol reacted as described below.

	Reacted Glycerol (g)	**Best possible (g)**	**Distillate (g)**
Glycerol	48.95	0	3.85
Acetol	0	39.37	33.51
Propylene glycol	0	0	1.63
Water	0	9.58	6.24

All reactions were performed at 240 ^{o}C and 98 kPa (vac). Glycerol feed rate was 33.33 g/h for semi-batch reaction.

Table 3.3. Effect of glycerol feed flow rate on conversion of glycerol to acetol in semi-batch reactive distillation

Glycerol feed flow rate (g/h)	Conversion (%)	Selectivity (%)	Residue: Initial-Glycerol Ratio (%)
100	88.94	60.92	20.45
50	91.49	65.21	19.81
33.33	92.71	85.11	9.30
18.75	91.58	87.32	8.73
14.29	90.15	87.49	7.59

All reactions were performed in semi-batch reactive distillation at 240 ^{o}C and 98 kPa (vac).

Table 3.4. Effect of catalyst to glycerol throughput ratio on conversion of glycerol to acetol in semi-batch reactive distillation

wt.% of catalyst	Conversion (%)	Selectivity (%)	Residue: Initial-Glycerol Ratio (%)
5	90.96	90.62	7.00
2.50	92.71	85.11	9.30
1.67	90.44	76.94	9.76
1.25	89.23	73.50	11.07
0.83	86.87	59.76	11.32

All reactions were performed in semi-batch reactive distillation with glycerol feed rate of 33.33 g/h at 240 ^{o}C and 98 kPa (vac).

Table 3.5. Effect of initial water content in the glycerol feedstock on residue formation

Water (wt. %)	Conversion (%)	Selectivity (%)	Residue: Initial-Glycerol Ratio (%)
0%	92.71	85.11	9.30
5%	90.74	90.65	7.02
10%	84.80	89.87	6.13
20%	82.58	89.84	5.31

All reactions were performed in semi-batch reactive distillation with glycerol feed rate of 33.33 g/h at 240 ^{o}C and 98 kPa (vac).

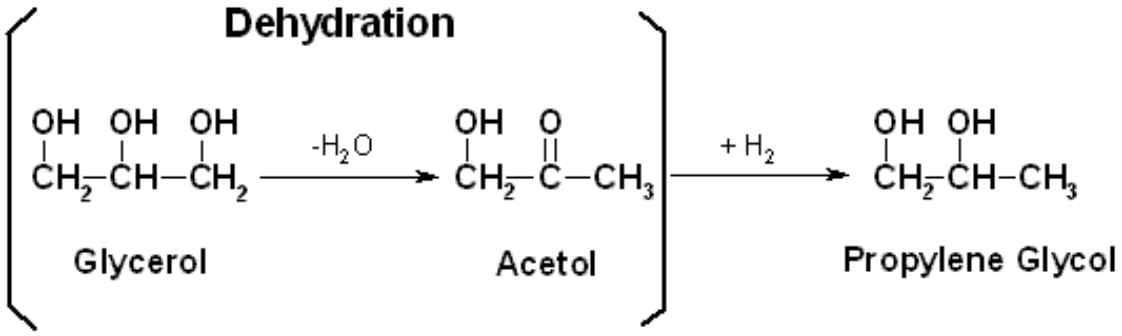

Figure 3.1. Proposed reaction mechanism for converting glycerol to acetol and then to propylene glycol.

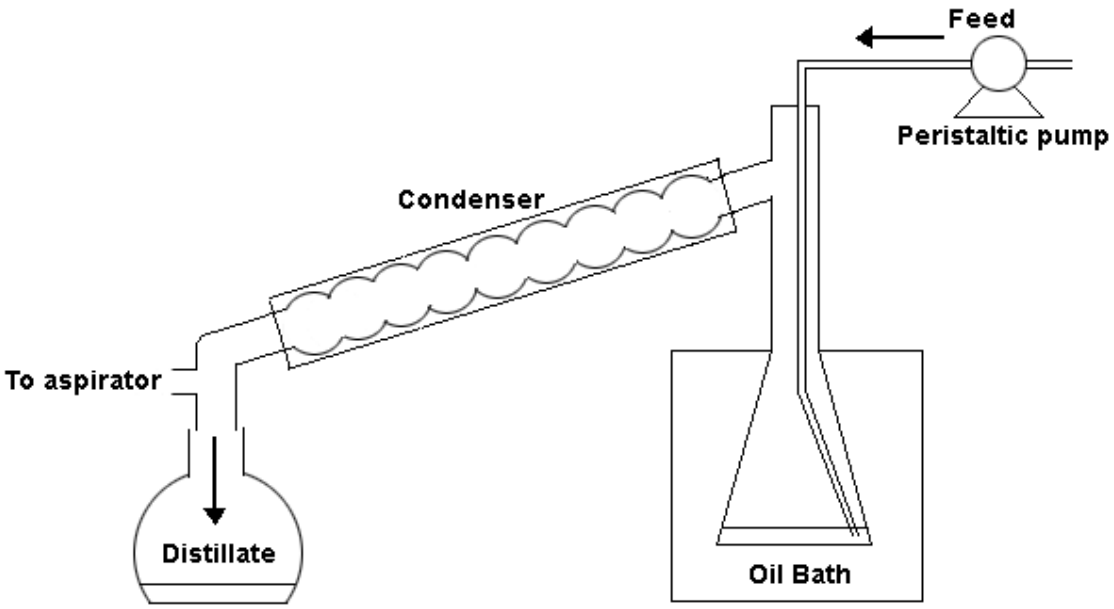

Figure 3.2. Diagram of semi-batch reactive distillation experimental setup.

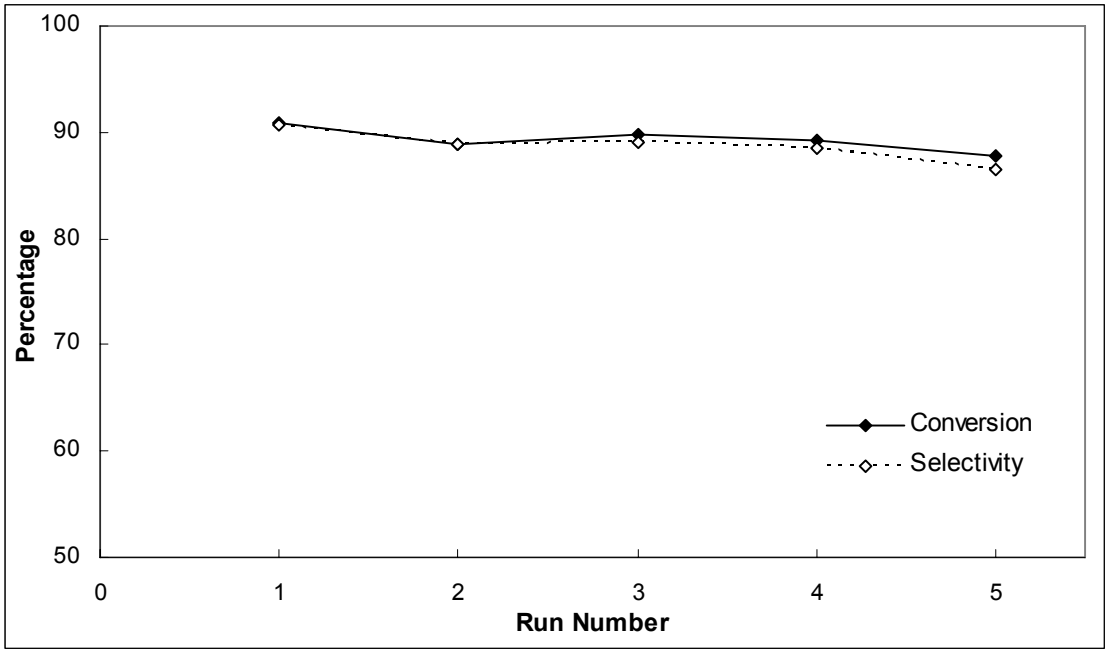

Figure 3.3. Copper-chromite catalyst reuse for conversion of glycerol to acetol. All reactions were performed using 5% copper-chromite catalyst loading in semi-batch reactive distillation with glycerol feed rate of 33.33 g/h at 240 ^{o}C and 98 kPa (vac).

CHAPTER 4

4. LOW-PRESSURE VAPOR-PHASE PACKED BED REACTOR FOR PRODUCING PROPYLENE GLYCOL FROM GLYCEROL

4.1 Abstract

This paper describes the investigations carried out on the vapor phase hydrogenolysis of glycerol to propylene glycol over a copper-chromite catalyst in a packed bed flow reactor. The effects of reaction method (liquid-phase versus vapor-phase mode), vapor-phase reaction with gas purge, reaction temperature, catalyst loading, and hydrogen purge rate were studied to arrive at optimum conditions. Operating the reactor in vapor-phase mode dramatically reduced the amount of unintended by-product formation, thereby, increased the overall yield of acetol and propylene glycerol. The optimum reaction temperature lied in near 220°C with increased hydrogen purge rates considering the both factors of propylene glycol production and glycerol conversion. The proposed production scheme has application for production of propylene glycol from the crude glycerol that contains various soluble salts.

4.2 Introduction

There has been a considerable interest in developing biodiesel as an alternative fuel in recent years due to its environmental benefits and because it is derived from renewable resources like vegetable oils or animal fats[2, 3, 4, 5]. With the demand for biodiesel expected to increase greatly, the amount of crude glycerol which is generated as a byproduct from transesterification will also rise. It is noted that known large-scale biodiesel production processes downplay the significance of the economic loss caused by glycerol by-product (approximately 10% of the biodiesel production).

Costly purification of crude glycerol is typically necessary to prepare it for third party usage, which the price that market will pay is typically minimal. The price of glycerol was already (in 2005) about half the price of past averages in Europe, where biodiesel production exceeded 1600 million liters per year. Increased biodiesel production is expected to further suppress glycerol prices. If this glycerol by-product can be converted to other valuable consumer products, this technology could increase the profitability of biodiesel industries and thereby reduce the costs of producing biodiesel.

Commercial petroleum-based propylene glycol is currently produced in large scale by hydration of propylene oxide through either the chlorohydrin process or the hydroperoxide process[31, 32]. It is employed in numerous applications, for example, moistening agent in the cosmetic and food industries, functional fluids (antifreeze, de-icing, and heat transfer agents), as a solvent for fats, oils, resins, dyestuffs etc. It also serves as raw product for manufacture of

other products. The hydrogenolysis of biodiesel's crude glycerol to propylene glycol used as antifreeze could have a significantly economic impact thereby providing higher profitability from biodiesel production.

4.2.1 Hydrogenolysis Catalysts

Propylene glycol can be produced by hydrogenating glycerol with a highly selective hydrogenolysis catalyst. Earlier work in our group has demonstrated that copper or copper based catalysts exhibit higher selectivity towards propylene glycol with little or no selectivity towards ethylene glycol and other degradation by-products[11]. In the absence of hydrogen, glycerol can be dehydrated to hydroxyacetone (acetol) via a reactive-distillation technique. From our previous studies, high acetol selectivities were obtained by using copper-chromite mixed oxide catalysts[12]. It is known that these catalysts exhibit poor hydrogenolytic activity toward C-C bonds and efficient activity for C-O bond hydro-dehydrogenation[15, 16].

4.2.2 Reaction Mechanism

The hydrogenolysis of glycerol to propylene glycol has been long known. Conventional processing of glycerol to propylene glycol uses metallic catalysts and hydrogen as reported in several United States patents[7, 8, 9, 10]. These research efforts reported the successful hydrogenolysis of glycerol to form propylene glycol. However, the concern was with laboratory scale attempts and without demonstrating suitability for large scale production due to some common

drawbacks of existing technologies, for example, high temperatures and high pressures, low production efficiency from using diluted solutions of glycerol, low selectivity to propylene glycol, and high selectivity to ethylene glycol and other by-products. Separation of propylene glycol and ethylene glycol is costly and difficult because of the close proximity of their boiling points.

In earlier work we proposed the novel reaction mechanism for converting glycerol to propylene glycol via a reactive intermediate as shown in Figure 4.1[11]. Relatively pure acetol was isolated from dehydration of glycerol as the transient intermediate indicates that the reaction process for producing propylene glycerol with high yield and selectivity can be done in two steps[12].

The technology has been developed to the point of commercial viability for converting glycerol to propylene glycol based on copper-chromite catalysis and a two-step synthesis involving the novel reactive-distillation and acetol hydrogenation[13]. The preferred method for preparing acetol and propylene glycol from glycerol includes a vapor-phase reaction over a copper-chromite catalyst in a packed bed reactor. In the presence of hydrogen, the vapor phase reaction approach allows glycerol to be converted to propylene glycol in a single reactor. This approach was demonstrated in a continuous process to address the concerns of scalability and catalyst recycle.

The present study is to develop a process applicable to the industrial scale production of propylene glycol from glycerol with considerably high conversions and yields. We focused on preparing acetol and propylene glycol from glycerol that involves a vapor phase reaction using in a packed bed reactor approach that

maintains the reaction mixture above its dew point temperature. The effects of reaction method (liquid-phase versus vapor-phase mode), vapor-phase reaction with gas purge (hydrogen versus nitrogen purge), reaction temperature, catalyst loading, and hydrogen purge rate on the product yields were experimentally studied using copper-chromite catalyst.

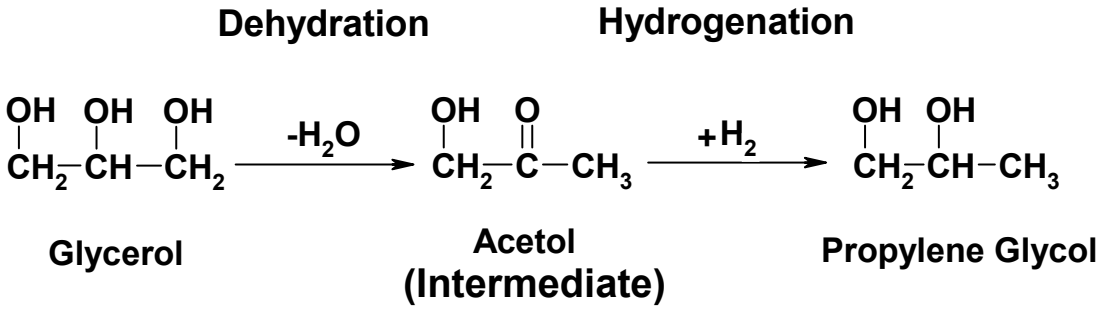

Figure 4.1. Proposed reaction mechanism for conversion of glycerol to propylene glycol.

4.3 Experimental Section

4.3.1 Materials

Glycerol (99.9%) propylene glycol, acetol, n-butanol, and Karl Fisher titrant were purchased from Sigma-Aldrich (Milwaukee, WI). Methanol (HPLC grade) was purchased from Fisher Scientific Co. (Fairlawn, NJ). Copper-chromite catalyst containing a mixture of copper and chromium impregnated on an activated carbon support was purchased from Sud-Chemie. Table 4.1 gives the specification of copper-chromite catalyst. The copper-chromite catalyst used in this study was reduced prior to reaction by the following procedures.

Table 4.1. The specification of copper-chromite catalyst.

Type	Cu/Cr
Form	tablets
Size (mm)	3 × 3
Surface area (BET, m^2/g)	30
Porous volume (cm^3/g)	0.2
Bulk density (g/cm^3)	0.8
Cu content (calculated as CuO in weight percent)	45
Cr content (calculated as Cr_2O_3 in weight percent)	47
MnO_2	3.5
Cr_2O_3	2.7

4.3.2 Catalyst Activation Procedures

Nitrogen and hydrogen were used to remove all of the heat generated during the activation process. The catalyst bed was heated using nitrogen until the minimum activation temperature of 130°C was reached. The catalyst was then activated by slow, stepwise, hydrogen addition beginning with hydrogen concentrations of 1% until over 95% hydrogen was present. An exotherm was observed each time the hydrogen concentration increased, thus the hydrogen addition was controlled carefully to limit the temperature in the catalyst bed to a maximum temperature of 170°C. After the hydrogen had reached the 95%

concentration, and after all exotherms had passed through the catalyst bed, the catalyst was slowly heated to a hold temperature of 180°C for 4 hours.

4.3.3 Experimental Setup

4.3.3.1 Vapor-phase Packed Bed Experiment

The experiments were carried out in a stainless steel tube packed bed reactor having a length of 6 m with an inside diameter of 19 mm. The copper-chromite catalyst in the form of 3 × 3 mm tables was inserted. A condenser was attached to the end of packed bed reactor through which chilled water was circulated. The packed bed reactor was heated by immersing it in a constant temperature oil batch, the temperature of which was maintained within ±1°C of the desired temperature. Thermocouples were placed concentrically in the reactor to measure the temperature in the catalyst bed. The glycerol was loaded into the evaporator at the start of the experiment and continuously introduced through an auxiliary feed to the evaporator during the experiment. The gas (hydrogen or nitrogen) was introduced at different flow rates measured by using a rotameter to contact with the glycerol in an evaporator operated at a temperature of 230°C which promotes evaporation of glycerol to form a vapor reactor influent. Figure 4.2 provides a description of experimental setup including glycerol and gas feeds.

The steady-state conditions were achieved by passing the reactants through the reactor kept at the operating temperature for 1 hour, the product samples were collected for 30 min and were analyzed by gas chromatography.

All experiments were carried out under isothermal conditions. The copper-chromite catalyst was reduced by the procedures as described in the section of catalyst activation procedures before reaction.

For the experiments conducted at pressures below 1 bar (vacuum), the use of vacuum by an aspirator was connected to the condenser at the end of the process. A vacuum promoted evaporation of glycerol at a temperature of 230°C to form a vapor reactor influent. The reduced pressure literally also pulled the vapors through the system and allowed the glycerol feed to evaporate at a temperature of 230°C than would occur at atmospheric pressure.

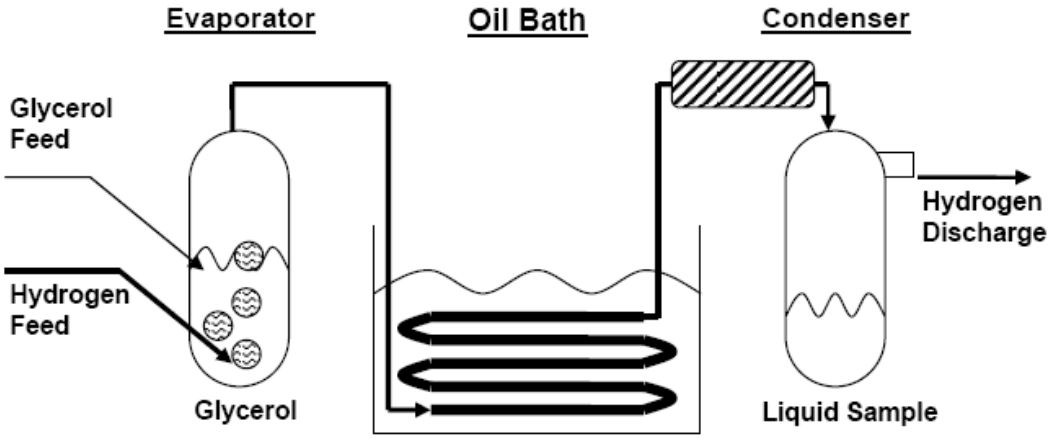

Figure 4.2. Experimental setup for converting glycerol to propylene glycol.

4.3.3.2 Liquid-phase Packed Bed Experiment

Liquid-phase packed bed experiments were carried out in the same packed bed reactor setup as described in the section of vapor-phase packed bed experiment. The preheat glycerol was continuously introduced into the packed

bed reactor with a constant flow rate by a peristaltic pump. All liquid-phase experiments were conducted at a reduced pressure of 0.1 bar by using an aspirator.

4.3.4 Analytical Methods

The liquid samples in the distillate were weighed and analyzed with a Hewlett-Packard 6890 (Wilmington, DE) gas chromatograph equipped with a flame ionization detector. Hewlett-Packard Chemstation software was used to collect and analyze the data. A Restek Corp (Bellefonte, PA) MXT® WAX 70624 GC column (30m x 250 μm x 0.5μm) was used for separation.

For preparation of the GC samples, a solution of n-butanol with a known amount of internal standard was prepared a priori and used for analysis. The samples were prepared for analysis by adding 100 μL of product sample to 1000 μL of stock solution into a 2mL glass vial. Two microliters of the sample was injected into the column. The oven temperature program consisted of: start at 45°C (0 min), ramp at 0.2 °C /min to 46°C (0 min), ramp at 30 °C /min to 220°C (2.5 min). Figure 4.3 shows a typical gas chromatogram of the reaction product. Using the standard calibration curves that were prepared for all the components, the integrated areas were converted to weight percentages for each component present in the sample. The concentration of water was measured by a Metrohm 758 KFD Titrino (Herisau, Switzweland) with Karl Fisher titrant. The samples were diluted with methanol before titration.

For each data point, the conversion of glycerol and the yield of product

were calculated. The conversion of glycerol is defined as the mole percent of glycerol reacted to that introduced into the reactor, and the yield as mole percent of the product produced to the glycerol introduced into the reactor, taking into account the stoichiometric coefficient. The stoichiometric coefficient was calculated on the basis that 1 mol of acetol or propylene glycol is produced from 1 mol of glycerol and 1 mol of water is produced from 1 mol of glycerol.

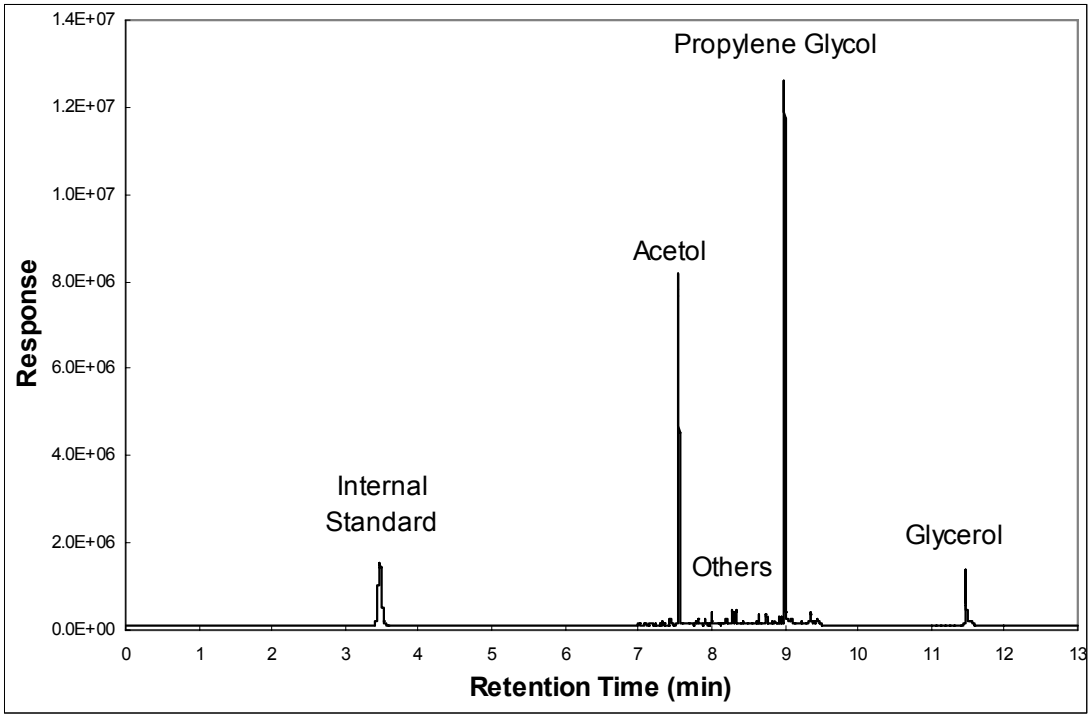

Figure 4.3. Gas chromatogram of the reaction product.

4.4 Results and Discussion

A series of experiments were conducted to evaluate the process variables that could impact the performance of low-pressure vapor-phase packed bed

reactor. The effects of reaction method (liquid-phase versus vapor-phase mode), vapor-phase reaction with gas purge (hydrogen versus nitrogen purge), catalyst loading, reaction temperature, and hydrogen purge rate for the glycerol hydrogenolysis reaction were determined using copper-chromite catalyst and the results are discussed in the following sections.

4.4.1 Liquid-phase versus Vapor-phase Packed Bed Method

Glycerol was reacted on each of liquid-phase and vapor-phase reactions over a copper-chromite catalyst to form acetol in a packed bed reactor. Relatively pure acetol was isolated from glycerol in absence of hydrogen at a reaction temperature of 230°C and a reduced pressure of 0.1 bar.

In the liquid-phase reaction, the preheated glycerol was continuously fed into the reactor at a constant rate of 90 g/h over a period of about 2 hours. In the vapor-phase reaction, glycerol was loaded into the evaporator at the start of the experiment and continuously introduced through an auxiliary feed to the evaporator during the experiment. A vacuum was used to promote evaporation of glycerol at a temperature of 230°C to form a vapor reactor influent. Condensate effluent (180 g) was collected over a period of about 2 hours.

Table 4.2 provides example conversion data over copper-chromite catalyst. The result illustrates the effectiveness of the vapor-phase reaction over a packed bed of catalyst for producing acetol in high yield and selectivity than liquid-phase reaction. Acetol tends to polymerize into dark gel at temperatures above 150°C. In the absence of hydrogen, acetol undergoes dehydration to form

acrolein. At the reaction conditions, in the absence of inhibitors, acrolein has high tendency to polymerize to highly cross linked solids which are infusible and insoluble in common solvents[38]. The vapor phase reaction reduces the polymer or oligomer formation by pull off any acetol along with vapor influent from the reaction mixture before it degrade/polymerize to form polymers or oligomers.

Table 4.2. Comparison of liquid-phase and vapor-phase packed bed reaction on formation of acetol and propylene glycol from glycerol [a].

	Glycerol conversion (%)	Product distribution (wt. %)				Total acetol and propylene glycol yield (%)
		Acetol	Propylene glycol	Water	Others[b]	
Liquid-phase	20.4	6.1	0.9	8.1	5.3	8.7
Vapor-phase	22.1	13.7	1.1	6.5	0.8	18.3

[a] All the reactions were performed over a copper-chromite catalyst of 50 g at a reaction temperature of 230°C and a reduced pressure of 0.1 bar in the packed bed reactor.

[b] The sum of unidentified compounds.

4.4.2 Vapor-Phase Packed Bed Reaction with Gas Purge

It was observed that propylene glycol was produced even in the absence of hydrogen. Since the only source of hydrogen for reacting with acetol or glycerol to form propylene glycol was from another acetol or glycerol molecule, it

was hypothesized that the absence of free hydrogen in the system led to scavenging of hydrogen from the glycerol and that this scavenging led to undesired by-products and loss in yield. To overcome the hypothesized problem with scavenging of hydrogen from glycerol, hydrogen was introduced to the system.

If glycerol is evaporated in the presence of gas, the gas overpressure can add to this pressure to increase overall pressure—glycerol has a vapor pressure of a mere 0.15 bar at 230°C. The hydrogen feed was introduced to the evaporator since this gas diluent would promote evaporation of glycerol. Table 4.3 provides example conversion data illustrating the beneficial impact of a hydrogen feed (purge) with the glycerol feed in the packed bed reactor. A higher yield to acetol and propylene glycol was observed compared with no gas purge.

Desired dehydration reaction produces one water molecule for every acetol molecule that is formed. Water present in excess of this indicates excess dehydration and lower selectivities. The ratio of actual to theoretical water content decreased from 1.47 to 1.05 as a result of hydrogen being present during the dehydration reaction. In addition, the ratio of undesired by-product “others” to desired products (acetol and propylene glycol) decreased from 0.05 to 0.02 as a result of hydrogen being present during the dehydration reaction.

In order to confirm that the desired results were a result of hydrogen rather than any diluent gas in the system, an experiment was performed using nitrogen instead of hydrogen. The ratio of actual to theoretical water increased to 1.66 with nitrogen. In addition, the ratio of the undesired by-product “others” to

desired products (acetol and propylene glycol) increased to 0.18. The result demonstrates that nitrogen was not as good as hydrogen based on higher water content and undesired by-products in the nitrogen reaction.

Table 4.3. Comparison of vapor-phase packed bed reaction with gas purge and without gas purge on formation of acetol and propylene glycol from glycerol.

Gas purge	Glycerol conversion (%)	Product distribution (wt. %)				Total acetol and propylene glycol yield (%)
		Acetol	Propylene glycol	Water	Others[c]	
No gas [a]	22.1	13.7	1.1	6.5	0.8	18.3
Hydrogen [b]	25.6	18.4	1.5	5.4	0.4	24.7
Nitrogen [b]	20.7	11.2	0.5	6.9	2.1	14.6

[a] All the reaction was performed on the vapor-phase reaction over a copper-chromite catalyst of 50 g at a reaction temperature of 230°C and a reduced pressure of 0.1 bar.

[b] All the reaction was performed on the vapor-phase reaction over a copper-chromite catalyst of 50 g at a reaction temperature of 230°C and atmospheric pressure with gas purge rate of 0.1 liter/min.

[c] The sum of unidentified compounds.

4.4.3 Effect of Catalyst Loading

In continuous operation, it was generally observed that as reaction proceeded, the activity of the copper-chromite catalyst tends to decrease after a

period of time. This catalyst can be regenerated by washing with a polar solvent and reducing it in the stream of hydrogen and in some cases has to be replaced with fresh catalyst.

In order to achieve the complete conversion, increasing catalyst loadings from 50 to 150g using crashed small catalyst (9-40 mesh) was evaluated to determine the impact of catalyst loading on conversion of glycerol to acetol and propylene glycol. Table 4.4 summarizes the conversion results. Doubling the catalyst mass doubled the conversion. Tripling the catalyst mass (50 to 150 g) tripled the conversion. To a first approximation, this reaction is zero-order.

In order to minimize the high cost of catalyst replacement and addition of fresh catalyst, reactions were carried out by packing various amounts of copper-chromite catalyst: 770, 1160, 1350, and 1560 g to find the minimum catalyst loading required to achieve the high product yield. Table 4.4 shows the effect of catalyst loading on the overall conversion of glycerol to acetol and propylene glycol. These data illustrate that the overall yield of acetol and propylene glycol increased with increasing catalyst loading from 760 to 1160 g. Higher catalyst loading provides more active sites for the conversion of glycerol to acetol and propylene glycol.

However, the overall yield increased until the catalyst loading of 1160 g and began to decrease as the catalyst loading was increased further. It was also observed that the amount of water and undesired by-product formation increased with increasing catalyst loading—decreased in selectivity to acetol and propylene glycol. It indicates that acetol and propylene glycol in the presence of heat

undergoes over hydrogenolysis, and the excess catalyst further promotes excessive reaction converting acetol and propylene glycol to degradation products. Hence, to get a good conversion of glycerol with high selectivity to acetol and propylene glycol, an optimal amount of catalyst should be used depending on production capacity.

Table 4.4. Effect of catalyst loading on formation of acetol and propylene glycol from glycerol.

Catalyst Loading (g)	Glycerol conversion (%)	Product distribution (wt. %)				Total acetol and propylene glycol yield (%)
		Acetol	Propylene glycol	Water	Others[c]	
Catalyst size: 9-40 mesh [a]						
50	31.9	23.1	1.7	6.5	0.6	30.8
100	63.5	44.7	2.4	13.0	3.4	58.5
150	92.9	64.1	6.4	18.8	3.6	87.4
Catalyst size: 3 × 3 mm [b]						
760	84.5	41.9	23.2	17.0	2.6	80.2
1160	100.0	44.0	28.6	21.4	5.8	89.3
1350	100.0	43.6	27.5	22.2	6.5	87.5
1560	100.0	42.3	26.9	22.9	7.9	85.1

[a] All the reactions were performed on the vapor-phase reaction over a copper-chromite catalyst at 230°C and atmospheric pressure with hydrogen purge rate of 0.1 liter/min.

[b] All the reactions were performed on the vapor-phase reaction over a copper-chromite catalyst at 220°C and atmospheric pressure with hydrogen purge rate of 2.4 liter/min.

[c] The sum of unidentified compounds.

4.4.4 Effect of Reaction Temperature

Temperature has a significant effect on the overall yield of acetol and propylene glycol. Experiments were carried out on the vapor-phase reaction over a copper-chromite catalyst at 200, 210, 220, 230, and 240°C and at atmospheric pressure with hydrogen purge in the packed bed reactor. Table 4.5 shows the effect of temperature on the conversion and yield of the reaction.

The glycerol conversion of 78% was obtained at a reaction temperature of 200°C. A 100% glycerol conversion was achieved at 220°C. At 210°C and 200°C, the conversion of glycerol was less than 100% due to the insufficient lower reaction rates. The selectivity to acetol and propylene glycol decreased as the temperature was further increased from 220 to 230 and 240°C. These trends indicate that at these higher temperatures (>220°C) excessive reaction converts the acetol and propylene glycol into undesired by-products which upon further degradation form degradation products appeared on the GC chromatogram as by-product “other” peaks. Under the present reaction conditions, the optimum reaction temperature for converting glycerol to acetol and propylene glycol is near 220°C on the basis of glycerol conversion and selectivity to desired products.

Table 4.5. Effect of reaction temperature on formation of acetol and propylene glycol from glycerol [a].

Temperature (°C)	Glycerol conversion (%)	Product distribution (wt. %)				Total acetol and propylene glycol yield (%)
		Acetol	Propylene glycol	Water	Others[b]	
200	78.1	26.1	35.3	15.8	2.3	78.0
210	91.6	30.6	39.3	18.6	3.2	85.6
220	100.0	32.1	42.4	20.9	4.6	91.2
230	100.0	32.3	38.7	23.2	5.9	87.0
240	100.0	31.4	35.1	25.6	8.3	81.5

[a] All the reactions were performed on the vapor-phase reaction over a copper-chromite catalyst of 1160 g at atmospheric pressure with hydrogen purge rate of 5 liter/min.

[b] The sum of unidentified compounds.

4.4.5 Effect of Hydrogen Purge Rate

Hydrogen is necessary for production of propylene glycol from glycerol or acetol products. It indicates that the addition of hydrogen would increase the yield of propylene glycol. The reactions were evaluated by introducing hydrogen in different flow rates from 0.1 to 7.1 liter/min to contact with glycerol in an evaporator at 230°C. This increase in hydrogen flow rate causes the partial pressure and the stoichiometric excess of hydrogen to increase.

Figure 4.4 summarizes the effect of hydrogen flow rate on conversion of glycerol to acetol and propylene glycol products at 220 and 230°C. As seen by

the figure, in every instance the increase in hydrogen pressure resulted in better selectivities of glycerol to products (acetol and propylene glycol) and higher conversions from acetol to propylene glycol. A similar trend was observed at other temperatures studied. Thus the propylene glycol formation appears to be directly proportional to the partial pressure of hydrogen—increasing hydrogen flow rate results in increase of partial pressure of hydrogen.

Under low hydrogen flow rate, there is a higher partial pressure of glycerol relative to hydrogen, glycerol is strongly adsorbed and displaces hydrogen from the active catalytic sites; thus the reaction tends to form acetol through glycerol dehydration. This confirms the observations made by our earlier work that acetol is formed by dehydration of a glycerol molecule, which further reacts with hydrogen to form propylene glycol with one mole of water by-product.

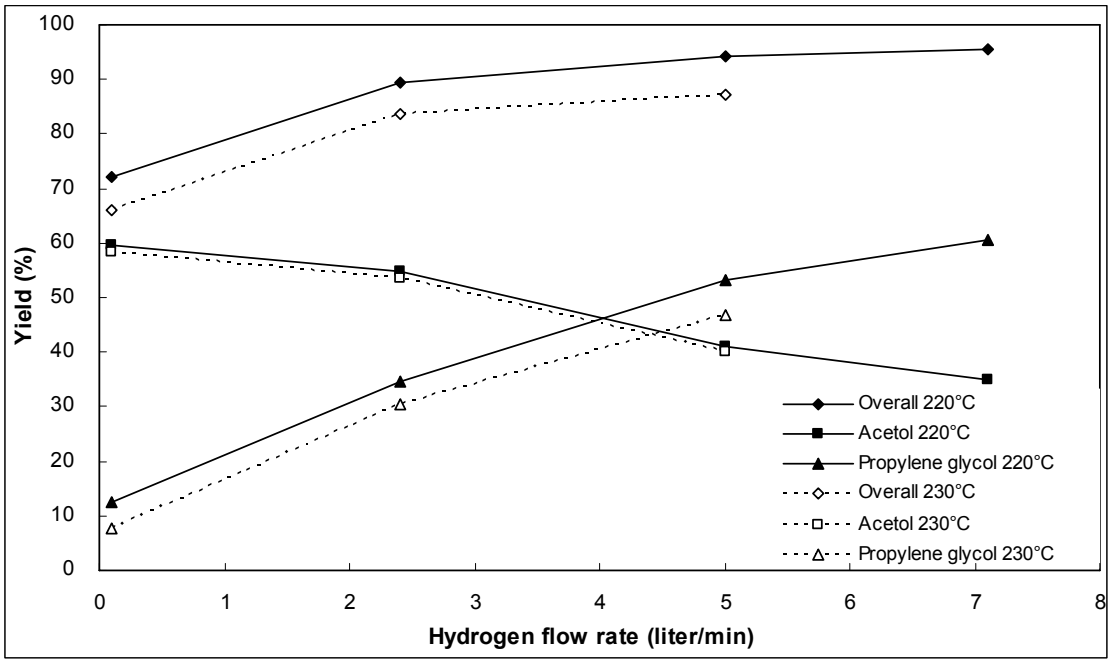

Figure 4.4. Effect of hydrogen purge rate on formation of acetol and propylene glycol from glycerol. All the reactions were performed on the vapor-phase reaction over a copper-chromite catalyst of 1160 g at atmospheric pressure with hydrogen purge.

4.4.6 Catalyst Life

The catalyst was found to perform satisfactorily for 15 reaction cycles of 4 hour duration. When operating at proper conditions (no liquid-phase in the reactor) the catalyst worked well for 15 cycles with no sign of deactivation. The catalyst life should be at least 50 cycles for the process to be commercially viable.

4.4.7 Process Concept

The process present here is applicable to the production of propylene

glycol from crude glycol produced from biodiesel industries. The primary intended application, however, is the selective catalytic synthesis of propylene glycol by the novel reaction mechanism from the crude glycerol, which contains various soluble salts. In the broader sense, the present process may potentially overcome operating problems and advance conventional methods by the two-step synthesis to, first, convert glycerol to acetol, and then acetol is hydrogenated in a further reaction step to produce propylene glycol. The new and novel low-pressure vapor-phase packed bed reactor operation in combination with the glycerol evaporator feed is the basis for the present process concept.

Figure 4.5 provides a process scheme for production of propylene glycol from the crude glycerol including glycerol and hydrogen feeds and an evaporator. The hydrogen is contacted with the glycerol in the evaporator operated near 230°C which promotes evaporation of glycerol to form a vapor reaction mixture. The evaporator is particular effective for processing crude glycerol that contains salts which poison the catalyst. Non-volatile components in the crude glycerol feed are removed from the evaporator in a continuous or semi-batch mode.

The partial pressure of glycerol is about 0.15 bar at 230°C. The partial pressure of glycerol should not exceed about 0.15 bar, above that the dew point is exceeded at 230 ^{o}C, with an optimal total pressure of about 1 bar. A stoichiometric addition of hydrogen feed could add an additional partial pressure to maintain the partial pressure of glycerol at 0.15 bar in the evaporator. The processes of this operation also can be maintained at pressures below 1 bar

through the use of vacuum source connected at the end of the process. For a practical perspective, a vacuum is used to pull off hydrogen that may accumulate in the system.

The crude glycerol is introduced stepwise or continuously into the evaporator. The vapor reaction mixture proceeds to the low-pressure vapor-phase packed bed reactor (packed bed reactor No.1) where the copper-chromite catalyst performs conversion of glycerol to acetol and propylene glycol in sequential reactions. The vapor product mixture is then cooled in a heat exchanger prior to hydrogenation in the packed bed reactor No. 2. The copper-chromite catalyst is also effective in the reactor No. 2. The separation and distillation processes are used to further purify the product. Water is produced as a reaction by-product can be kept with the propylene glycol product or removed.

The effluent of reactor No. 2 is recycled along with the overhead of the separator. A blower or pump may need to overcome pressure drops of the recycle. The hot recycle steams may reduce or eliminate the need for auxiliary heat addition to the evaporator. This heat integration by direct-contact heat exchange and evaporation is very efficient to substantially reduce the utility cost.

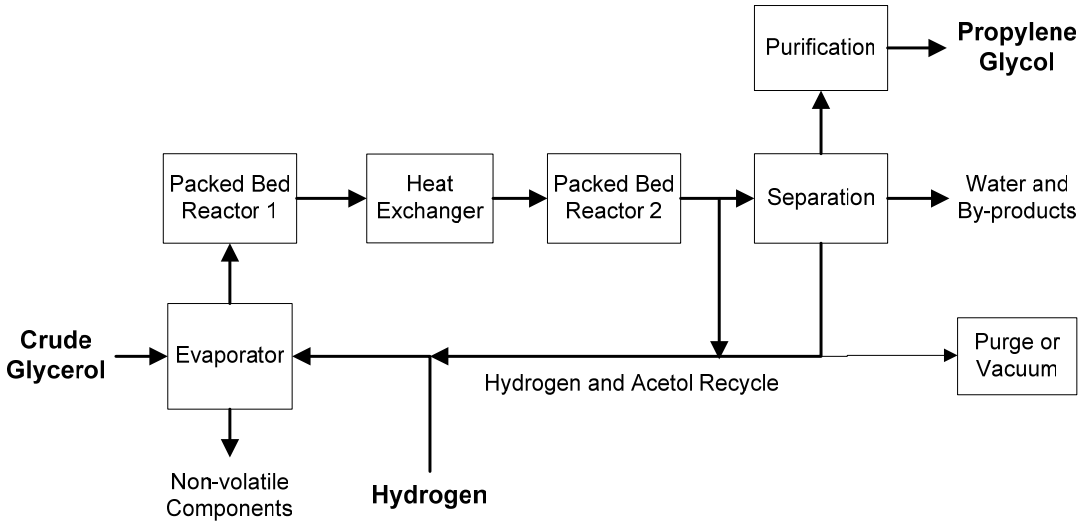

Figure 4.5. Process concept for production of propylene glycerol from crude glycerol.

4.5 Conclusions

The formation of acetol and propylene glycol from glycerol through the novel reaction mechanism was preformed in a low-pressure vapor-phase packed bed reactor using copper-chromite catalyst. This catalytic process has been demonstrated as feasible for producing propylene glycol from glycerol. Effects of various reaction parameters on the products yield were tested. Operating the reactor in vapor-phase mode dramatically reduced the amount of undesired by-product formation. Higher yields of propylene glycol were observed at higher hydrogen purge rates. At temperatures of greater than 220°C excessive reaction takes place resulting in undesired by-product formation which upon further degradation forms degradation products. 100% glycerol conversion and single-pass yields of propylene glycol >50% were attained at the temperature range of

220-230°C and atmospheric pressure with hydrogen purge. A two-step reaction process to produce propylene glycol from the crude glycerol via an acetol intermediate was proposed and validated. A large scale process is thereby potentially viable.

CHAPTER 5

5. BY-PRODUCT FORMATION IN RESPECT OF OPERATING CONDITIONS ON CONVERSION OF GLYCEROL TO PROPYLENE GLYCOL

5.1 Formation of Reaction By-products

The chemical reaction of converting glycerol to propylene glycol (PG) is achieved through a reactive intermediate (acetol). First, glycerol is dehydrated to form acetol, and then this acetol is hydrogenated in a further reaction step to produce propylene glycol. In the presence of hydrogen, two reactions can be occurred in parallel in a packed bed flow reactor. However, while the reaction of glycerol to propylene glycol achieves a high selectivity toward propylene glycol, it has shown little selectivity toward ethylene glycol and other unknown by-products. The selectivity on conversion of glycerol to propylene glycol is decreased as side reactions become prominent.

As the process economic aspect, a large portion of cost in a chemical production plant is owing to the separation and purification involving large energy expenses for evaporation and distillation under vacuum conditions. The entire downstream processing costs are most significantly affected by the product quality achievable in the reaction. In other words, a minimum of by-product formation is desirable, since such by-products reduce the yield and product quality and increase the downstream processing costs.

In order to optimize the reaction process achieving maximum propylene glycol production, identification of trends on these unknown by-products was evaluated. Propylene glycol and seven unknown by-products that are present in the highest concentration were selected to carry out the study where the trends were studied in relation to propylene glycol production and reaction operating conditions. The seven unknown by-products 8.74, 8.78, 9.11, 9.15, 9.28, 9.32, and 9.405 are named as the retention time shown in the gas chromatogram. The latest laboratory result on by-product identification indicates that the peak 9.11 was identified as ethylene glycol (EG). Factors taken into consideration in the reaction are operating pressure and temperature. The reactions were carried out at 1, 2, and 4 bar in a vapor-phase packed bed flow reactor. The reaction temperature ranges from 180 to 240°C.

5.2 Experimental Section

In this study, the packed-bed reactor for producing propylene glycol from glycerol by means of packed-bed catalytic vapor phase reaction include a catalytic reaction zone, a glycerol evaporator and a heat exchange condenser. 650 g of pre-reduced copper-chromite catalyst purchased from Engelhard Corporation (Elyria, Ohio) was packed in the catalytic reaction zone for producing propylene glycol as a main product. The reactor has a length of 8 ft with an outside diameter of 0.75 in equipped with thermocouples. The details of experimental setup are thoroughly described in the section of experimental setup in chapter 4 and 6.

To properly assess these unknown by-products, a Hewlett-Packard 6890 (Wilmington, DE) gas chromatograph equipped with a flame ionization detector was used to analyze the finish products and collect the data. Chromatogram and area percentage data generated by the gas chromatograph were used to prepare the graphs using Microsoft Excel. Unknown by-products were compared in the ratio of internal standard (IS) and propylene glycol peak areas. All reactions were performed in the vapor-phase packed bed reactor with glycerol feed rate of 100 g/h and hydrogen flow rate of 5 l/min.

5.3 Results and Discussion

5.3.1 Reaction of Glycerol to Propylene Glycol

Reaction temperature and pressure have a significant effect on the overall yield of propylene glycol. Reactions were carried out at reaction temperatures from 220 to 240°C and at system pressures of 1, 2, and 4 bar in the presence of a copper-chromite catalyst. Figure 5.1 presents the effect of temperature on production of propylene glycol from glycerol at different levels of pressure. The results indicate that as the reaction temperature decreases from 240 to 220°C there is an increase in the production of propylene glycol. Also, more propylene glycol was produced at higher system pressures.

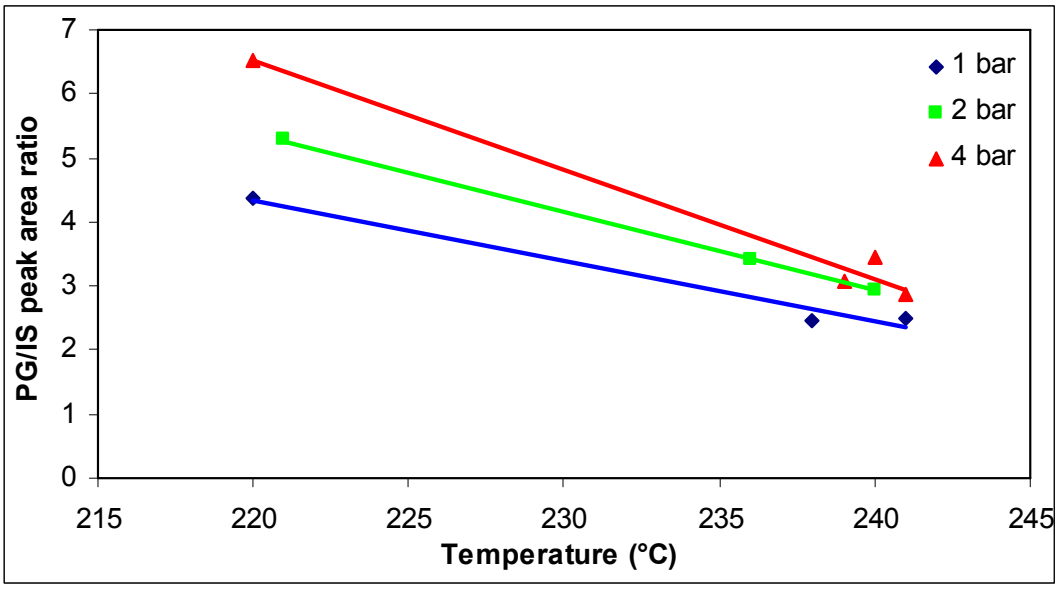

Figure 5.1. Effect of reaction temperature and pressure on propylene glycol production from glycerol.

5.3.1.1 Trends in 7 Unknown By-products

Figure 5.2 to 5.15 present the effect of temperature (220 to 240°C) on the other seven unknown by-products at pressures of 1, 2, and 4 bar. These figures indicate that increasing the reaction temperature results in more by-product formation, and this trend is repeated at each of the three pressure levels for all unknown by-products. Higher pressures lead to a fewer by-product formation at a given temperature.

It was observed that the by-product 9.11 (ethylene glycol) (see Figure 5.7) is the only by-product studied that follows the trend of propylene glycol production—the formation of ethylene glycol increases with increased propylene glycol production. As the reaction temperature increases, there is a decrease in

the formation of ethylene glycol, and more ethylene glycol is produced at higher pressures. In summary, the results from studies on the impact of temperature indicate that more by-products can be formed (except ethylene glycol) at higher temperatures; it dramatically decreases the selectivity on converting glycerol to propylene glycol.

8.74:

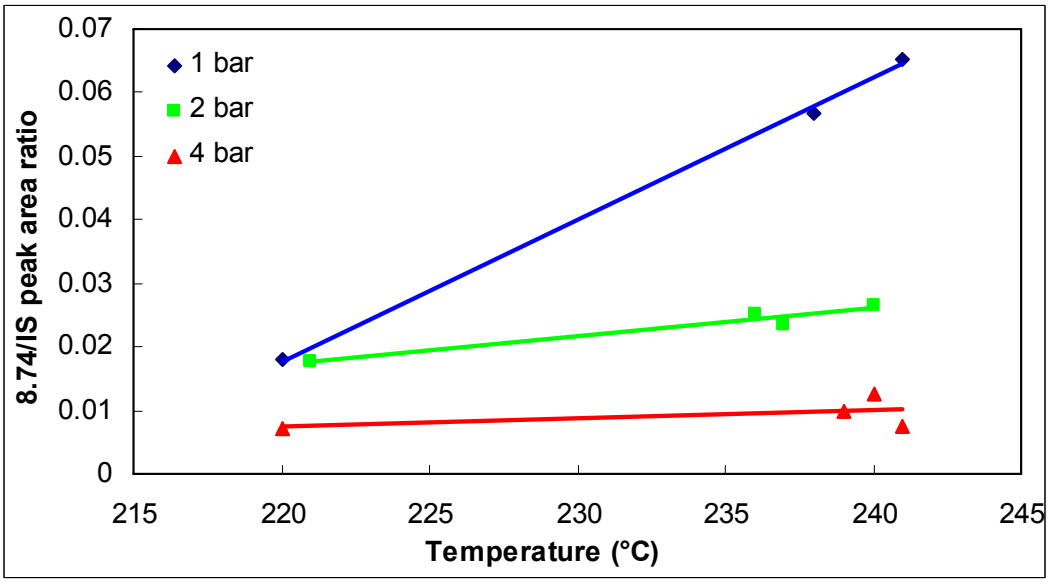

Figure 5.2. Effect of reaction temperature and pressure on unknown by-product 8.74 formation of the glycerol to propylene glycol reaction (Data were plotted by 8.74/IS peak area ratio vs. Temperature)

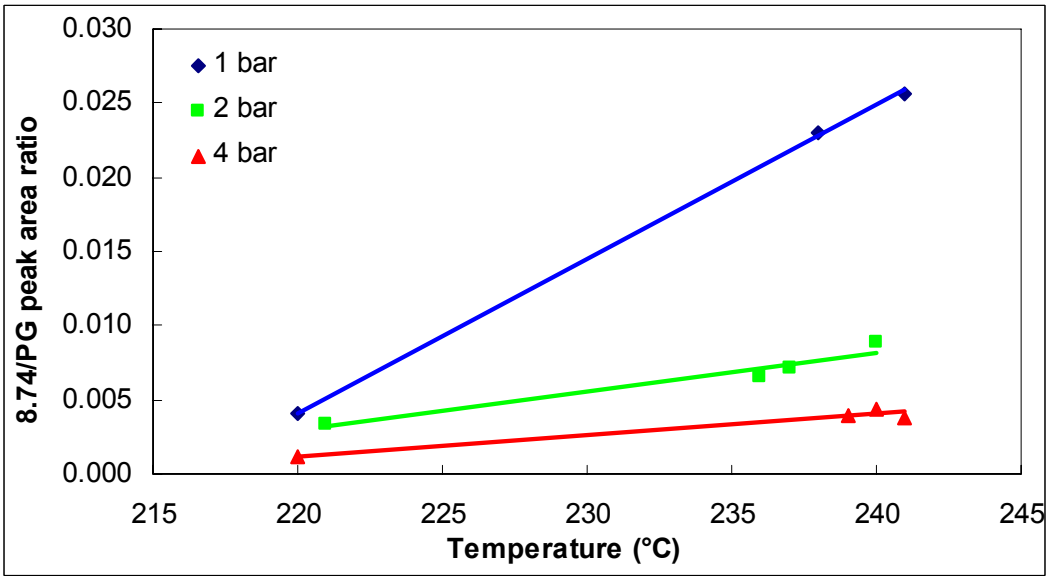

Figure 5.3. Effect of reaction temperature and pressure on unknown by-product 8.74 formation of the glycerol to propylene glycol reaction (Data were plotted by 8.74/PG peak area ratio vs. Temperature)

8.78:

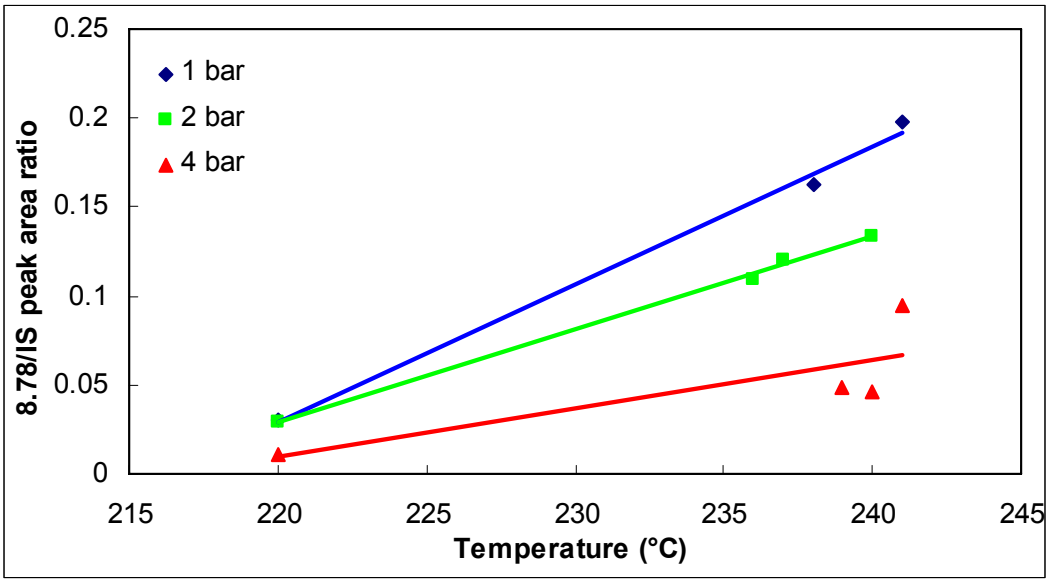

Figure 5.4. Effect of reaction temperature and pressure on unknown by-product 8.78 formation of the glycerol to propylene glycol reaction (Data were plotted by 8.78/IS peak area ratio vs. Temperature)

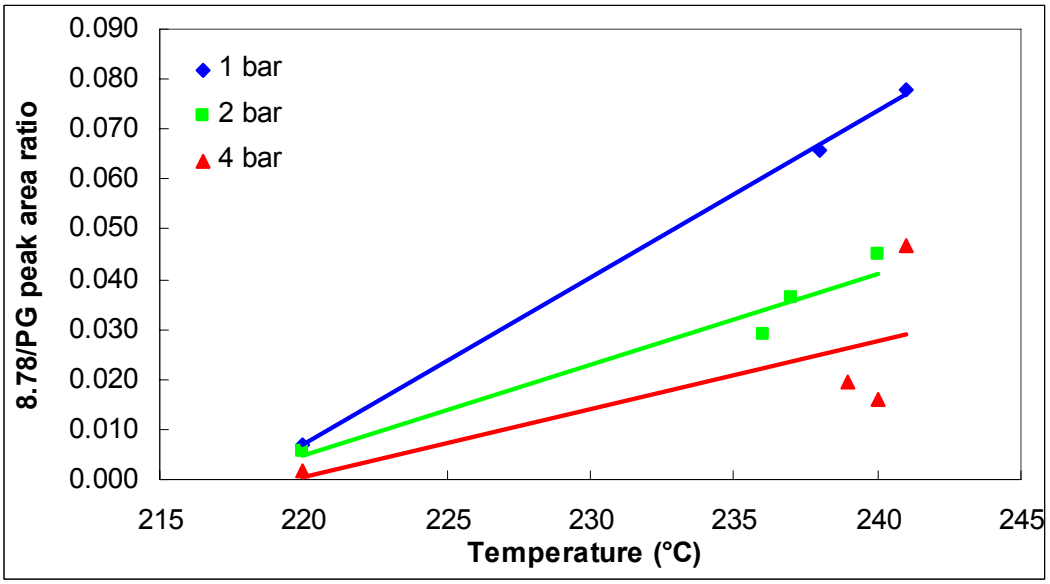

Figure 5.5. Effect of reaction temperature and pressure on unknown by-product 8.78 formation of the glycerol to propylene glycol reaction (Data were plotted by 8.78/PG peak area ratio vs. Temperature)

9.11(EG):

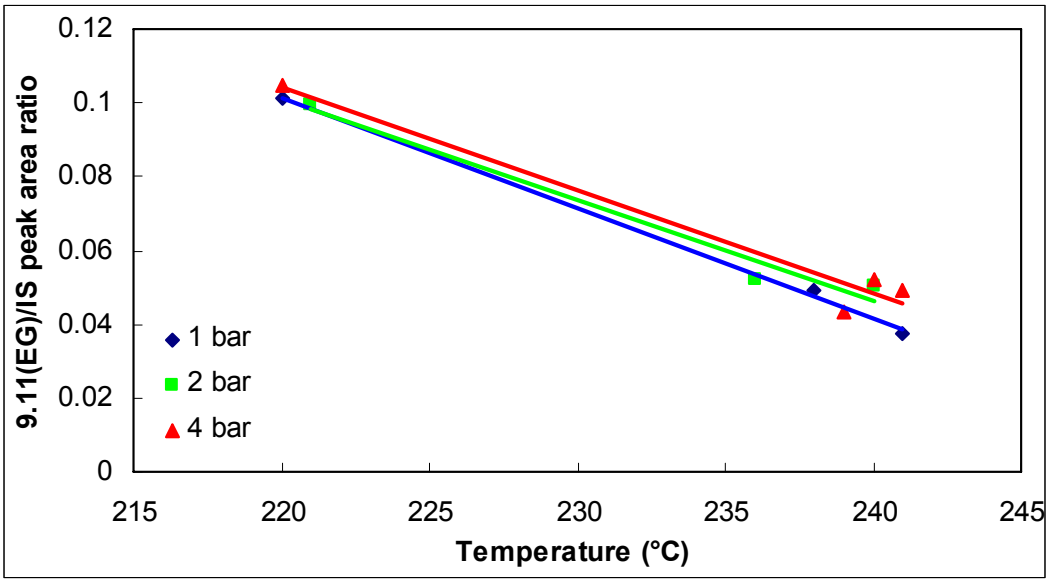

Figure 5.6. Effect of reaction temperature and pressure on unknown by-product 9.11 (EG) formation of the glycerol to propylene glycol reaction (Data were plotted by 9.11(EG)/IS peak area ratio vs. Temperature)

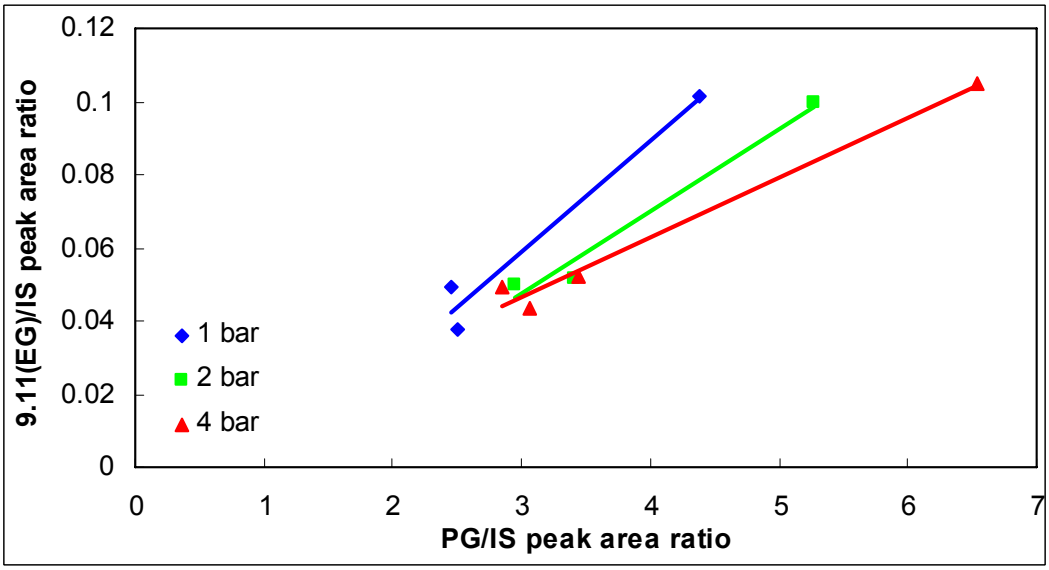

Figure 5.7. Unknown by-product 9.11 (EG) formation versus propylene glycol production of the glycerol to propylene glycol reaction (Data plotted by 9.11(EG)/IS peak area ratio vs. PG/IS peak area ratio)

9.15:

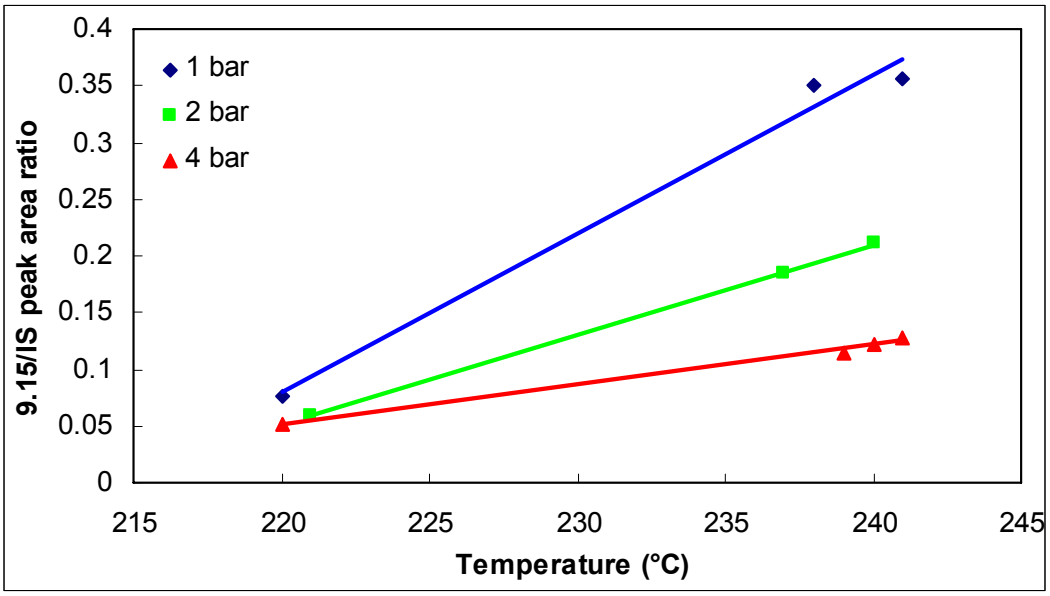

Figure 5.8. Effect of reaction temperature and pressure on unknown by-product 9.15 formation of the glycerol to propylene glycol reaction (Data were plotted by 9.15/IS peak area ratio vs. Temperature)

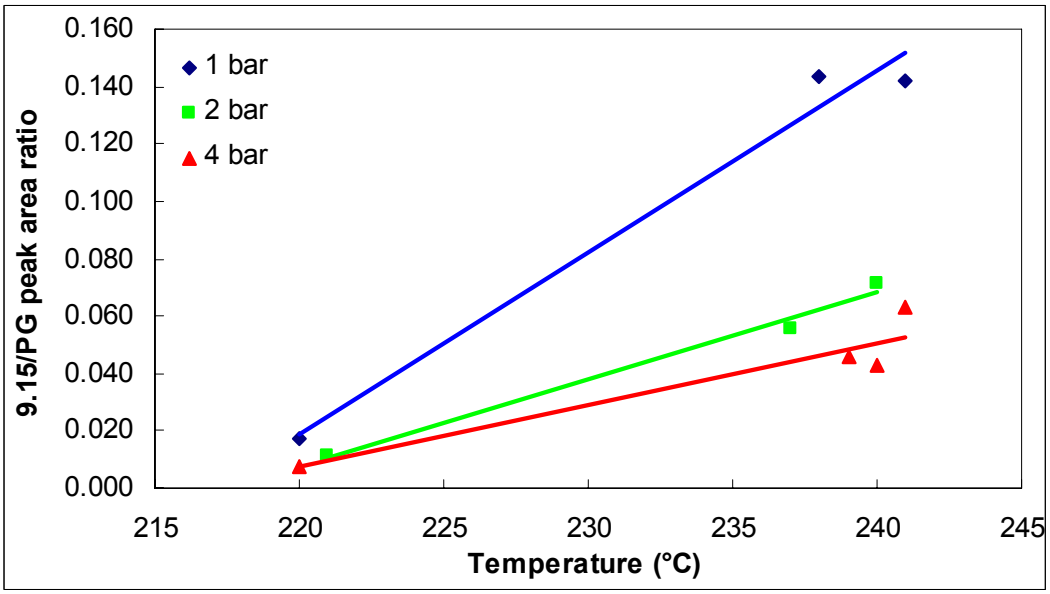

Figure 5.9. Effect of reaction temperature and pressure on unknown by-product 9.15 formation of the glycerol to propylene glycol reaction (Data were plotted by 9.15/PG peak area ratio vs. Temperature)

9.28:

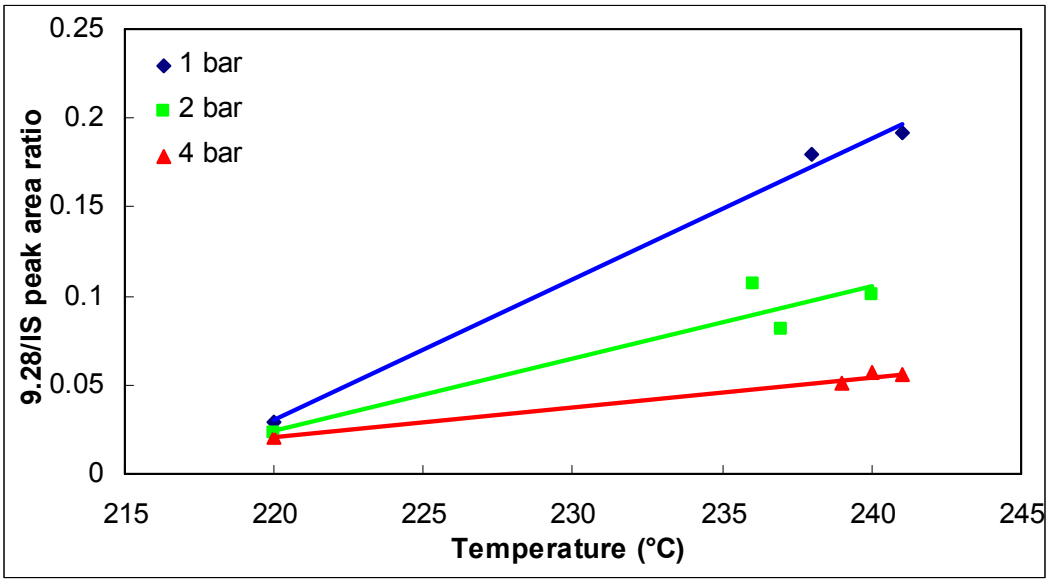

Figure 5.10. Effect of reaction temperature and pressure on unknown by-product 9.28 formation of the glycerol to propylene glycol reaction (Data were plotted by 9.28/IS peak area ratio vs. Temperature)

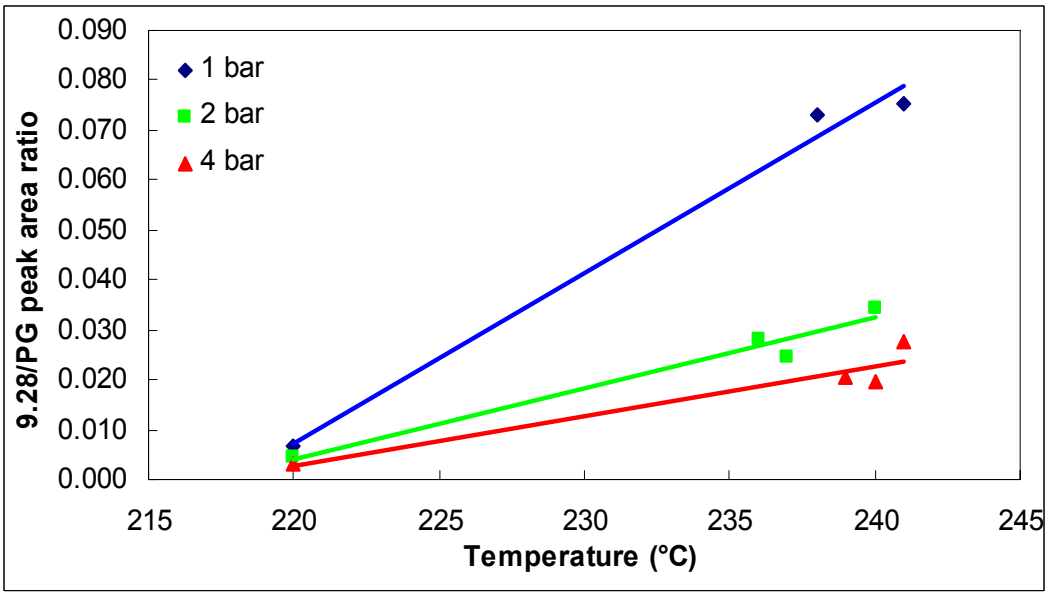

Figure 5.11. Effect of reaction temperature and pressure on unknown by-product 9.28 formation of the glycerol to propylene glycol reaction (Data were plotted by 9.28/PG peak area ratio vs. Temperature)

9.32:

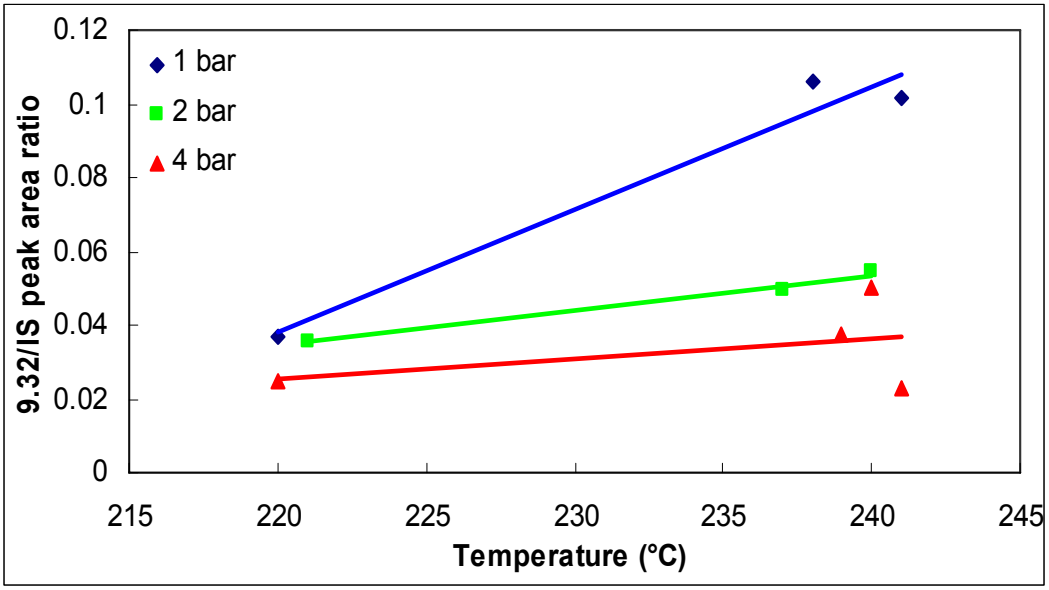

Figure 5.12. Effect of reaction temperature and pressure on unknown by-product 9.32 formation of the glycerol to propylene glycol reaction (Data were plotted by 9.32/IS peak area ratio vs. Temperature)

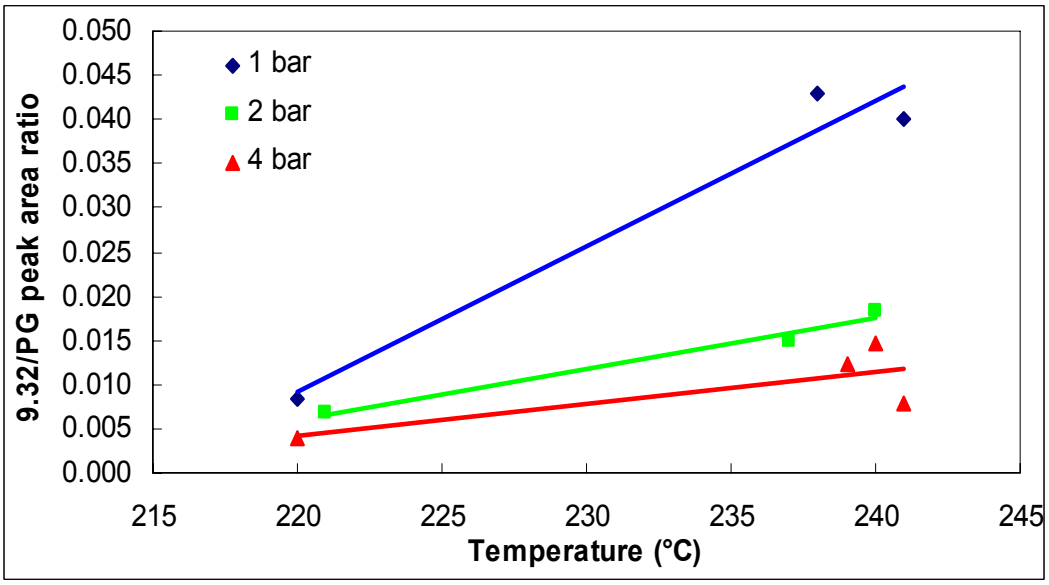

Figure 5.13. Effect of reaction temperature and pressure on unknown by-product 9.32 formation of the glycerol to propylene glycol reaction (Data were plotted by 9.32/PG peak area ratio vs. Temperature)

9.405:

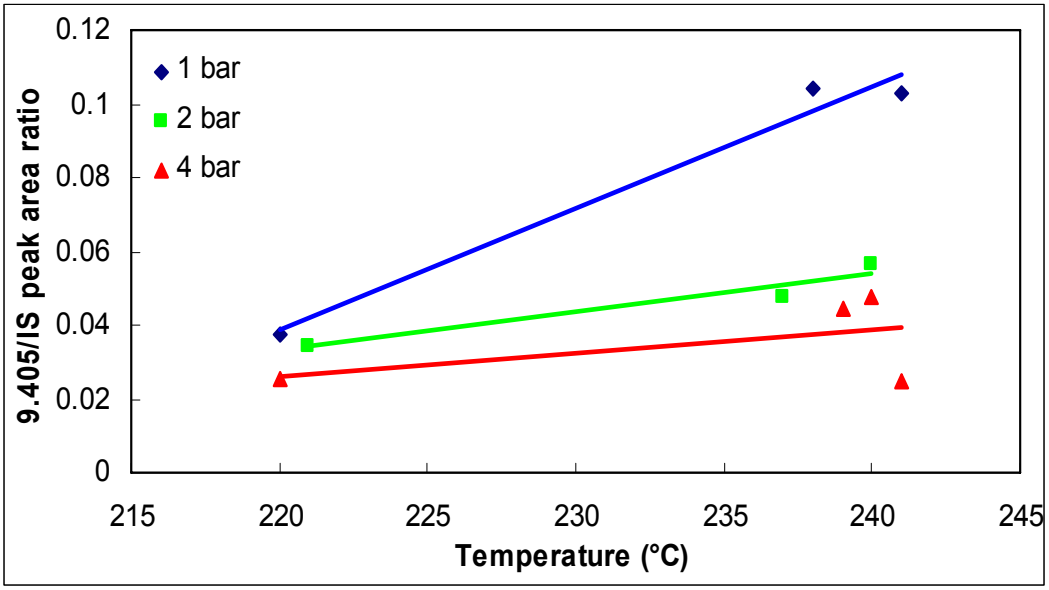

Figure 5.14. Effect of reaction temperature and pressure on unknown by-product 9.405 formation of the glycerol to propylene glycol reaction (Data were plotted by 9.405/IS peak area ratio vs. Temperature)

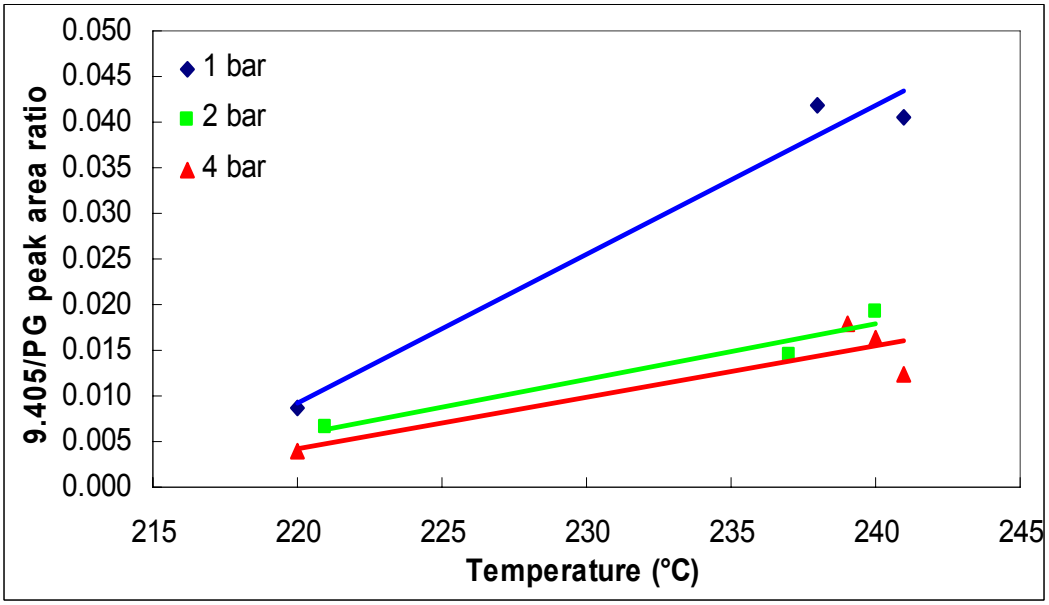

Figure 5.15. Effect of reaction temperature and pressure on unknown by-product 9.405 formation of the glycerol to propylene glycol reaction (Data were plotted by 9.405/PG peak area ratio vs. Temperature)

5.3.2 Reaction of Acetol to Propylene Glycol

The effect of temperature (180 to 240°C) on the conversion of acetol to propylene glycol at three different pressures (1, 2, and 4 bar) is presented in Figure 5.16. This figure indicates that more propylene glycol is produced at lower reaction temperatures, and this behavior is evident at each of the three pressure levels. It was also observed that more propylene glycol is produced at higher pressures. In the reaction of acetol to propylene glycol, more propylene glycol is produced at lower temperatures and higher pressures. The result of this reaction is similar to the reaction of glycerol to propylene glycol as presented in Figure 5.1.

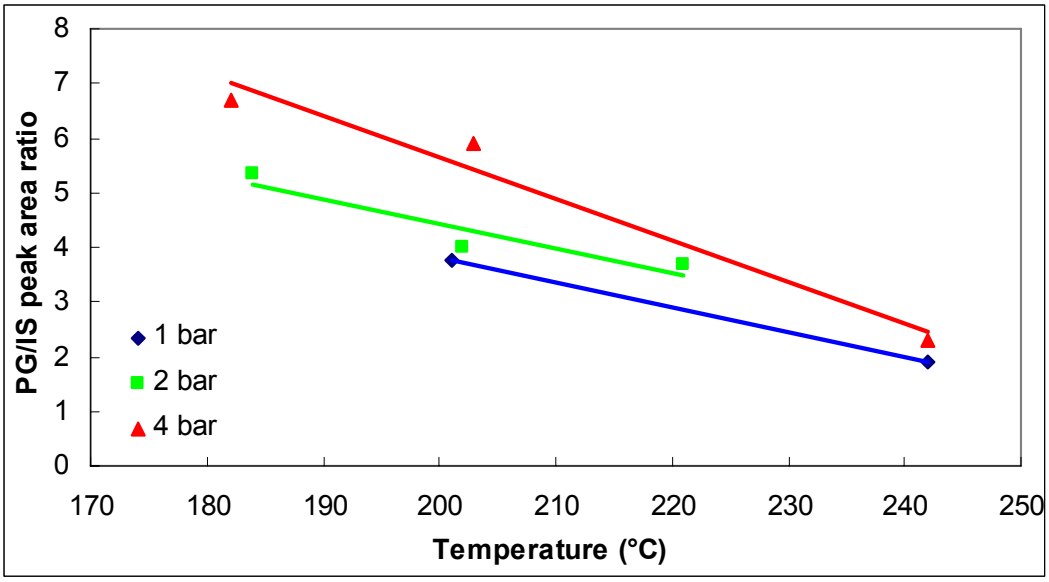

Figure 5.16. Effect of reaction temperature and pressure on propylene glycol production from acetol

5.3.2.1 Trends in 7 Unknown By-products

Trends of all unknown by-products in the reaction of acetol to propylene glycol agreed with the trends of all unknown by-products observed in the glycerol to propylene glycol reaction. Figure 5.17 to 5.30 present the effect of temperature (180 to 240°C) on seven unknown by-product formation of the reaction of acetol to propylene glycol at three different pressures (1, 2, and 4 bar). These figures indicate that increasing the reaction temperature results in more by-product formation, and this trend was repeated at each of the three pressure levels for all unknown by-products. Fewer by-products are produced with an increase in pressure at a given temperature. The formation of ethylene glycol (9.11) is about 5 to 10 times less than that is formed in the glycerol to propylene glycol reaction. In this reaction, ethylene glycol (see Figure 5.22) is the only by-product studied that follows the trend of propylene glycol production.

8.74:

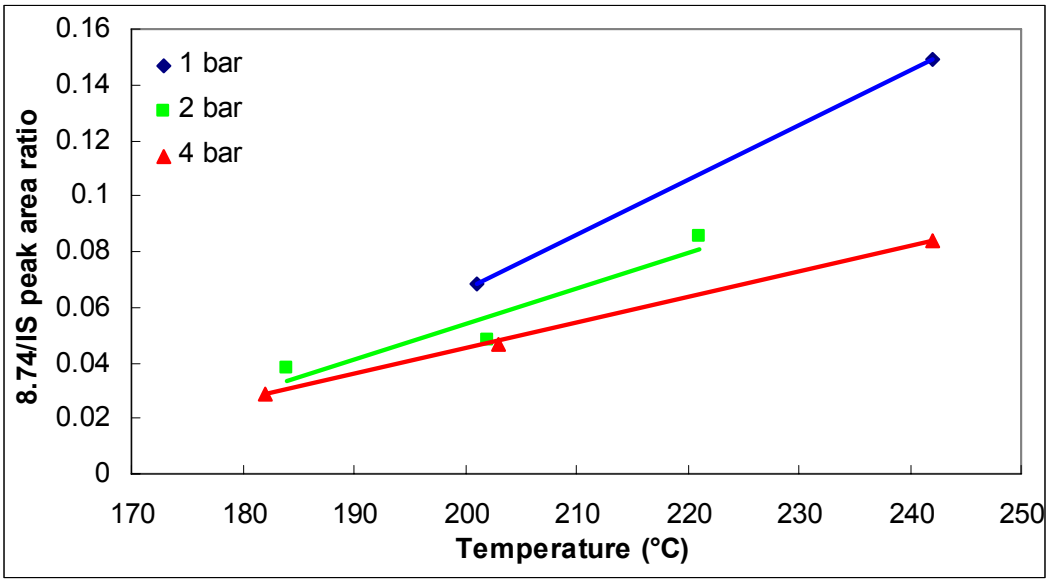

Figure 5.17. Effect of reaction temperature and pressure on unknown by-product 8.74 formation of the acetol to propylene glycol reaction (Data were plotted by 8.74/IS peak area ratio vs. Temperature)

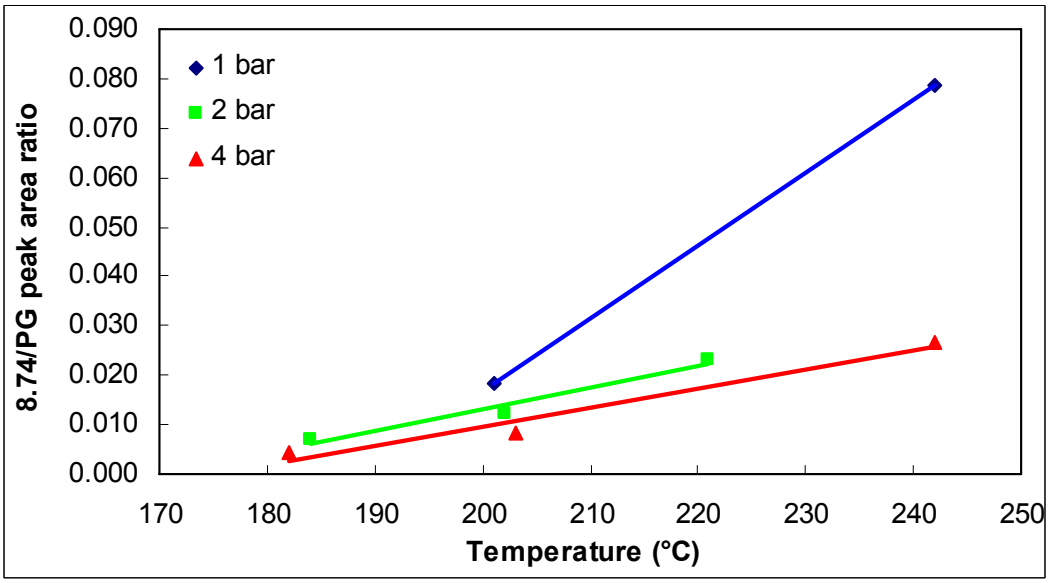

Figure 5.18. Effect of reaction temperature and pressure on unknown by-product 8.74 formation of the acetol to propylene glycol reaction (Data were plotted by 8.74/PG peak area ratio vs. Temperature)

8.78:

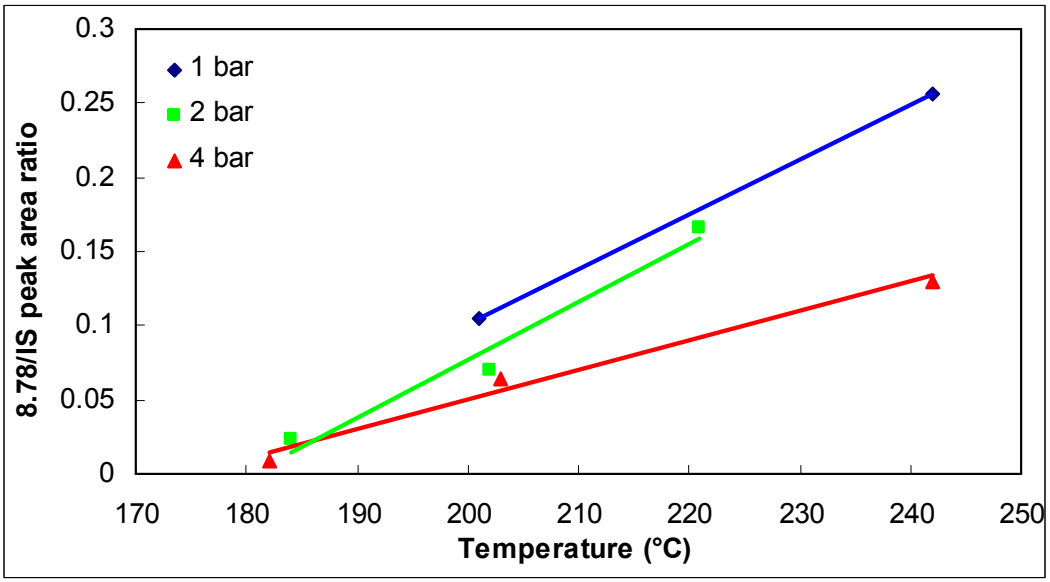

Figure 5.19. Effect of reaction temperature and pressure on unknown by-product 8.78 formation of the acetol to propylene glycol reaction (Data were plotted by 8.78/IS peak area ratio vs. Temperature)

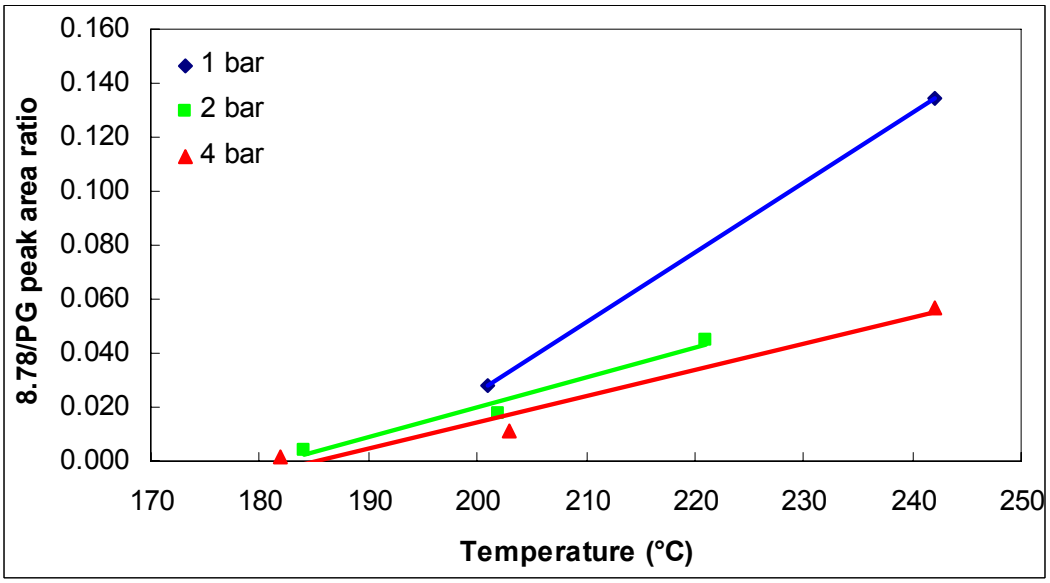

Figure 5.20. Effect of reaction temperature and pressure on unknown by-product 8.78 formation of the acetol to propylene glycol reaction (Data were plotted by 8.78/PG peak area ratio vs. Temperature)

9.11 (EG):

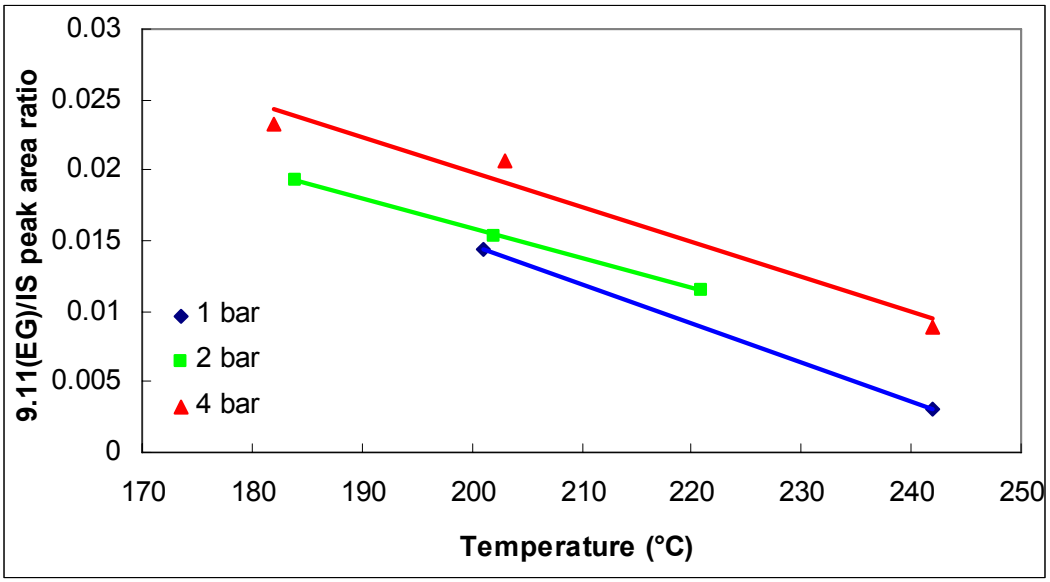

Figure 5.21. Effect of reaction temperature and pressure on unknown by-product 9.11 formation of the acetol to propylene glycol reaction (Data were plotted by 9.11/IS peak area ratio vs. Temperature)

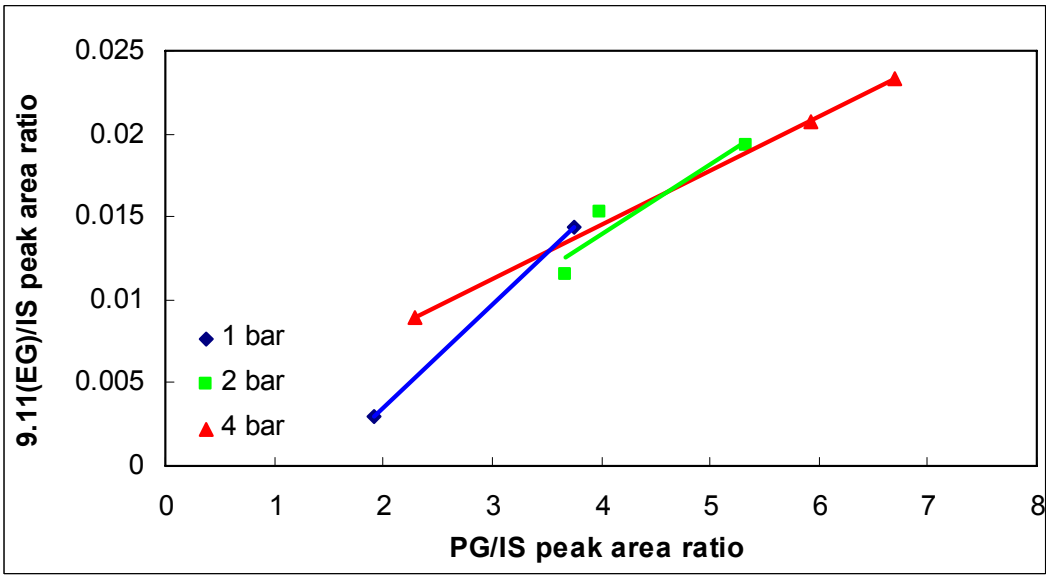

Figure 5.22. Unknown by-product 9.11 (EG) formation versus propylene glycol production of the acetol to propylene glycol reaction (Data plotted by 9.11(EG)/IS peak area ratio vs. PG/IS peak area ratio)

9.15:

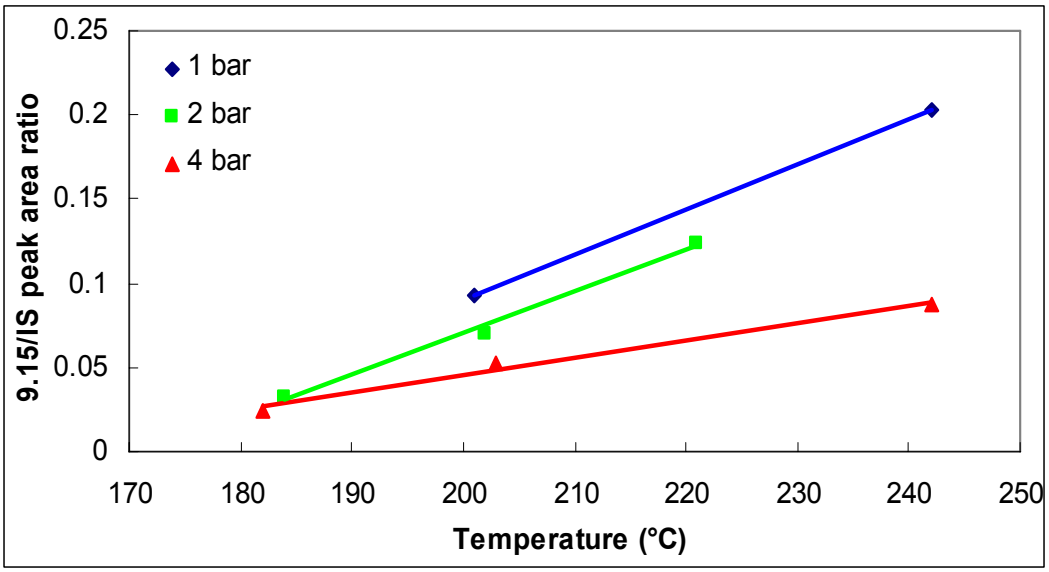

Figure 5.23. Effect of reaction temperature and pressure on unknown by-product 9.15 formation of the acetol to propylene glycol reaction (Data were plotted by 9.15/IS peak area ratio vs. Temperature)

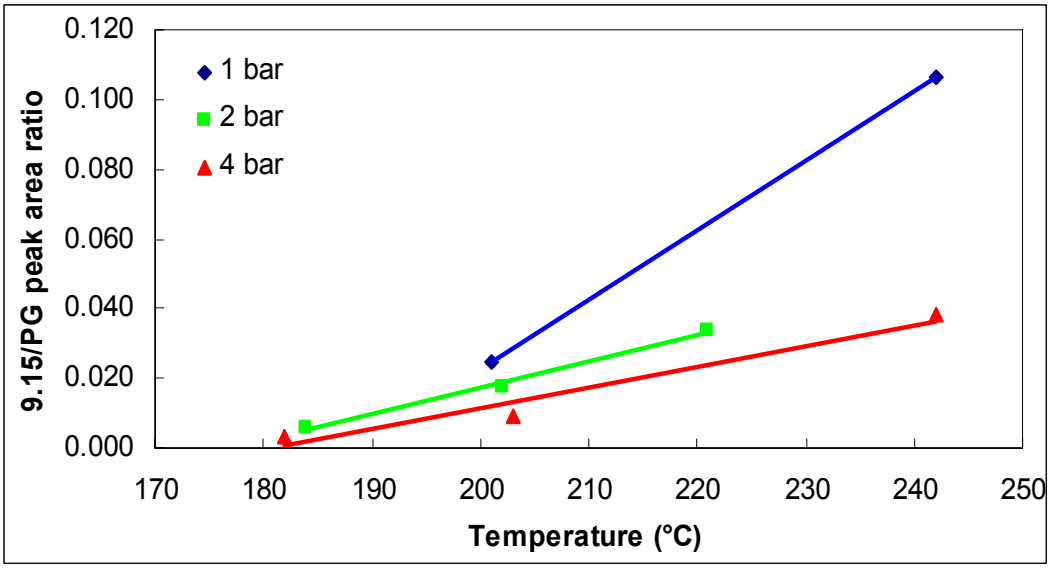

Figure 5.24. Effect of reaction temperature and pressure on unknown by-product 9.15 formation of the acetol to propylene glycol reaction (Data were plotted by 9.15/PG peak area ratio vs. Temperature)

9.28:

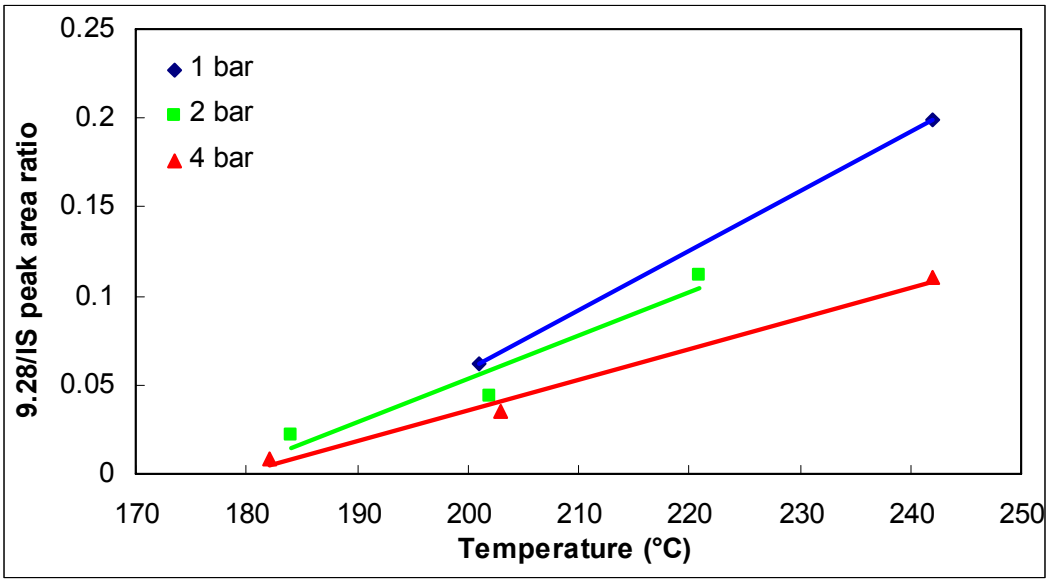

Figure 5.25. Effect of reaction temperature and pressure on unknown by-product 9.28 formation of the acetol to propylene glycol reaction (Data were plotted by 9.28/IS peak area ratio vs. Temperature)

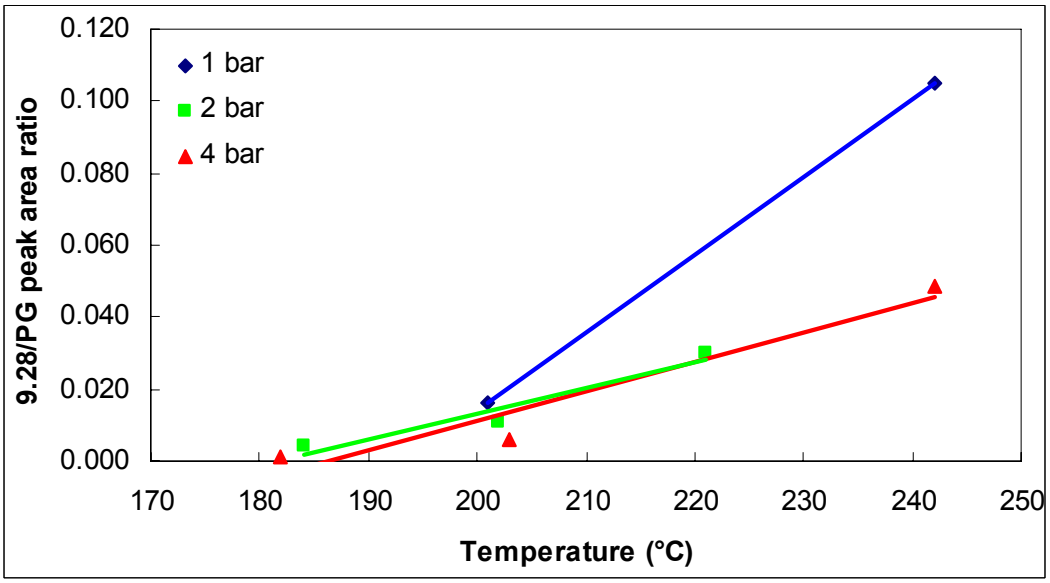

Figure 5.26. Effect of reaction temperature and pressure on unknown by-product 9.28 formation of the acetol to propylene glycol reaction (Data were plotted by 9.28/PG peak area ratio vs. Temperature)

9.32:

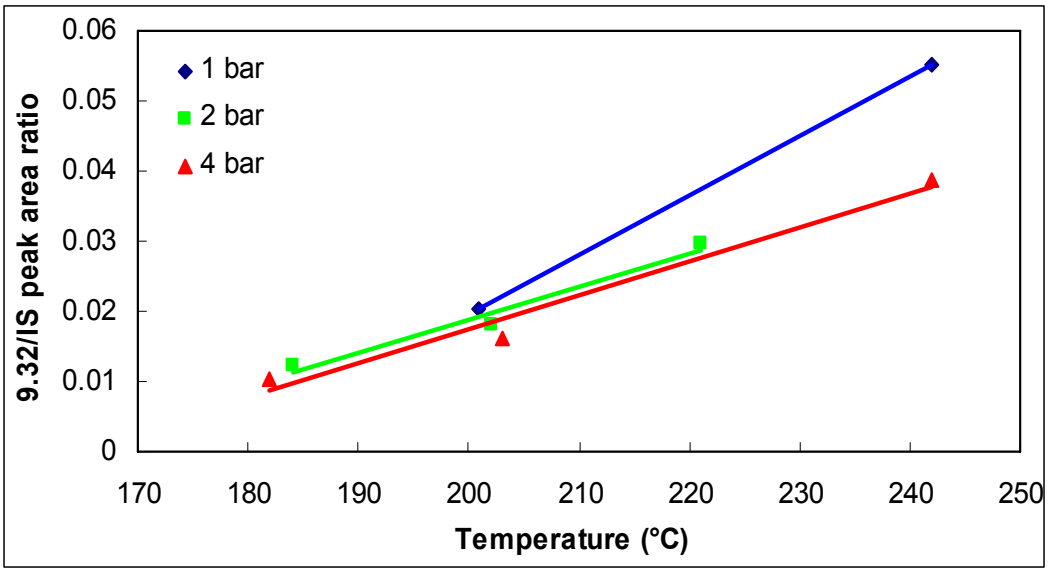

Figure 5.27. Effect of reaction temperature and pressure on unknown by-product 9.32 formation of the acetol to propylene glycol reaction (Data were plotted by 9.32/IS peak area ratio vs. Temperature)

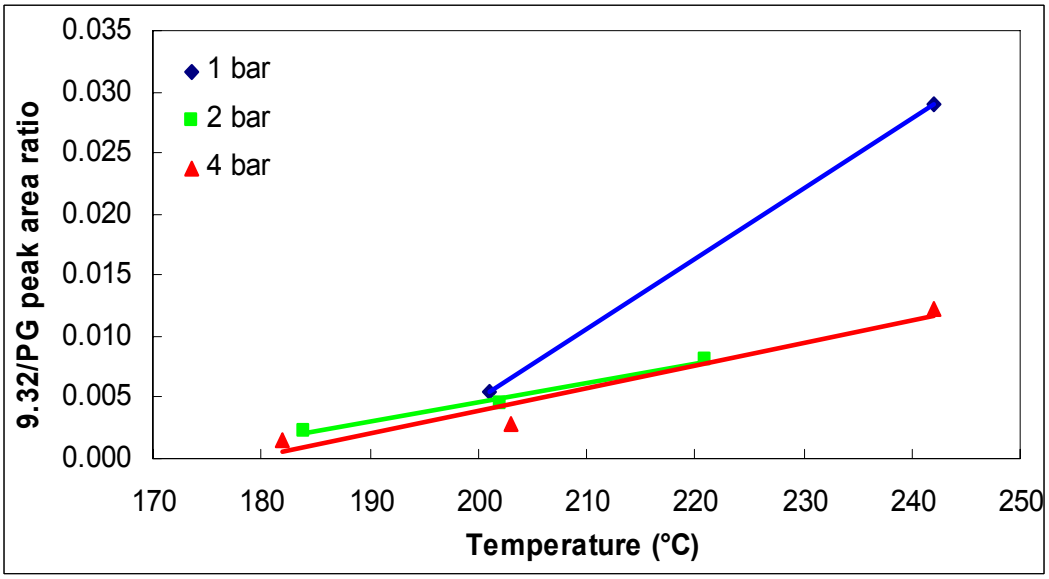

Figure 5.28. Effect of reaction temperature and pressure on unknown by-product 9.32 formation of the acetol to propylene glycol reaction (Data were plotted by 9.32/PG peak area ratio vs. Temperature)

9.405:

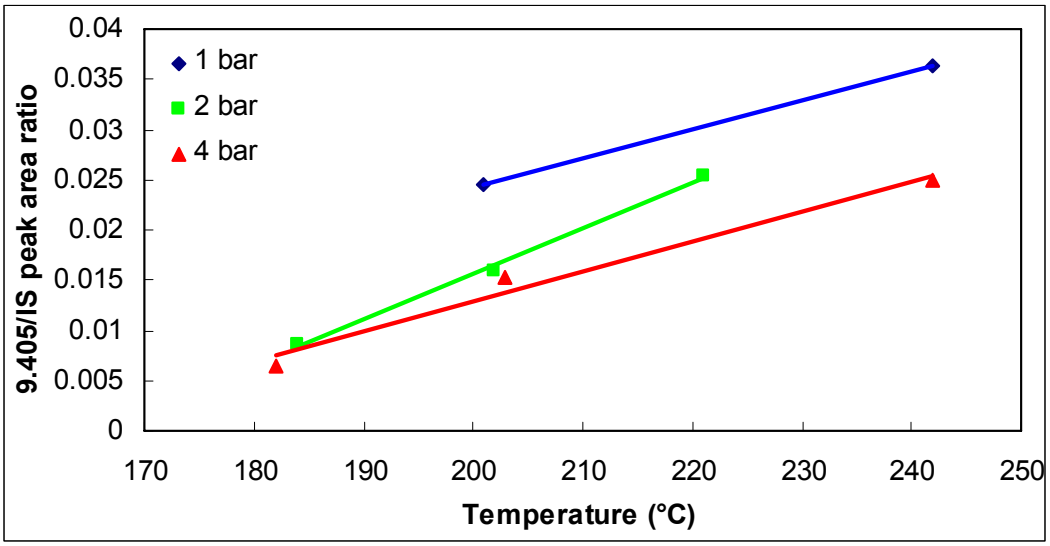

Figure 5.29. Effect of reaction temperature and pressure on unknown by-product 9.405 formation of the acetol to propylene glycol reaction (Data were plotted by 9.405/IS peak area ratio vs. Temperature)

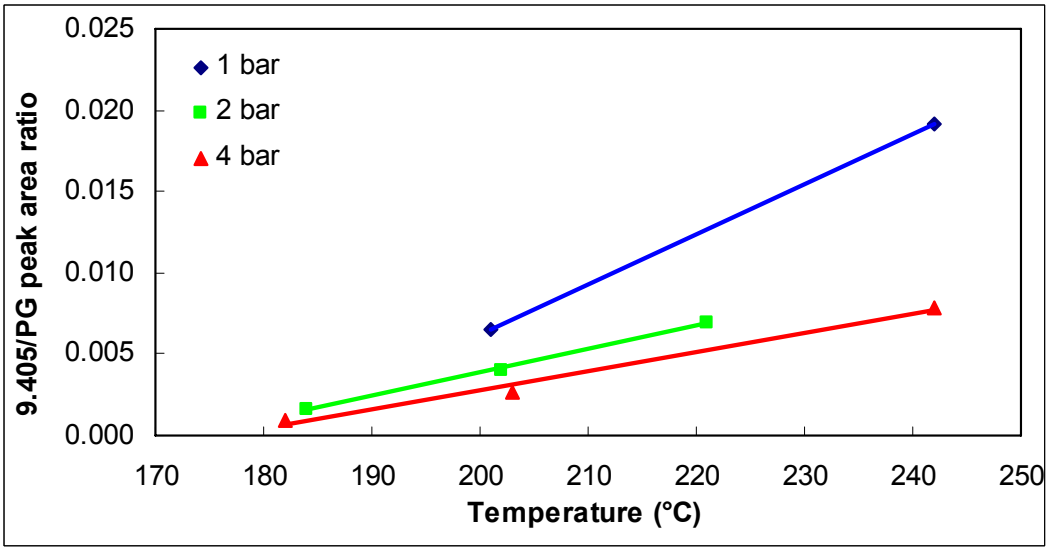

Figure 5.30. Effect of reaction temperature and pressure on unknown by-product 9.405 formation of the acetol to propylene glycol reaction (Data were plotted by 9.405/PG peak area ratio vs. Temperature)

5.3.3 Reaction of Propylene Glycol to Acetol

Figure 5.31 shows the results of the propylene glycol to acetol reaction at different temperatures (180 to 240°C) and pressures (1, 2, and 4 bar). This figure indicates that, for a specific pressure, at higher temperatures more acetol is produced. Lower pressures cause more acetol to be produced from propylene glycol at a given temperature. This behavior is in agreement with results obtained for the reactions of glycerol to propylene glycol and acetol to propylene glycol that the second step of the reaction (acetol to propylene glycol) is a reversible reaction and it is expected to be equilibrium limited.

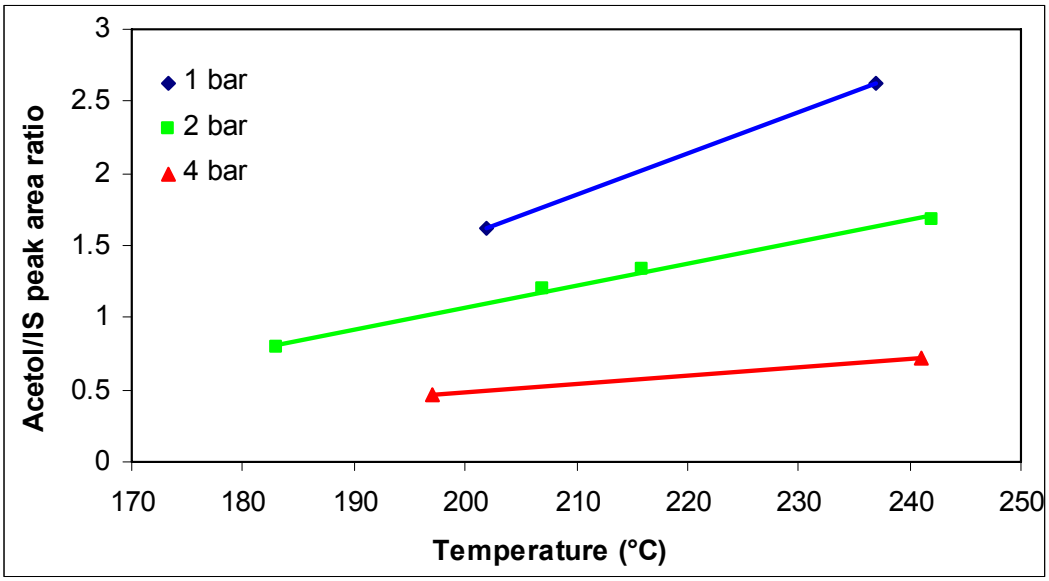

Figure 5.31. Effect of reaction temperature and pressure on conversion of propylene glycol to acetol.

5.3.3.1 Trends in 7 Unknown By-products

Trends of all unknown by-products in the reaction of propylene to acetol agree with the trends of all unknown by-products observed in the reactions of glycerol to propylene glycol and acetol to propylene glycol. The effect of temperature (180 to 240°C) on all unknown by-product formation for the propylene glycol to acetol reaction at three different pressures (1, 2 and 4 bar) is presented in Figure 5.32 to 5.37. The results indicate that more unknown by-products are produced at an increased reaction temperature. The same effect was also observed at each of the three pressure levels. At a given temperature, higher pressures produce fewer by-products. Ethylene glycol (9.11) was not observed in this reaction—ethylene glycol is not formed in this reversed reaction of propylene glycerol to acetol. It indicates that ethylene glycerol is produced from glycerol and not propylene glycol.

8.74:

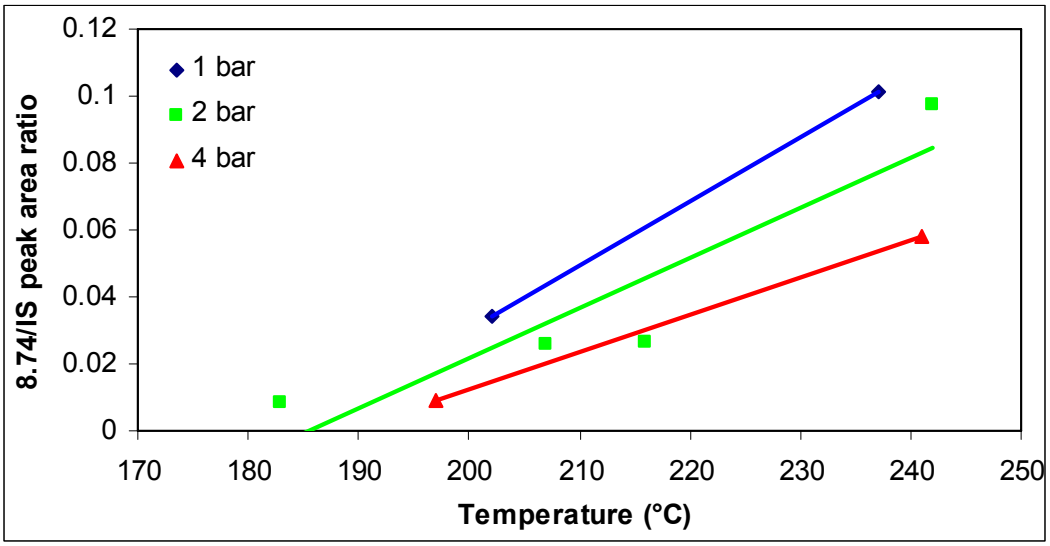

Figure 5.32. Effect of reaction temperature and pressure on unknown by-product 8.74 formation of the propylene glycol to acetol reaction (Data were plotted by 8.74/IS peak area ratio vs. Temperature)

8.78:

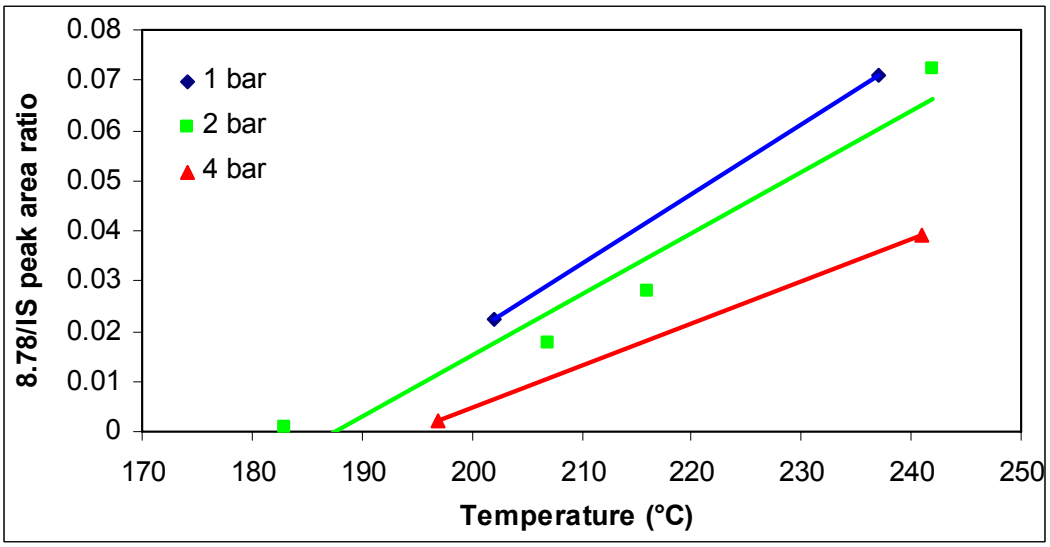

Figure 5.33. Effect of reaction temperature and pressure on unknown by-product 8.78 formation of the propylene glycol to acetol reaction (Data were plotted by 8.78/IS peak area ratio vs. Temperature)

9.15:

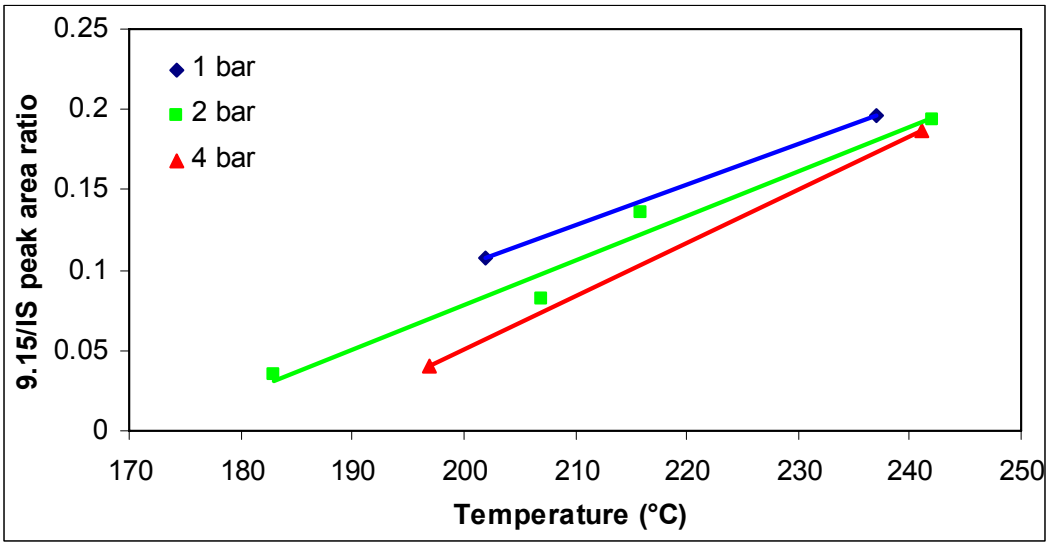

Figure 5.34. Effect of reaction temperature and pressure on unknown by-product 9.15 formation of the propylene glycol to acetol reaction (Data were plotted by 9.15/IS peak area ratio vs. Temperature)

9.28:

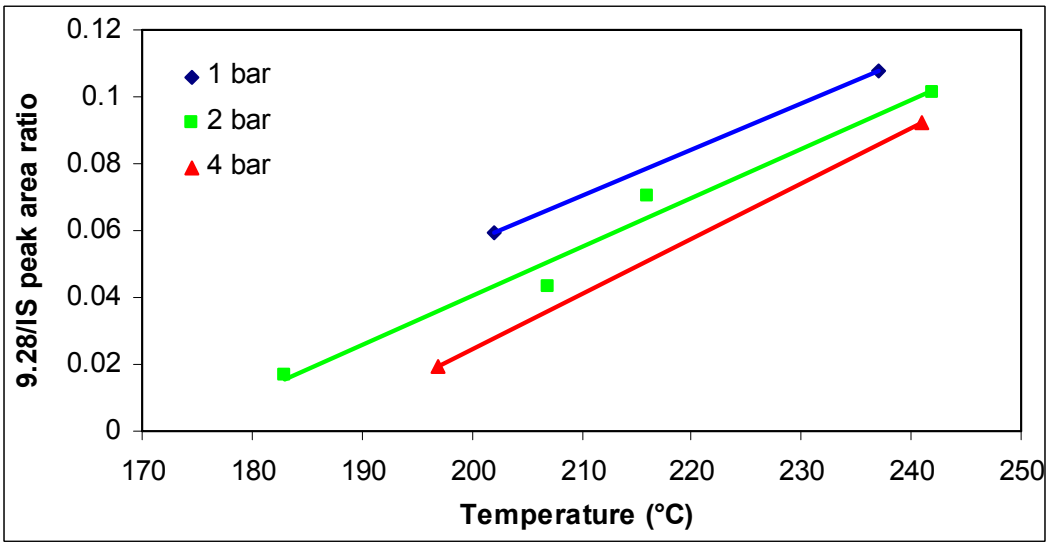

Figure 5.35. Effect of reaction temperature and pressure on unknown by-product 9.28 formation of the propylene glycol to acetol reaction (Data were plotted by 9.28/IS peak area ratio vs. Temperature)

9.32:

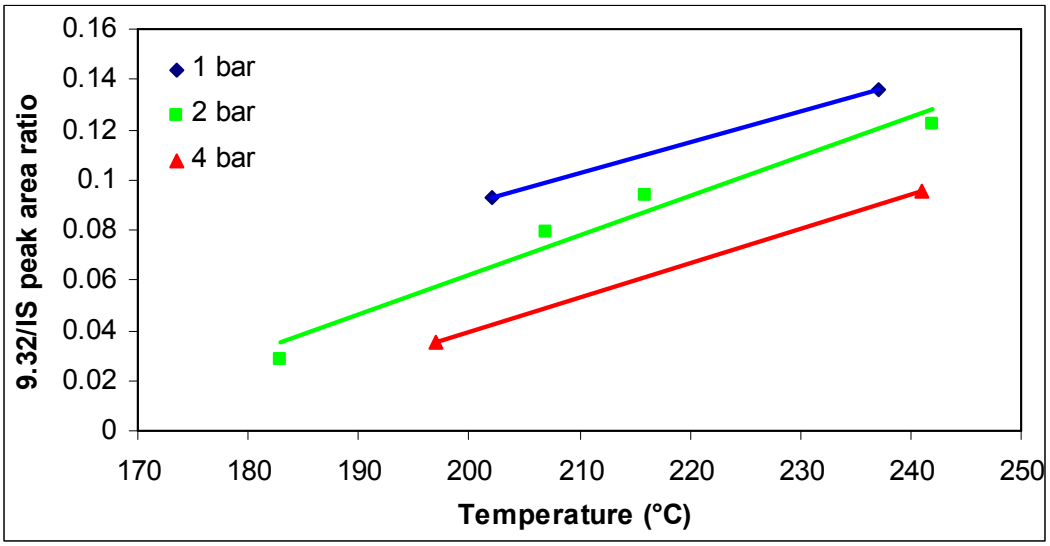

Figure 5.36. Effect of reaction temperature and pressure on unknown by-product 9.32 formation of the propylene glycol to acetol reaction (Data were plotted by 9.32/IS peak area ratio vs. Temperature)

9.405:

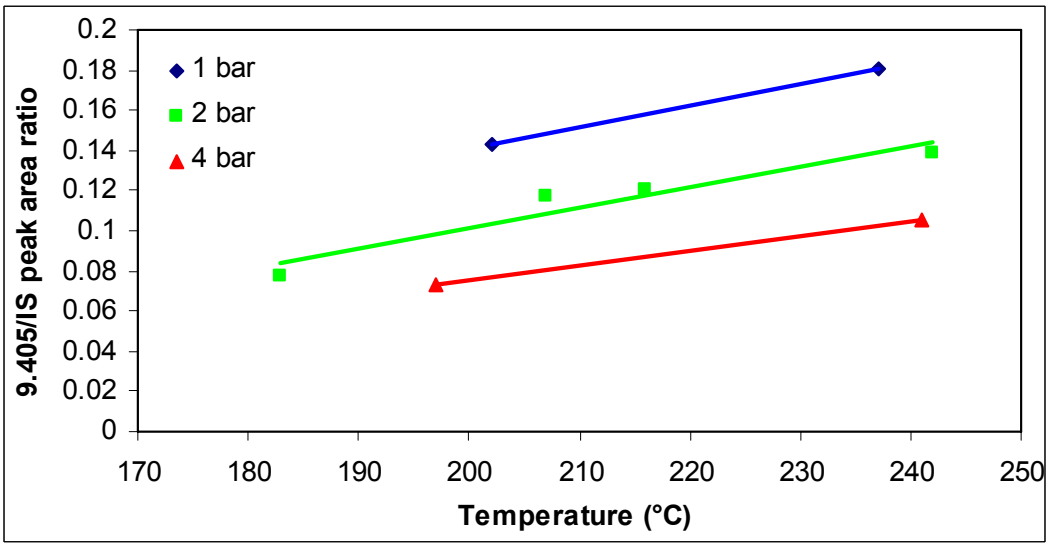

Figure 5.37. Effect of reaction temperature and pressure on unknown by-product 9.405 formation of the propylene glycol to acetol reaction (Data were plotted by 9.405/IS peak area ratio vs. Temperature)

5.4 Conclusions

For the reactions of glycerol to propylene glycol and acetol to propylene glycol, at higher temperatures the by-product formation has a notable dependence on system pressure, in contrast, at lower temperatures the dependence of by-product formation on pressure is less. Ethylene glycol is the only by-product that follows the trend of propylene glycol production, and it is likely produced directly from glycerol.

For the overall reaction of producing propylene glycol from glycerol, lower temperature and higher pressure operation results in a higher yield in propylene glycol because of the reaction equilibrium on the second step of reaction (see Chapter 8). Concentration profiles of the by-products suggest that the preferred operating conditions for converting glycerol to propylene glycol with high selectivities are lower temperatures and higher pressures.

CHAPTER 6

6. PILOT-SCALE STUDY ON THE PRODUCTION OF PROPYLENE GLYCOL FROM GLYCEROL

6.1 Introduction

6.1.1 Scale-up

Scale-up is inherent in all industrial activity. When a new chemical process or a change of a process moves from laboratory to the pilot plant to the manufacturing facility, unexpected problems are often encountered. The problems could be of either chemical or physical in nature, or a variation of both. One of the most frustrating difficulties that can be encountered is the presence of impurities that are not considered or studied in the small laboratory scale. To be successful at the scale-up of chemical processes requires the utilization of a broad range of fundamental knowledge and a mature understanding of the total problem under study.

Ju and Chase[39] classified the scale-up of a chemical process into three stages:

1. Laboratory scale, where elementary studies are carried out.
2. Pilot scale, where the process optimizations are determined.
3. Plant scale or production scale, where the process is brought to economic fruition.

Scale-up is a procedure for the design and construction of a large scale system on the basis of the results of experiments with small-scale equipment. Hence, the two big steps in scale-up are from the laboratory to the pilot plant, and then from the pilot plant to manufacturing. Each of those transitions call for new types of observations and new types of solutions to problems. The purpose of scale-up is to actually observe, measure, analyze, and record data. This chapter focuses on the first step that is from the laboratory experiment to the pilot plant processing.

6.1.2 Pilot Scale Processing

The ultimate purpose of all pilot plant is crystallized in a phrase by L. H. Baekeland that has become famous: “Commit your blunders on a small scale and make your profits on a large scale”[40]. George E. Davis, author of the word’s first handbook of chemical engineering, emphasized the value of experiments on a scale intermediate between that of the laboratory and full-scale production: “A small experiment made upon a few grammes of material in the laboratory will not be much use in guiding to the erection of a large scale works, but there is no doubt that an experiment based upon a few kilogrammes will give nearly all the data required.....”[41].

The main purpose of a pilot plant employed in chemical engineering is as forerunner to a full-sized production plant that is not yet built. The small-sale equipment is called a pilot plant, and its principal function is usually to provide design data for the ultimate large one, although it may also be required to

produce small quantities of a new product. Pilot-plant experiments are likely to be conducted on trial-and-error principles. The chief function is to exhibit the effects of change in shape or operating conditions more quickly and economically than would be possible by experiments on the full-sized prototype.

Pilot plants are used at various stages of the process development cycle and fulfill different purposes depending on the needs at that time. The following are the purposes of the pilot plant in this study:

- To confirm laboratory scale chemistry on industrial style equipment
- To provide design information for subsequent scale-up and individual process items
- To test and optimize the performance of proprietary plant equipments
- To produce material for downstream processing and trials
- To investigate the production of new product grades and formulations

6.1.3 Packed-Bed Exothermic Catalytic Reactor

As mentioned in chapter 4, propylene glycol can be produced from glycerol via a vapor phase reaction using in a packed bed reactor approach. Packed-bed tubular reactors are today the most commonly used reactor for practicing vapor phase catalytic reactions. These reactors are usually large capacity units, reaching in some cases, as in ammonia synthesis, capacities of half a million tons per year. The reactors are not single packed tubes. With all the auxiliary equipment for gas processing such as feeding, compressing, and

heating or cooling, and the support units, the reactors are indeed complicated. Large capacity reactors can have tens of thousands of tubes operating in parallel. At the heart of these reactors is still a single tube packed with a supported catalyst in one form or another. A coolant is circulated around the tubes to dissipate heat that is released from the exothermic controlled catalytic reaction. An effective heat removal prevents occurrence of hot spots and efficiently obtains the desired product.

6.1.4 Hot Spot

It is well established that transversal hot zones, with a temperature much higher than that of the adjacent zones, may exist in packed-bed reactors. Several potential causes have been proposed to explain the occurrence of hot zones in packed-bed reactors. The first is nonuniformity in the packing of the reactor or the activity of the catalyst. Boreskov et al.[42] reported hot zone formation due to nonuniform packing of the catalyst. The second potential cause is a nonuniform flow field generated by the interaction between the chemical reaction and the change in the physical properties of the fluid (such as viscosity and density). Colin and Balakotaiah[43], Nguyen and Balakotaiah[44], and Benneker et al.[45] showed that this type of interaction may generate flow maldistributions and local hot zones in packed-bed reactors.

The reactants are pre-mixed and fed to the reactor. The exothermic reaction causes hot spots to form near the reactor entrance, due to slow heat removal from the reactor tubes to the coolant fluid. Reports of the existence of

hot zones in industrial reactors were reported by Jaffe[46] and Barkelew and Gambhir[47]. Boreskov et al.[42] presented a map of the temperature distribution in a 60-cm-diameter reactor that showed several hot spots existed at the bottom of the reactor. Hot spot formation is undesirable, because it can create safety problems, reduce catalyst life, reduce reactor performance, and lead to reaction runaway if not properly controlled. Mills and Harold[48] summarized the options available to reduce the severity of hot spots in multi-tubular packed-bed reactors by (1) reduce coolant temperature; (2) increase gas flow rate; (3) increase bed thermal conductivity; (4) reduce tube diameter; and (5) dilute the catalyst bed (activity profiling).

6.1.5 Temperature Control on Packed-Bed Exothermic Catalytic Reactor

Control of temperature with respect to time and/or location is one of the most important aspects to operate exothermic reactions. The rates and equilibrium of reactions are profoundly affected by temperature, so are side reactions, by-product formation, yield, selectivity. Reaction temperatures must be controlled in order to ensure selectivity of the process, reproduce results accurately and to prevent thermal runaways. Heat transfer is not only important in the reaction but in the work up as well. In many chemical processes the rate of external heating may not be important, but the rate of external cooling can be very critical when exotherms take place. Heat evolved is proportional to number of moles of reactants participated during the reaction. Removal of heat is also

proportional to surface area. Hence as reactor size increases, volume-to-surface ratio also increases. It means that heat transfer becomes more difficult.

The hydrogenolysis of glycerol to propylene glycol is highly exothermic. This reversible exothermic reaction poses a space-time yield issue since an increase in temperature, while increasing the conversion of acetol, decreases the equilibrium yield of propylene glycol. A threat of by-product formation also increases due to increased temperatures. To achieve near total conversion to propylene glycol with less by-product formation one might:

1. Abandon adiabaticity and employ a near-isothermal tubular reactor whereby heat exchange provides a near-constant modest temperature commensurate with high reaction rate and high equilibrium conversion.
2. Retain the far less expensive adiabatic reactor but cool between adiabatic stages and operate initial stages at higher temperatures, which effectively shifts the equilibrium conversion point to the larger desired value as the process stream moves from the first to *n*-th adiabatic stage.

6.2 Experimental Section

In this study, pilot plant reactors for producing acetol and propylene glycol from glycerol by means of packed-bed catalytic vapor phase reaction include a catalytic reaction zone for producing propylene glycol as a main product. Pre-reduced copper-chromite catalyst purchased from Engelhard Corporation (Elyria, Ohio) was packed in the catalytic reaction zone. The investigation involves

exploring the features of typical two types of reactors to approach a proper temperature control and maximum propylene glycol production.

6.2.1 Experimental Setup

The experimental setup is divided into three distinct parts: glycerol evaporator, reactor, and heat exchange condenser shown in Figure 6.1.

Glycerol evaporator

The glycerol evaporation system consists of a wrapped coil (soft refrigerated copper tubing of 0.5 in outside diameter) with an electric heating tape wrapped around a stainless steel pipe to evaporate the liquid glycerol along with gas. The vapor temperature on the evaporator outlet was measured by a thermocouple.

Packed-bed reactor

The details of packed-bed reactors (shell-and-tube and tube-cooled reactors) employed are thoroughly described in the sections of reactor description.

Heat exchange condenser

The heat exchange condenser consists of a copper coil (soft refrigerated copper tubing of 0.5 in outside diameter) submerged in a cooling water bath and followed by a glass condenser which chilled water was circulated.

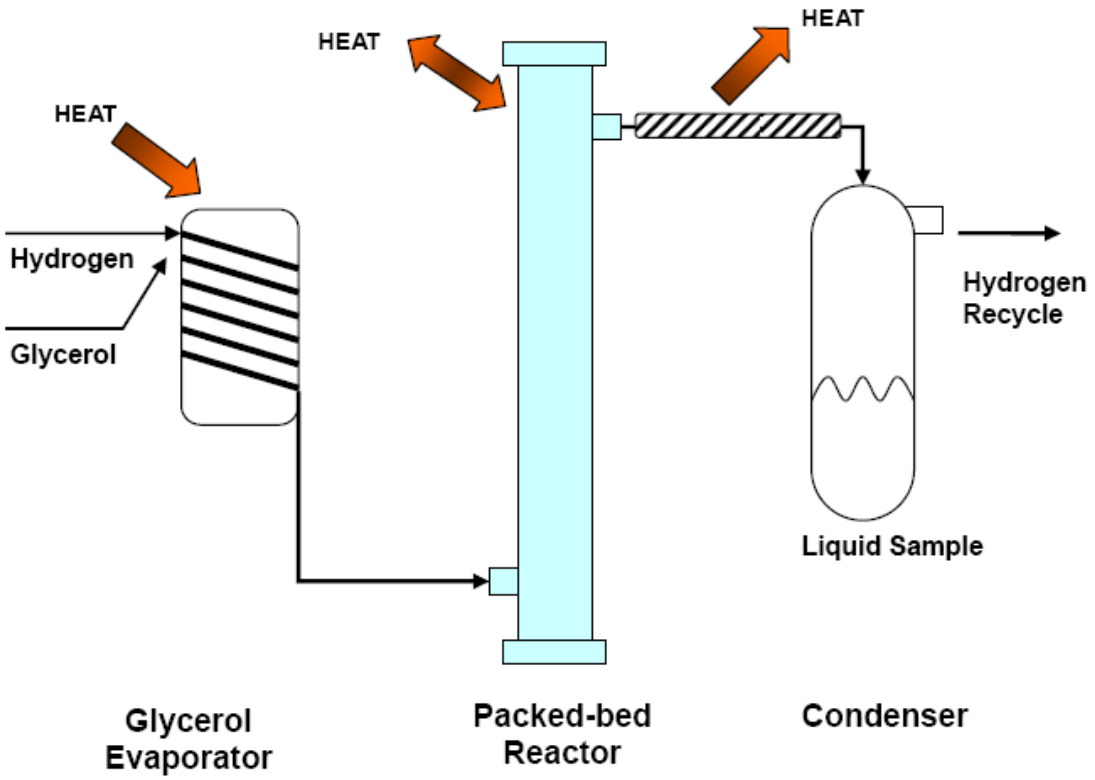

Figure 6.1. Pilot-scale experimental setup.

6.2.2 Analytical Methods

Exit liquid samples were analyzed with a Hewlett-Packard 6890 (Wilmington, DE) gas chromatograph equipped with a flame ionization detector. Hewlett-Packard Chemstation software was used to collect and analyze the data. A Restek Corp (Bellefonte, PA) MXT® WAX 70624 gas chromatography (GC) column (30m x 250 μm x 0.5μm) was used for separation. A solution of *n*-butanol with a known amount of internal standard was prepared a priori and used for analysis. The samples were prepared for analysis by adding 0.1 mL of

product sample to 1 mL of stock solution in a 2 mL glass vial. A 2 μL portion of the sample was injected into the column. The oven temperature program consisted of the following segments: start at 45 °C (0 min), ramp at 0.2 °C /min to 46 °C (0 min), and ramp at 30 °C /min to 220 °C (2.5 min). Using the standard calibration curves that were prepared for all the components, the integrated areas were converted to weight percentages for each component present in the sample. The concentration of water was measured by a Metrohm 758 KFD Titrino (Herisau, Switzweland) with Karl Fisher titrant. The samples were diluted with methanol before titration.

For each data point, the conversion and overall selectivity of propylene glycol was calculated. Conversion of glycerol is defined as the ratio of the number of moles of glycerol consumed in the reaction to the total moles of glycerol initially present. The overall selectivity is defined as the ratio of the number of moles of acetol and propylene glycol produced to the moles of glycerol consumed in the reaction, taking into account the stoichiometric coefficient.

6.3 Results and Discussion

Great quantities of heat are released in this exothermic catalytic reaction from glycerol to propylene glycol and, furthermore, acceptable selectivities are usually ensured only within a fairly narrow temperature range. If a plant were to be built at short notice, the choice would probably be between the shell-and-tube packed-bed reactor and the tube-cooled packed-bed reactor, since these reactor types can provide efficient control of temperature. These reactors have been

well established commercially, and it would seem appropriate to discuss their merits and drawbacks for production of propylene glycol from glycerol.

6.3.1 Shell-and-Tube Packed-Bed Reactor

6.3.1.1 Reactor Description

A Fixed-bed catalytic vapor-phase reaction for producing propylene glycol from glycerol was performed in a pilot plant reactor constructed as a shell-and-tube heat exchanger having its tube space filled with a copper-chromite catalyst and its shell space filled with a recirculating heat-transfer fluid. Figure 6.2 is a schematic view showing the structure of the pilot-plant reactor, wherein the reactor comprising one catalytic tube, and the structure of a catalytic bed disposed inside of the catalytic tube.

Two pilot plant reactors were designed, constructed, and tested. The #1 reactor has a length of 16 ft with an outside diameter of 0.75 in. The reactor tube was filled with 1.5 kg of copper-chromite catalyst. The #2 reactor has a length of 10 ft with an outside diameter of 1 in. The reactor tube was filled with 2.2 kg of copper-chromite catalyst. The shell space was filled with a heat-transfer medium, and the heat-transfer medium the shell space was maintained as close to an isothermal temperature or a temperature difference of 0-5°C by pumping through hot thermal oil at 215-230°C with a high flow rate. Also, in order to protect catalyst from a highly exothermic reaction, the process was performed at a limited temperature difference between the temperature at a hot spot and the temperature of the heat-transfer medium. Several thermocouples, pressure

gauges, and sampling valves were mounted along the reactor (#1 reactor) to measure the pressure, concentration and temperature axial profiles. The product samples were collected for each 20 min until steady state of the reaction is reached (after 1-2 hour depending on the operating conditions) and were analyzed by gas chromatography. Catalyst activity was regularly checked by sampling the reactor outlet.

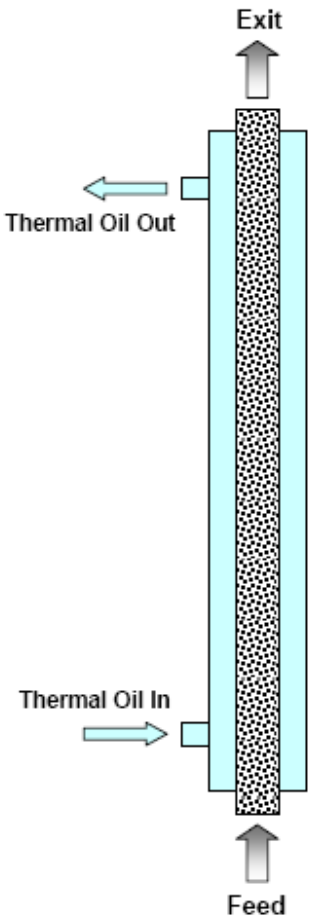

Figure 6.2. Shell-and-tube packed-bed pilot plant reactor.

6.3.1.2 Performance

For shell-and-tube type reactor, the temperature of the overall reactor system is controlled by the heat-transfer medium in the shell. Reaction heat is removed by heat transfer across the tube wall into the circulated heat-transfer fluid used in the process. The temperature increase at the reactor inlet was observed due to exothermic nature—hot spots appear and disappear periodically (flickering) on the bottom of the reactor during the reaction. The maximum temperature difference between the tube centerline and the heat-transfer fluid was 5-8°C. An optimum temperature profile can be maintained in the catalyst bed, obtaining high conversion yields, and with this optimum temperature control a very active copper-contain catalyst can be used.

Temperature measurements in the catalyst bed were performed during the reaction. The results are depicted in Figure 6.3 which also contains the temperature profile in the tube-cooled packed-bed reactor. No deactivation was observed at reaction temperature of 220°C after more than 72 hours of operation (see Figure 6.4).

In the manufacturing plant scale, this type of catalytic reactor with a plurality of parallel reaction tubes is particularly suitable for the direct catalytic hydrogenation of glycerol with hydrogen. The improved heat-control system for reactors can secure the heat stability of the catalyst layer, reduce the amount of by-products, and increase the yield of a final product. However, it is necessary to limit the pressure drop through the catalyst beds and to reduce the reactor volume.

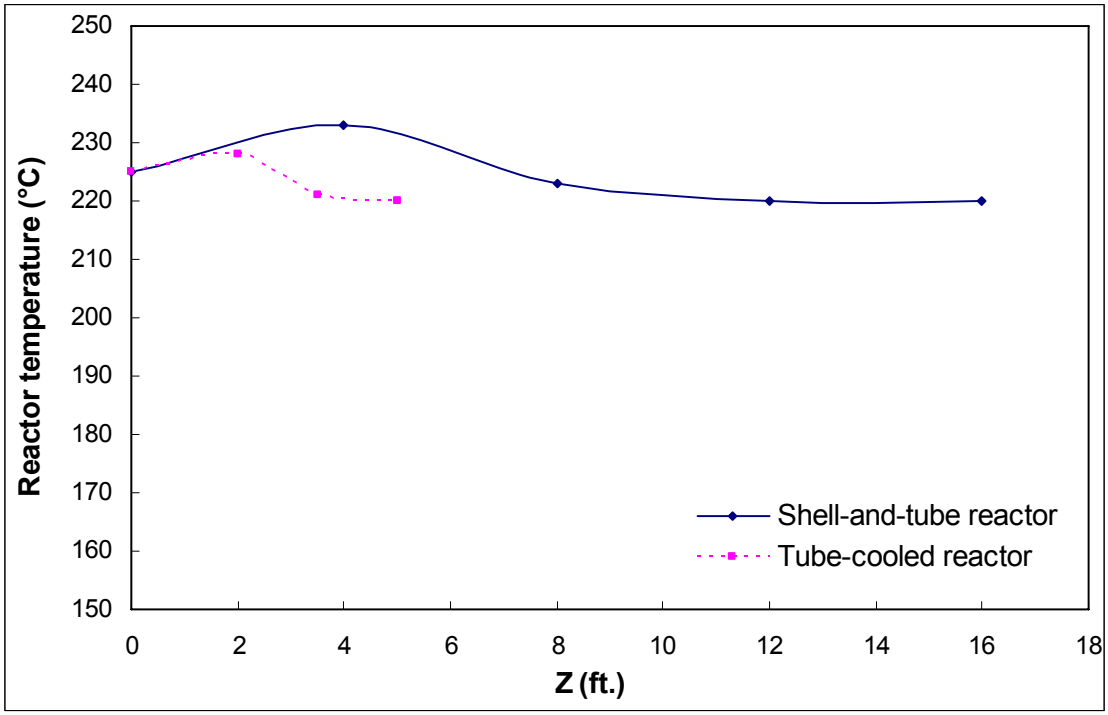

Figure 6.3. Axial temperature profile for the #1 shell-and-tube packed-bed reactor and the tube-cooled packed-bed reactor at 220°C operating temperature.

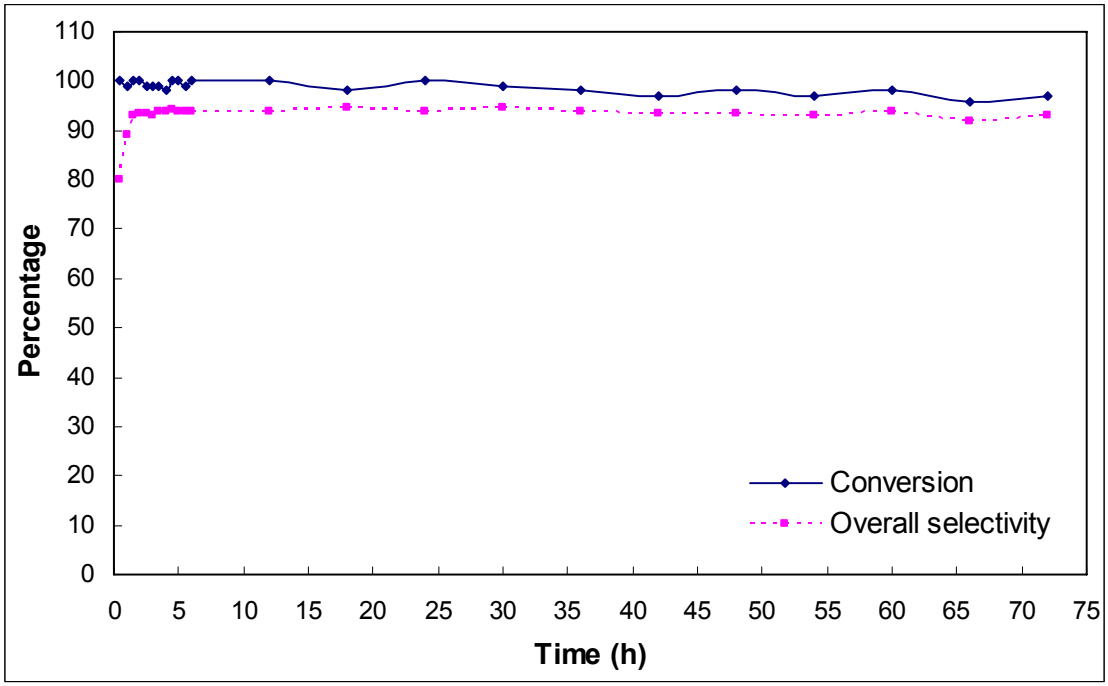

Figure 6.4. Stability test of the #1 shell-and-tube packed-bed reactor at reaction temperature = 220°C; glycerol feed rate = 0.8 kg/hr; hydrogen flow rate = 50 l/min.

6.3.2 Tube-Cooled Packed-bed Reactor with Inert Packing

6.3.2.1 Reactor Description

The tube-cooled packed-bed reactor has a 2 in inside diameter, 5 ft length, and three 0.5 in outside diameter tubes running thermal oil for heat removal. Figure 6.5 shows an axial and radial cross section of the pilot reactor. The reactor shell space was filled with 3.6 kg of copper-chromite catalyst. Several thermocouples and pressure gauges were mounted along the reactor to measure the pressure and temperature axial profiles. The thermal oil was manifolded in the three tubes on one side and manifolded out on the other. In order to

minimize the temperature increase at the reactor inlet caused by the rapid exothermic reaction, the shell side has alternating sections of inert material packing and catalyst, where hot spots are to be generated in a reaction zone.

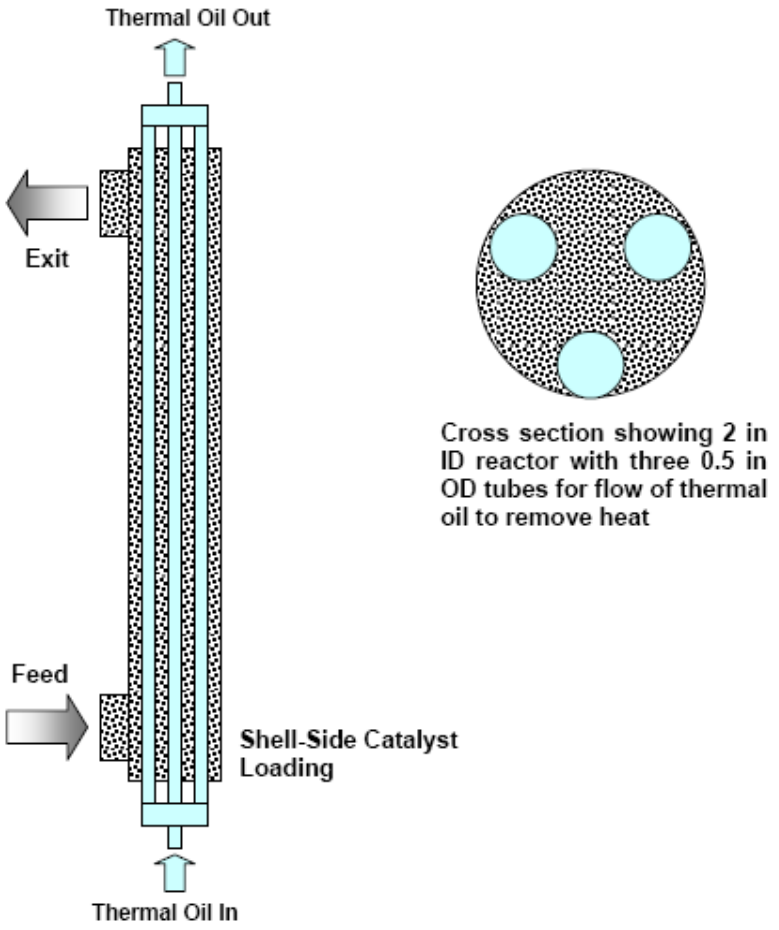

Figure 6.5. Tube-cooled packed-bed pilot plant reactor.

6.3.2.2 Performance

This tube-cooled packed-bed reactor offers a larger cross-sectional area and reduced distance of travel for flow compared to the shell-and-tube reactor.

Consequently, the pressure drop is reduced (about 0.25 psi pressure drop is across the every 2.5 ft section). The temperature held constant with excellent control during the reaction period. The maximum temperature difference between each thermocouple was 2-5°C. The ability to use inert packing to assure temperature control was successful, thereby increasing the lifetime of a catalyst and producing propylene glycol in both high yield and selectivity. This design is considered fully scalable without hot spots and minimal pressure drop.

It was also observed that more unconverted glycerol (~5%) appeared in the product mixture because the larger gas-volume formed during the experiment entails high gas velocities in the reactor and both can generate channels in the catalyst bed. Table 6.1 provides the comparison of conversion data from two reactor types.

Table 6.1. Comparison of the #1 shell-and-tube and tube-cooled reactors on converting glycerol to propylene glycol.

Reactor Type	#1 Shell-and-Tube Packed-bed Reactor	Tube-Cooled Packed-bed Reactor
Reactor Size		
Length (ft.)	16	5
Reactor dia (in)	2 ID	2 ID
Tube dia. (in)	0.75 OD tube × 1	0.5 OD tube × 3
Catalyst mass (kg)	1.5	3.6
Catalyst packing	Tube-side	Shell-side with inert packing
Heat-transfer medium	Shell-side	Tube-side
Operating Conditions		
Operating temperature (°C)	220	220
Glycerol feed rate (kg/hr)	0.8	1.3
Reaction Data		
Pressure drop across reactor (pai)	8	0.5
Glycerol conversion (%)	100-99.5	95
Overall selectivity (%)	94%	94%
Propylene glycol production (kg/hr)	0.4	0.625
Catalyst productivity (kg PG/hr /kg of catalyst)	0.267	0.174
Glycerol evaporation	Sufficient	Limited

6.3.2.3 Scalability

The tube-cooled reactor had lower glycerol conversion despite having a higher catalyst to glycerol ratio, possibly, glycerol vapors were by-passing the catalysts and were in the product stream at conditions that the shell-and-tube reactor exhibited less than 0.2% glycerol in the product mixture. The by-passing (channeling) was possible due to the low depth of the packing—a packing of 3.75 ft of catalyst (total 5 ft of catalyst less inert) as compared to 10 and 16 ft of catalyst (axial length of packing) in the shell-and-tube reactors. In the commercial facility, the depth of catalyst packing will typically be around 18 to 24 ft; therefore, this bypassing issue should be resolved.

The heat transfer in the tube-cooled reactor is over the same dimensions as heat exchange in the shell-and-tube reactors. The reactor is fully scalable by simply increasing the shell diameter while keeping the spacing of the heat exchange tubes the same. The shell surface was insulated against heat loss.

In the tube-cooled reactor design, a shell side loading of the reactor is possible in the recommended configuration because access from the top (U-side) allows easy loading of catalyst in the reactor and allows inert packing to be strategically placed in the reactor. Even in the pilot scale study, the shell side loading was much easier to work with and the reactor had a much lower pressure drop. The advantages of this configuration over tube-side loading in the shell-and-tube reactors are as follows:

- Reduction in reactor size.
- The pressure drop is considerably less.

- Filling catalyst in the shell side is considerably easier. Basically 2-6 shells are loaded with catalyst as opposed to 50,000 tubes (5 X volume).

This tube-cooled packed-bed reactor design is considered crucial to the successful operation. Figure 6.6 illustrates the orientation of the reactor and internals.

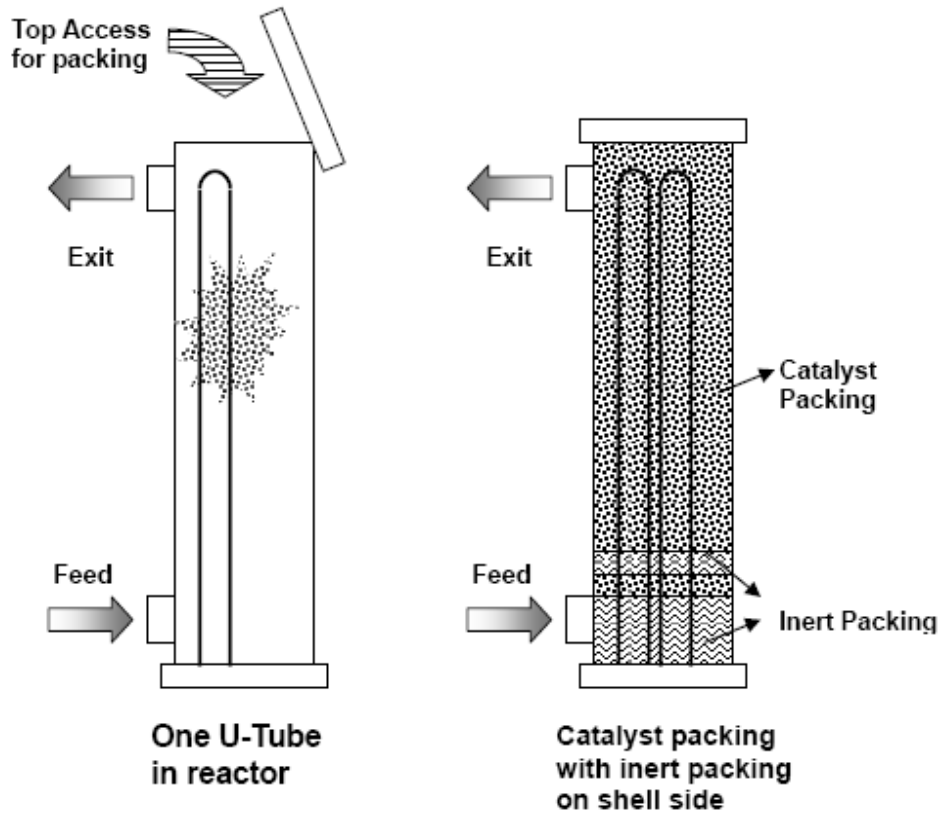

Figure 6.6. Recommended configuration for the tube-cooled packed-bed reactor.

CHAPTER 7

7. SEPARATION SCHEME AND RELATIVE VOLATILITY EATIMATION

7.1 Introduction

The process for converting glycerol to propylene glycol involves two reactions via a reactive intermediate—first, dehydrate glycerol to acetol, and then acetol is hydrogenated in a further reaction step to produce propylene glycol[12]. The reaction of glycerol to propylene glycol achieves a high selectivity toward propylene glycol, however, it has shown little selectivity toward ethylene glycol and other unknown by-products. Downstream processing involving product recovery and purification is essential to be followed by the commercial production plant to bring the propylene glycol product to a desired purity. The commercial-scale process will produce 100 million pounds of propylene glycol annually, and the propylene glycol product needs to have over 99.5% purity.

7.1.1 Multicomponent Distillation

Distillation is one of the more important and common unit operations in chemical engineering. The purification of reaction products in a chemical production plant is typically accomplished through distillation. Most practical distillation problems, however, involve multicomponent mixtures. In this case, the impurities make the distillation multicomponent. Evaluating and synthesizing the best possible multistage distillation column setup therefore requires rapid and

accurate methods to calculate the design requirements for specified separations. Several procedures that are grouped into three main areas: heuristics, shortcut calculations and rigorous modeling, have been commonly suggested to optimize the design of distillation columns. Many investigators[49, 50, 51, 52, 53] have presented different short-cut and rigorous methods. The Fenske-Underwood-Gilliland model (FUG) is one of these shortcut methods, which has been demonstrated to be a very effective model for multicomponent distillation.

7.1.2 Fenske-Underwood-Gilliland (FUG) Shortcut Method for Design of Multicomponent Distillation Columns

The FUG shortcut distillation method was applied to the light key (*LK*) and to the heavy key (*HK*) components, under column's condition of total reflux. The light key component is defined as one which is present in the bottom in important amounts. All components lighter than the light key are present only in small amounts in the bottom. The heavy key component is present in the distillate in important amounts. All components heavier than the heavy key are present only in small amounts in the distillate.

The calculations are based on the standard Fenske, Underwood, Gilliland and Kirkbride equations applying the assumptions of constant relative volatility and constant molar overflow to provide an initial estimate of number of theoretical stages, reflux ratio and optimal feed stage location[49]. However, these calculations are not applicable for separations of major components with widely divergent molar enthalpies of vaporization (violates the assumption of constant

molar flow) or mixtures with large deviations from ideal solution behavior, including azeotropic mixtures (violates the assumption of constant relative volatility).

These estimates are most effective when generated before performing full simulation calculations to set up initial values for those simulation calculations. The Fenske method estimates the minimum number of theoretical stages at total reflux by assuming constant relative volatility of the components. The Underwood method estimates the minimum reflux for an infinite number of theoretical stages assuming constant molar flow through the column, an optimal feed stage location, and saturated reflux. The Gilliland method estimates the number of theoretical stages required for a given split with the reflux at a fixed multiplier of the minimum reflux ratio. The Kirkbride method estimates an optimal feed stage location.

Fenske equation[50] can be used to calculate the minimum number of stages for the specified splits of the two key components:

$$N_{\min} = \frac{\ln\left[\left(\frac{x_{LK,D}}{x_{LK,B}}\right)\left(\frac{x_{HK,B}}{x_{HK,D}}\right)\right]}{\ln\alpha_{LK,HK}} \qquad (1)$$

The subscripts *D* and *B* refer to the distillate and bottom. The minimum number of stages corresponds to the state of total reflux. It is influenced by the presence of the nonkey components only if they have any effect on the relative volatility between the key components.

Underwood equations are used to determine the minimum reflux ratio required to achieve the specified separation of the two keys. The minimum reflux ratio corresponds to a column of infinite stages, and the point at which this occurs is referred to as a pinch point. Shiras et al.[51] classified multicomponent systems as having one or two pinch points. For Class 1 separation (single pinch point), all components in the feed distribute to both the distillate and bottom products. If one or more of the components appear in only the distillate or bottom products, two pinch points occur in the column, and the separation is classified as Class 2 separation.

Class 1 separation can occur when narrow-boiling mixtures are distilled or when the degree of separation between the key components is not sharp. For the rectifying section pinch point of a continuous column, the following equation attributed to Underwood[52] can be written from mass balances and equilibrium relationships:

$$\frac{L_\infty}{D} = R_{\min} = \frac{\frac{x_{LK,D}}{x_{LK,\infty}} - \alpha_{LK,HK}\frac{x_{HK,D}}{x_{HK,\infty}}}{\alpha_{LK,HK} - 1} \qquad (2)$$

For Class 2 separation, the two equations devised by Underwood are:

$$\sum \frac{\alpha_{i,j} z_{i,F}}{\alpha_{i,j} - \theta} = 1 + q \qquad (3)$$

$$\sum \frac{\alpha_{i,j} x_{i,D}}{\alpha_{i,j} - \theta} = 1 + R_{\min} \qquad (4)$$

Equation 3 is first solved for *m* roots of θ where *m* is one less than the number of distributing components. Equation 4 is then written for each value of θ, and the *m* equations are solved simultaneously to yield R_{min} and the splits of the distributing components.

The actual reflux ratio is generally established by economic considerations at some multiple of the minimum reflux. The value of R/R_{min} usually lies between 1.1 and 1.5. The number of theoretical stages for the specified separation is then determined from Gilliland's empirical correlation relating R_{min}, N_{min}, R, and N. The Gilliland correction is very useful for preliminary exploration of design variables. One equation form of Gilliland's correlation is[53]:

$$\frac{N - N_{\min}}{N + 1} = 1 - \exp\left[\left(\frac{1 + 54.4X}{11 + 117.2X}\right)\left(\frac{X - 1}{X^{0.5}}\right)\right] \qquad (5)$$

where

$$X = \frac{R - R_{\min}}{R + 1}$$

The feed stage location can be located using the Kirkbride equation. The distribution of the nonkey components at actual reflux is approximated to be close to that estimated by Fenske equation at total reflux.

7.2 Problem Statement

The aim of this project is to design a separation process followed by a commercial production plant as “Procedure for Purifying Propylene Glycol for Production Operation When Reactor Produces Out-of-Spec Product”. The detailed problem statement is provided in the cover sheet as the topic of Comprehensive Exam. A typical composition and conditions of the stream that reaches the distillation section of the plant is given in Table 7.1. The feed consists of 10 components, water, hydroxyacetone (acetol), propylene glycol (PG), and 7 unknown by-products. The laboratory results on by-product identification indicate that the peak 9.11 was identified as ethylene glycol (EG), and the peak 8.78 was identified as propionic acid. By-product identification was done by matching the peak in the gas chromatogram using a flame ionization detector. The latest GC/MS results indicate that the peak 9.11 was further confirmed as ethylene glycol; however, the peak 8.78 was not confirmed as propionic acid. In the present work, the peak 8.78 was still considered as propionic acid and used for the ChemCAD process simulation. The information on the feed flow rate and conditions (temperature and pressure) are provided by Mr. Bryan Sawyer. The column operating pressure and temperature are representative and depend on economic factors.

Table 7.1. Problem description: base case process

Feed Specification	
flowrate (kg/hr)	12913
pressure (bar)	0.6
temperature (°C)	85
Feed Composition (wt. %)	
Unknown[a]	
8.75	0.12
8.78	0.49
9.11 Ethylene glycol (EG)	1.15
9.15	0.88
9.28	0.38
9.32	0.39
9.405	0.34
Total Unknown	3.75
Water	20.00
Hydroxyacetone (Acetol)	22.26
Propylene glycol (PG)	53.51

[a] Unknowns (unidentified compounds) are named as the retention time shown in the gas chromatogram

7.3 Solution Methods

ChemCAD process simulation program was used to perform shortcut calculations and rigorous equilibrium model for this multicomponent distillation

process. The pseudo components used to imitate the unknown by-products in the simulation modeling were created by applying the pseudocomponent method. The information of required entry (normal boiling point) for creating pseudo components was generated from experimentally obtained values of the relative volatility.

7.3.1 Relative Volatility Calculation and Normal Boiling Point Estimation

7.3.1.1 General Theory

The vapor-liquid equilibrium for a mixture is described by a *K*-value, where *K* for each component *i* is the ratio of mole fractions in the vapor and liquid phases at equilibrium:

$$K_i \equiv \frac{y_i}{x_i} \tag{6}$$

For the system where the liquid phase is an ideal solution that follows Raoult's law and where the gas phase follows the ideal gas laws, the *K*-value becomes

$$K_i = \frac{y_i}{x_i} = \frac{P_i^{Sat}}{P} \tag{7}$$

The *K*-values are strongly temperature dependent because of the change in vapor pressure, however, the relative values of *K* for two components change

only moderately with temperature by assuming that both P_i^{Sat} and P_j^{Sat} are identical functions of temperature. The ratio of *K*-values is the same as the relative volatility of the components:

$$\alpha_{ij} = \frac{K_i}{K_j} = \frac{\frac{P_i^{Sat}}{P}}{\frac{P_j^{Sat}}{P}} = \frac{P_i^{Sat}}{P_j^{Sat}} \tag{8}$$

Since relative volatility is generally a much less strong function of temperature than the component vapor pressures; in many systems, it is acceptable to assume that the relative volatility is constant over a range of temperatures and compositions.

In a two component mixture, relative volatility becomes:

$$\alpha_{ij} = \frac{K_i}{K_j} = \frac{y_i / x_i}{y_j / x_j} \tag{9}$$

where $y_j = (1 - y_i)$, and $x_j = (1 - x_i)$. Hence, it is possible to calculate relative volatility by generating X-Y diagram and assuming that the relative volatility is a constant independent of temperature.

7.3.1.2 Relative Volatility Calculation

For vapor-liquid separation operations, relative volatility is an index of the

relative separability of two chemical species. The number of theoretical stages required to separate two components to a desired degree is strongly depend on the value of this index—the greater the departure of the relative volatility from a value of one, the fewer the equilibrium stages required for a desired separation. In other words, the relative volatility of a key component in the distillate product to that of a key component in the bottom product can be used to estimate the minimum number of equilibrium stages for a multicomponent distillation. Fenske equation (Equation 1) applies to any two components, *i* and *j*, in a conventional distillation at total reflux by assuming relative volatility is constant. The equation has the form:

$$N_{\min} = \frac{\ln\left[\left(\frac{x_{i,D}}{x_{i,B}}\right)\left(\frac{x_{j,B}}{x_{j,D}}\right)\right]}{\ln\alpha_{ij}} \qquad (10)$$

Fenske equation is not restricted to the two key components. Once N_{min} is obtained from two key components, it can be used to calculate relativity volatility (α_{ij}) for all unknown nonkey components. In this work, the relativity volatility data were calculated from experimental separation data— $x_{i,D}$ (the peak area ratio of the gas chromatogram of species *i* in the distillate) and $x_{i,B}$ (the peak area ratio of the gas chromatogram of species *i* in the bottom). *j* is the reference component, in this case, *j* is propylene glycol. The average experimental separation data and calculated results are shown in Figure 7.2.

Table 7.2. Experimental separation data and calculated relative volatility values

	Distillate ($x_{i,D}$)[b]	Bottom ($x_{i,B}$)[b]	Calculated (α_{ij})
Two key			
Acetol (*i*)	0.2833	0.0362	
Propylene glycol (*j*)	0.6575	0.9298	
α_{ij} [c]= 4.56			
N_{min}= 1.88			
Unknown[a] nonkey			
8.75	0.0098	0.0004	6.06
8.78	0.0106	0.0006	5.72
9.11 Ethylene glycol (EG)	0.0072	0.0159	0.79
9.15	0.0190	0.0046	2.70
9.28	0.0088	0.0015	3.35
9.32	0.0021	0.0059	0.66
9.405	0.0017	0.0051	0.63

[a] Unknowns (unidentified compounds) are named as the retention time shown in the gas chromatogram

[b] The peak area ratio of the gas chromatogram of species *i* in the distillate and bottom

[c] α_{ij} is generated from X-Y diagram by using ChemCAD

7.3.1.3 Approximate Normal Boiling Point Estimation

If the relative volatility between two components is very close to one, it is an indication that they have very similar vapor pressure characteristics. It means that they have very similar normal boiling points and therefore, it would be difficult to separate the two components. The relative volatility is closely related to the normal boiling points of components. Basically, the experimentally determined boiling points and equilibrium data are necessary to develop the relation between the boiling points and the relative volatilities of the components of the system. However, analytic expressions can be obtained if an additional idealizing assumption is made. The following equations were suggested by Bowman (1951)[54]. Base on the previous assumption of constant relative volatility, it gives:

$$P(\alpha,T) = \alpha P_0(T) \tag{11}$$

In this case, let the vapor pressure-temperature function for the key component is assumed to be:

$$\ln P_0 = \frac{A}{T} + B \tag{12}$$

Therefore

$$P(\alpha,T) = \alpha e^{\frac{A}{T}+B} \tag{13}$$

This is the general vapor pressure-temperature function for the components of this ideal system. Setting the pressure equal to the total pressure yields the general relation between the boiling temperature and the relative volatility.

$$\ln \frac{P}{\alpha} = \frac{A}{T} + B \qquad (14)$$

A and *B* are experimental parameters which are determined by plotting the data. In this study, the relative volatility data and normal boiling temperatures of identified components were regressed with linear regression, and the values of *A* and *B* were obtained (Figure 7.1). Equation 14 allows normal boiling point data to be independently calculated by experimentally obtained values of the relative volatility. Table 7.3 shows the calculated normal boiling point data.

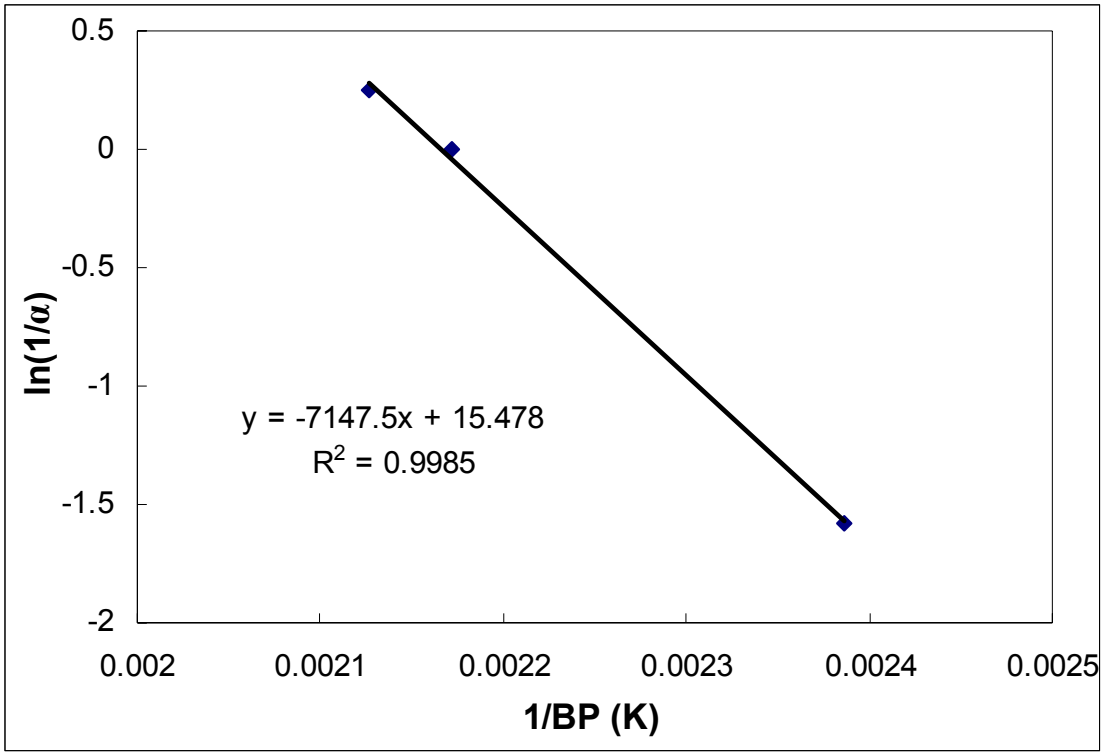

Figure 7.1. Relative volatilities and true boiling points of identified components

Table 7.3. Comparison between the true and calculated normal boiling points

	True Boiling Point (°C)	Calculated Relative Volatility (α_{ij})	Calculated Boiling Point (°C)
Hydroxyacetone (Acetol)	146.0	4.56	147.14
Propylene glycol (PG)	187.4	1	188.62
Unknown[a]			
8.78		5.72	141.60
9.11 Ethylene glycol (EG)	197.2	0.79	195.72
8.75		6.06	140.19
9.15		2.70	160.62
9.28		3.35	154.99
9.32		0.66	201.43
9.405		0.63	202.50

[a] Unknowns (unidentified compounds) are named as the retention time shown in the gas chromatogram

7.3.2 Distillation Process Modeling Using ChemCAD Simulation Program

For the process simulation and design, the chief advantage in using process simulation program is to avoid the nuisance having to perform countless series of tedious and repetitive calculations. ChemCAD is a common chemical engineering process simulation package available to universities and industries. This program enables the user to design Process Flowsheet Diagrams (PFD),

and regulates and edits virtually every aspect. It is also loaded with vast databanks containing the physical properties of thousands of chemicals, various thermodynamic and equilibrium packages for more accurate modeling that are useful for formulating control strategies.

In this work, the boiling point of each unknown by-product estimated from experimental value of the relative volatility was used to create new components in ChemCAD simulation program. The pseudocomponent method was selected for this purpose because the pseudocomponent method is a lumped component method usually applied to hydrocarbon mixtures. For the pseudocomponent method, normal boiling point is a required entry to predict some pure component properties base on API oriented methods.

In order to confirm if the pseudocomponent method is appropriate to use for creating new components in this case, X-Y equilibrium curves were generated from true components and created pseudo components by using ChemCAD. The following two X-Y diagrams (Figure 7.2 and Figure 7.3) show the comparison of true component and created pseudo component for ethylene glycol and acetol to propylene glycol mixtures. Good agreement between true and created pseudo component data was obtained.

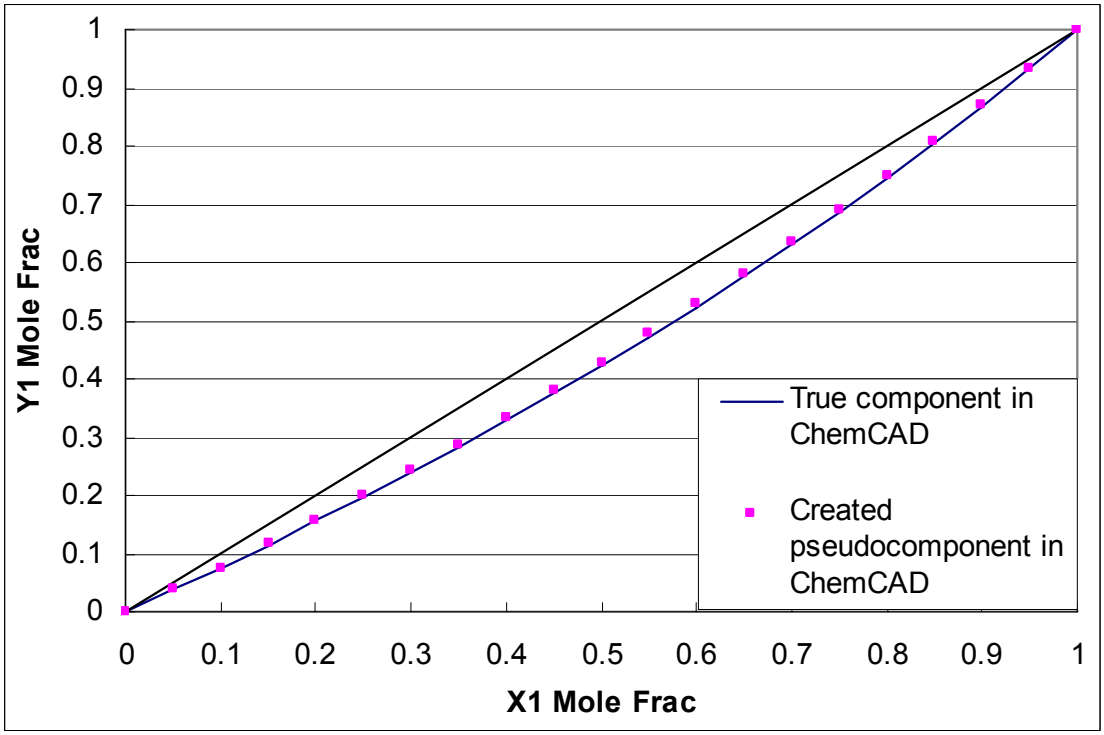

Figure 7.2. Comparison of true and created pseudo components for the ethylene glycol-propylene glycol mixture at a pressure of 135mmHg. The solid line represents the true component and point (■) represents the created component in ChemCAD

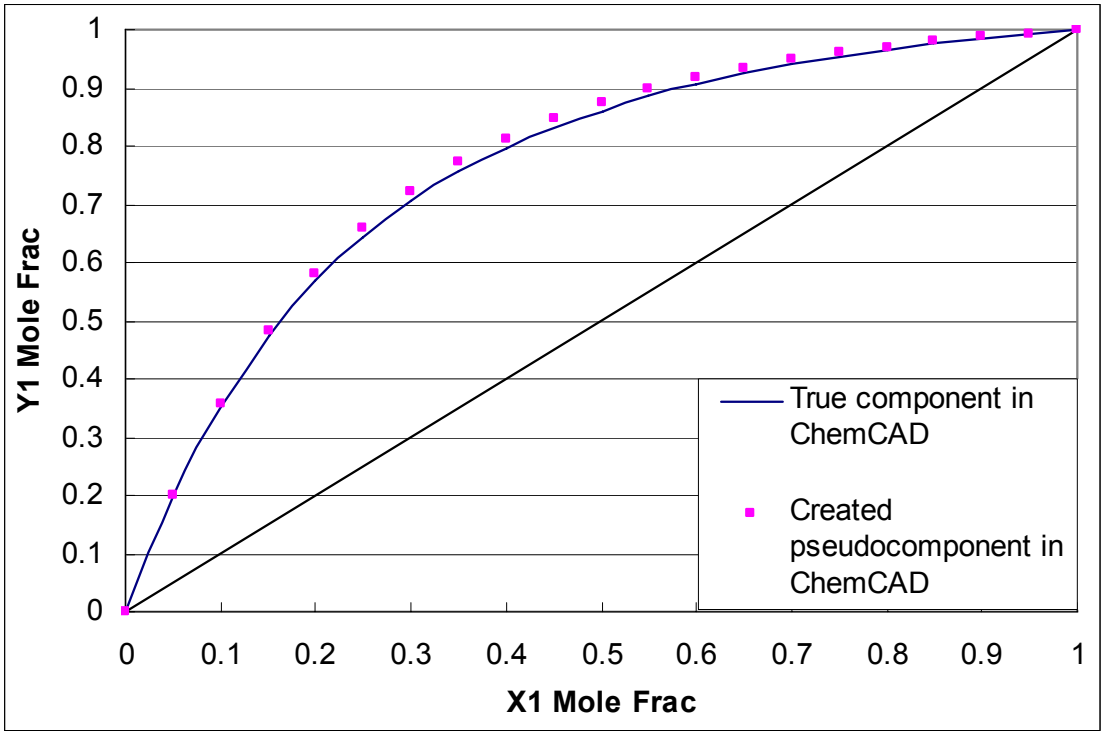

Figure 7.3. Comparison of true and created pseudo components for the acetol-propylene glycol mixture at a pressure of 135mmHg. The solid line represents the true component and point (■) represents the created component in ChemCAD

7.3.2.1 Solution Procedures for Base Case Process

A sequential procedure composed of shortcut calculations and rigorous distillation module calculations was developed for the efficient optimization of multicomponent distillation process design. In the first step, possible splits and distillation segments were generated and evaluated with the help of shortcut calculations. The results were then exported to a rigorous distillation model, where they were used for an efficient initialization and tight bounding of the

optimization variables.

7.3.2.1.1 Simple Distillation Model (FUG shortcut method)

The shortcut distillation calculations used the Fenske-Underwood-Gilliland method (FUG) to calculate a simple distillation column with one input stream and two product streams (distillate and bottom). In the FUG shortcut method, the Fenske equation was used to calculate a minimum number of stages; the Underwood equation for minimum reflux; the Gilliland correlation; and the Fenske or Kirkbride correlations for feed stage location. This shortcut method may not be suitable for column design, but the output data from shortcut method is extremely useful to set up initial values for a rigorous distillation column.

A center concept in the FUG shortcut method is that of a “key component”. Figure 7.4 shows the approximate distribution of components in this multicomponent distillation system with the selected key components. Components have been arranged in descending order of volatility. The line separating components indicates that those components appearing above the line are predominantly in the distillate product. Those components appearing below the line are predominantly in the bottom product. The light key was chosen from the components that are above the line and the heavy key was chosen from the components that are below the line. In shortcut columns, the number of stages, the reflux ratio, and the location of the feed stage were calculated to achieve splits of 0.95 and 0.05 on the propylene glycol and ethylene glycol respectively. These numbers give us some idea of what the rigorous

distillation column should look like to achieve 99.5% pure propylene glycol in the distillate product of column No. 2. It is necessary to use a rigorous distillation model in next step to confirm any shortcut results. Table 7.4 shows the calculated results of the number of stages, the reflux ratio, and the feed stage for shortcut columns.

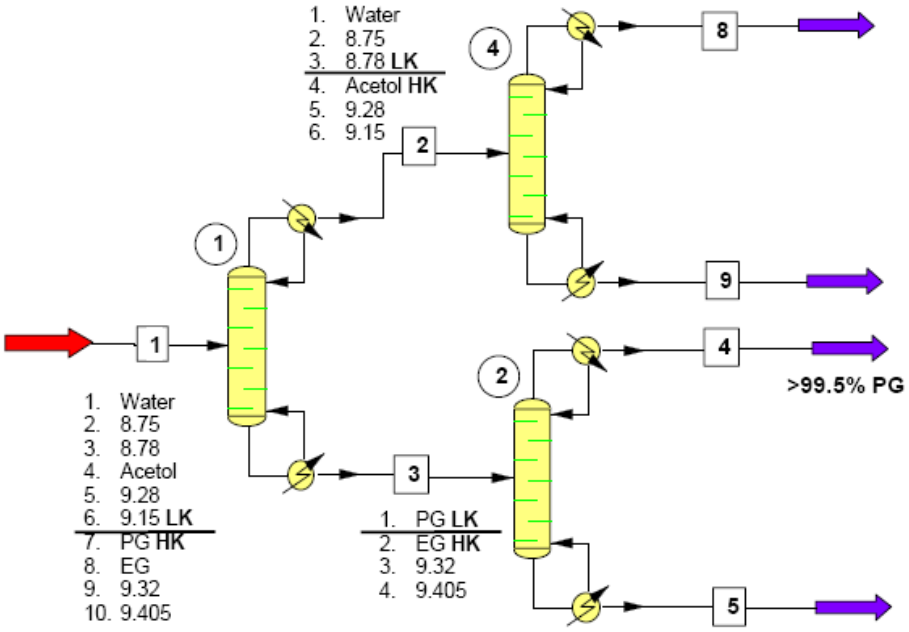

Figure 7.4. Process flow diagram of the base case process with approximate distribution of components (FUG shortcut method)

Table 7.4. The calculated results using Fenske-Underwood-Gilliland shortcut method

	Column 1	Column 2	Column 4
Minimum stages (N_{min})	7.80	18.31	8.49
Number of stages	21.66	35.01	20.41
Feed stage	6.10	18.00	6.04
Minimum reflux	0.121	2.78	0.34
Reflux ratio	0.157	3.62	0.44

7.3.2.1.2 Rigorous Equilibrium Stage-to-Stage Model (SCDS rigorous method)

Once the number of stages, the feed stage, and the reflux ratio were obtained from shortcut method, this information was used to run the rigorous distillation model for columns No. 1 to No. 4. Rigorous multicomponent calculation is difficult to converge. It requires accurate initial values, and even then, it usually takes longer time to complete.

SCDS is a rigorous multi-stage vapor-liquid equilibrium module which simulates any single column calculation. SCDS is mainly designed to simulate non-ideal K-value chemical systems. It uses a Newton-Raphson convergence method and calculates the derivatives of each equation rigorously, including the DK/DX (derivative of K-value with respect to composition) term which is significant in chemical system simulation. Side products and side heaters/coolers can also be modeled rigorously by SCDS. SCDS offers a variety

of specifications, such as total mole flow rate, heat duty, reflux ratio, temperature, mole fraction, recovery fraction, component flow rate, and flow ratio of two components in products. Figure 7.5 is the process flow diagram of the base case process with SCDS column setup. The approximate product compositions and flow rates obtained from shortcut method were compared with those obtained from rigorous distillation model in Table 7.5.

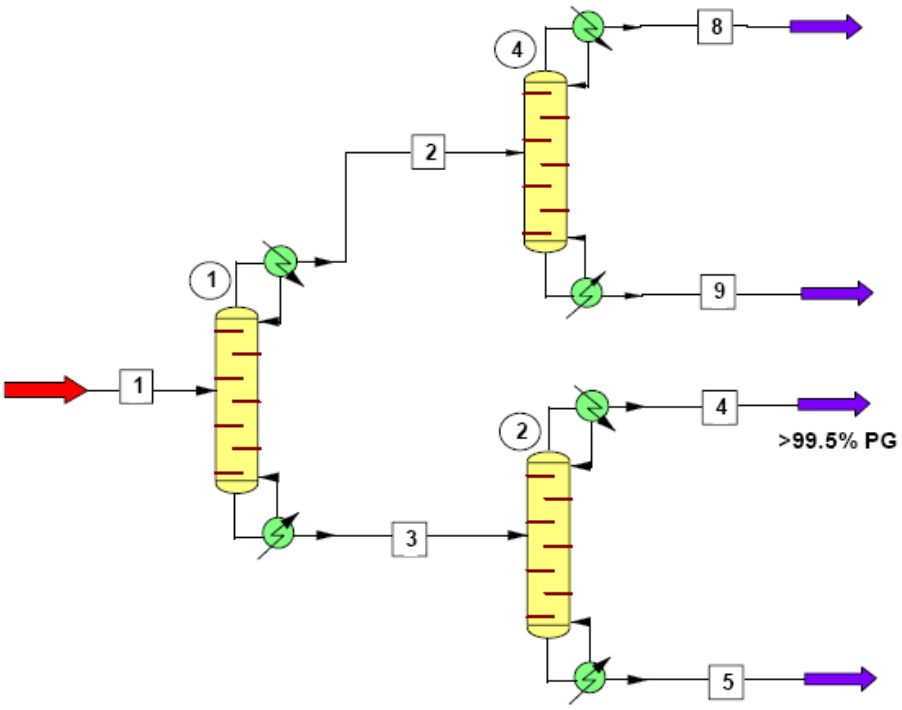

Figure 7.5. Process flow diagram of the base case process (SCDS rigorous method)

Table 7.5. Comparison between FUG shortcut and rigorous methods using ChemCAD

Column Specification		
	FUG Shortcut	**SCDS Rigorous**
Number of stages		
1	21.66	20
2	35.01	35
4	20.41	20
Performance Parameters		
	Stream 4	Stream 4
PG flowrate (kg/hr)	6324.18	6186.69
% PG recovered	91.08	89.1
purity of PG (wt. %)	99.63	99.58
Product Compositions (wt. %)		
	Stream 4	Stream 4
Unknown[a]		
8.75	0.000	0.000
8.78	0.000	0.000
9.11 Ethylene glycol (EG)	0.188	0.224
9.15	0.018	0.046
9.28	0.008	0.020
9.32	0.082	0.082
9.405	0.045	0.048
Water	0.000	0.000
Hydroxyacetone (Acetol)	0.029	0.001
Propylene glycol (PG)	99.631	99.578

[a] Unknowns (unidentified compounds) are named as the retention time shown in the gas chromatogram

7.3.2.1.3 Distillation process with propylene glycol recycle stream

In order to meet the following specifications in the final design, the process has been optimized and improved by setting up an additional distillation column with a propylene glycol recycle stream.

Product purity (weight basis):

- ＞99.5% propylene glycol in the distillate product (stream No. 4) of column No. 2

Recovery (weight basis):

- ＞98% overall recovery of propylene glycol in the distillate product stream (stream No. 4) of column No. 2

Both the purity of product and propylene glycol recovery were improved base on this design. Figure 7.6 and Figure 7.7 show the process flow diagrams of FUG shortcut method and SCDS rigorous model for this improved design process, respectively. The acetol will be recycled to the hydrogenolysis reactors for reuse. At the present time, acetol recycle stream is left in the state it is as it exits the column.

In order to confirm if propylene glycol in the stream No. 6 can have good separation when it is recycled to the column No. 2, the column No. 5 in the FUG shortcut process (Figure 7.6) was setup to simulate the propylene glycol recycle

stream No. 6 in the SCDS rigorous process (Figure 7.7). The calculated result of the number of stages of column No. 5 is in agreement with the results in column No. 2 in the FUG shortcut process. The product components results from FUG shortcut method was further confirmed with SCDS rigorous model. The comparison of results from FUG shortcut method and from SCDS rigorous model is shown in Table 7.6.

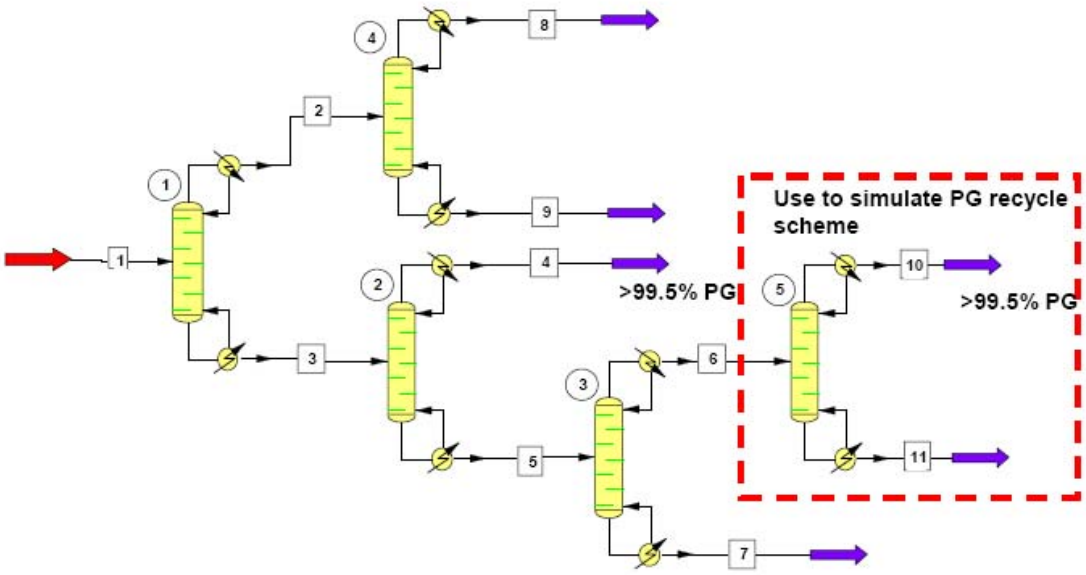

Figure 7.6. Process flow diagram of the base case process with propylene glycol recycle (FUG shortcut method)

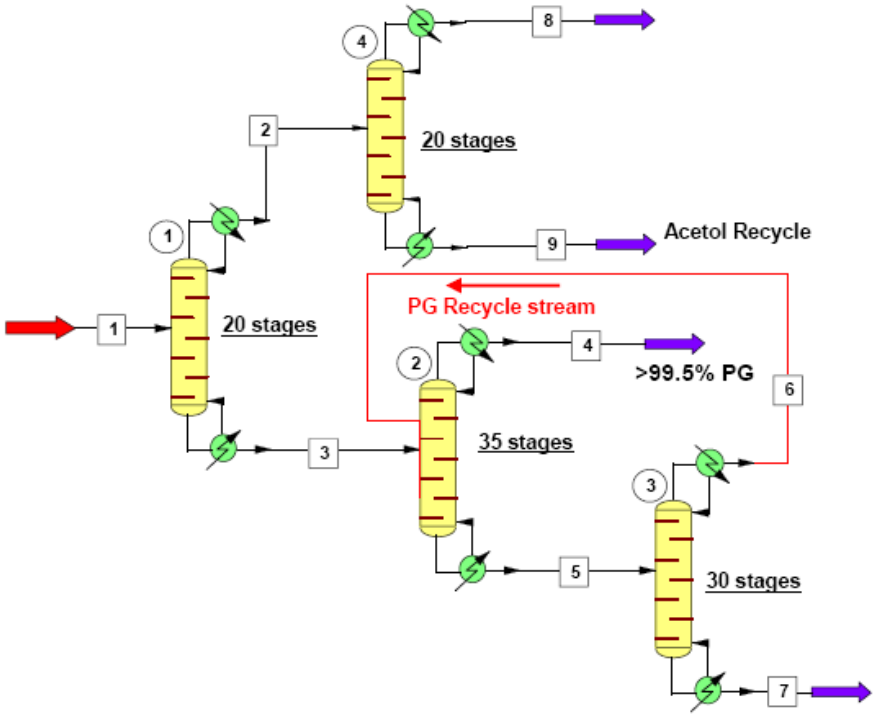

Figure 7.7. Process flow diagram of the base case process with propylene glycol recycle (SCDS rigorous method)

Table 7.6. Comparison between FUG shortcut and rigorous methods on the improved process using ChemCAD

Column Specification			
	FUG Shortcut		**SCDS Rigorous**
Number of stages			
1	21.66		20
2	35.01		35
3	30.93		30
4	20.41		20
5	34.96		
Performance Parameters			
	Stream 4	Stream 10	Stream 4
PG flowrate (kg/hr)	6324.17	455.34	6836.13
purity of PG (wt. %)	99.63	99.61	99.58
Product Compositions (wt. %)			
	Stream 4	Stream 10	Stream 4
Unknown[a]			
8.75	0.000	0.000	0.000
8.78	0.000	0.000	0.000
9.11 Ethylene glycol (EG)	0.188	0.239	0.229
9.15	0.018	0.000	0.042
9.28	0.008	0.000	0.018
9.32	0.082	0.111	0.082
9.405	0.045	0.043	0.047
Water	0.000	0.000	0.000
Hydroxyacetone (Acetol)	0.029	0.000	0.001
Propylene glycol (PG)	99.631	99.607	99.581

[a] Unknowns (unidentified compounds) are named as the retention time shown in the gas chromatogram

7.4 Conclusions

In this work, the solution method is divided into two sections. In the first section, the relative volatilities of seven unknown by-products were calculated from experimental separation data. The normal boiling temperatures of identified components were observed to be in good agreement with the values estimated by Equation 14 and experimentally obtained values of the relative volatility. The estimated approximate boiling points of unknowns were used to create new pseudo components in ChemCAD process simulation program using the pseudocomponent method.

In the second section, ChemCAD process simulation program was used to model the distillation process. There are four separation segments in the preliminary design. (Figure 7.8). The objectives are to produce propylene glycol at over 99.5% purity with at least 98% recovery based on an annual production of 100 million pounds of propylene glycol. The purpose of the first separation step is to remove the relative more volatile components. The purpose of second separation step is to remove the most close boiling point component, ethylene glycol. In the preliminary design, the first step columns for light components removal have 20 stages, the second step ethylene glycol removal columns have 40 stages. At the end of the second separation step, the purity of propylene glycol in the step is reached up to 99.5 %; this can be drained off as the final propylene glycol product. In the actual operation, the second ethylene glycol removal (column No. 3) is used to improve the product recovery and also function as adding flexibility on the present separation process, when the

propylene glycol production excesses 100 million pounds per year. In other words, the propylene glycol recycle scheme provides a design flexibility of the present process.

The example problems were used for process model testing and validation. The design processes were rigorously simulated using ChemCAD, and the results of FUG shortcut method were compared to these results. Agreement between the shortcut method and rigorous model was excellent.

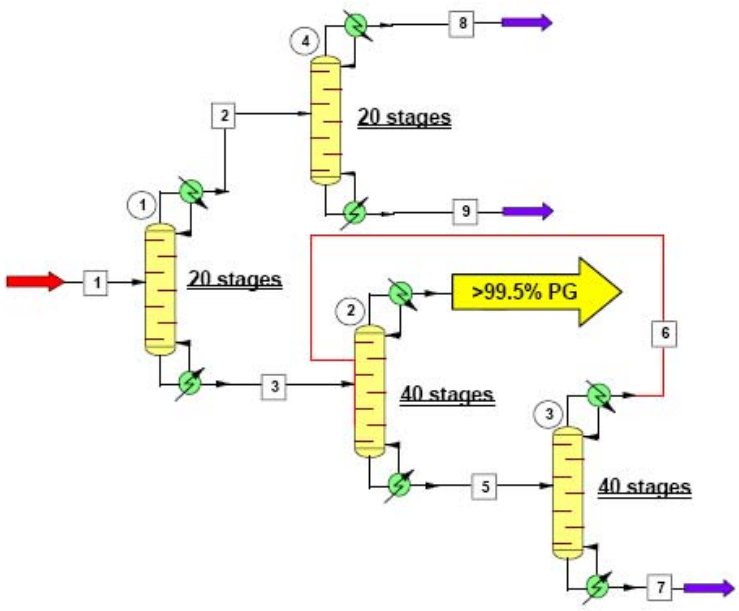

Figure 7.8. Process flow diagram of preliminary design

CHAPTER 8

8. KINETIC AND EQUILIBRIUM STUDIES OF CONVERSION OF GLYCEROL TO PROPYLENE GLYCOL IN A PACKED BED REACTOR

8.1 Kinetic Studies of Converting Glycerol to Propylene Glycol

The glycerol hydrogenolysis over a copper-chromite catalyst was studied using a vapor-phase packed bed catalytic reactor. Pre-reduced copper-chromite catalyst purchased from Engelhard Corporation (Elyria, Ohio) was packed in the catalytic reaction zone. The reactor has an outside diameter of 0.75 inches equipped with thermocouples. The details of experimental setup are thoroughly described in the section of experimental setup in chapter 4 and 6. The reaction was studied at a temperature of 220, 230, and 240°C and 1 bar of total pressure. The mass of catalyst loading was varied between 25 and 750g. All reactions were performed in the vapor-phase packed bed reactor with glycerol feed rate of 100 g/h and hydrogen flow rate of 5 l/min. The objective of this work was to study the kinetics of converting glycerol to propylene glycol, and it is important when doing process design, control and optimization.

8.1.1 Initial Reaction Rate

The initial reaction rate was observed by reacting glycerol and hydrogen to vary amounts of catalyst at a constant glycerol feed rate of 100 g/h and hydrogen

flow rate of 5 l/min. The dependence of the glycerol conversion upon *W/F* at 220, 230, and 240°C is given in Figure 8.1, 8.2, and 8.3, respectively.

For a packed bed reactor, the differential form of the design equation for a heterogeneous reaction is[55]:

$$F_{A0}\frac{dX}{dW} = -r_A \tag{1}$$

where *W* is the weight of the catalyst (g), *F* is the glycerol feed flow rate (mol/h), *X* is the fractional conversion (%). A reaction is of zero-order when the rate of reaction is independent of the concentration of reactants; thus

$$-r_A = -\frac{dC_A}{dt} = k_0 \tag{2}$$

Combine equation 1 and 2, we have:

$$\frac{dX}{d\left(\frac{W}{F}\right)} = k_0 \tag{3}$$

$$X = k_0\frac{W}{F} \tag{4}$$

k_0 is the zero-order rate constant (mol/h · g of catalyst). From equation 4, note that a plot of *W/F* versus *X* will yield a straight line, with the slope of the line

equal to k_0. This is consistent with the data reported in Figure 8.1, 8.2, and 8.3, indicating that the reaction is zero-order with respect to glycerol conversion over the range of conditions studied.

There are a number of mechanisms which may be proposed that will explain the observed zero-order kinetics. One possible explanation is that the vaporous glycerol is uniformly and rapidly adsorbed on the catalytic surface during the dehydration reaction. Based on this assumption, the reaction would be limited by the rate at which active sites become available. The availability of active sites would then be determined by the rate at which the glycerol can be dehydrated in the first step reaction or the rate at which the intermediate product acetol and the second-step hydrogenation product propylene glycol are desorbed.

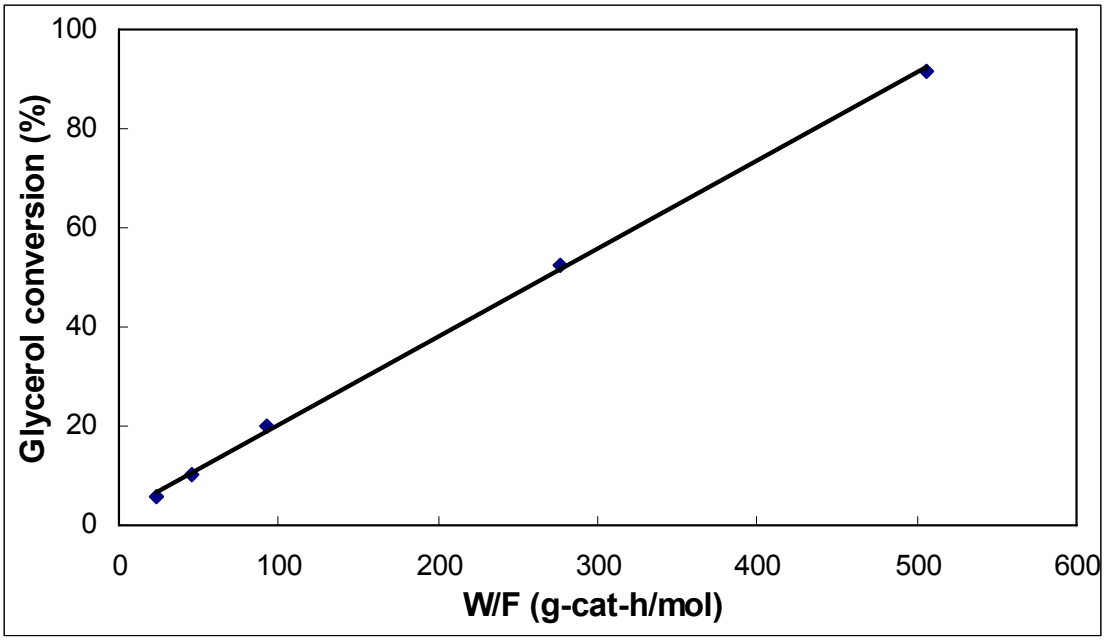

Figure 8.1. Effect of *W/F* on glycerol conversion at 220°C and 1 bar.

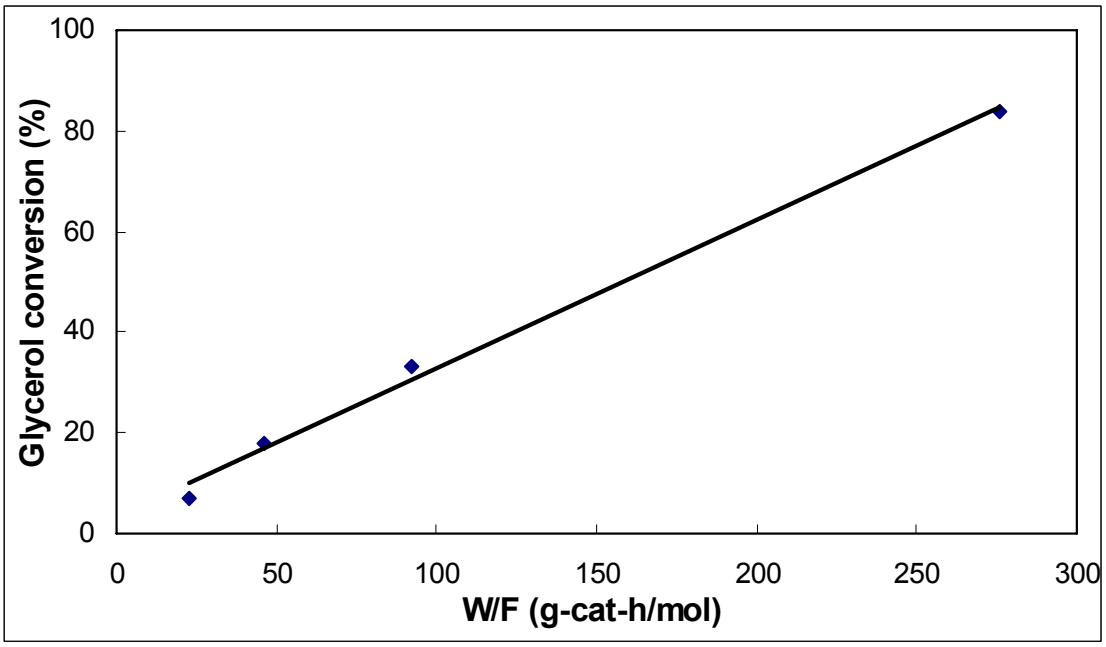

Figure 8.2. Effect of *W/F* on glycerol conversion at 230°C and 1 bar.

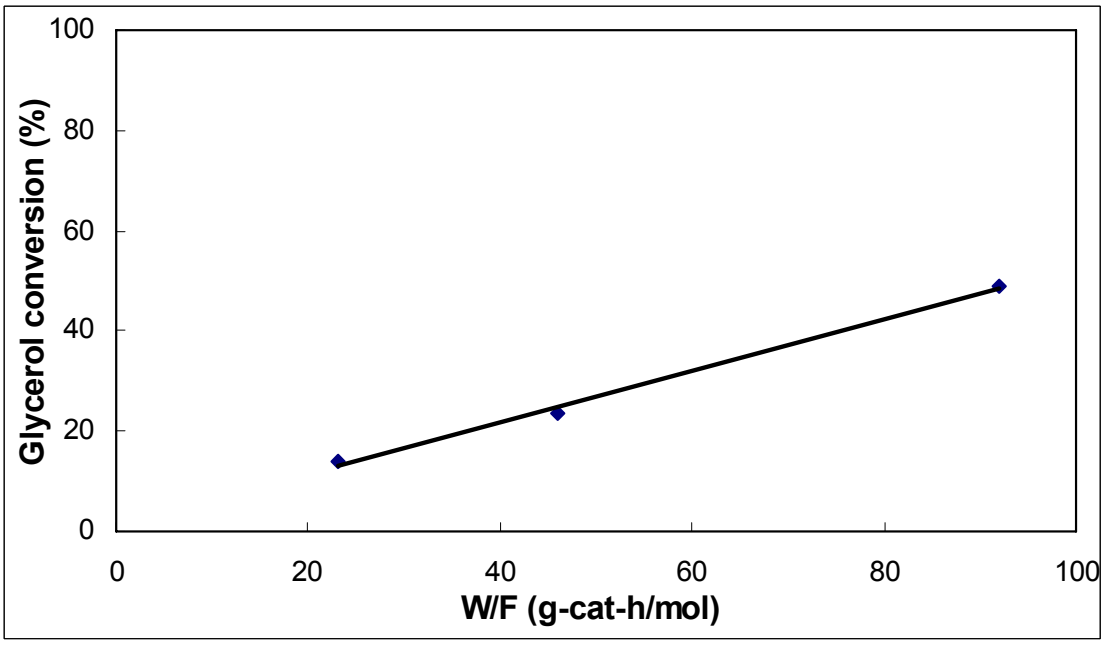

Figure 8.3. Effect of *W/F* on glycerol conversion at 240°C and 1 bar.

8.1.2 Effect of Reaction Temperature on Rate Constant

Table 8.1 shows the effect of reaction temperature on the zero-order rate constant. The reaction temperature has a strong effect on initial rate of reaction and the glycerol conversion was found to increase with increase in reaction temperature. The temperature dependence of the zero-order rate constant is illustrated in Figure 8.4. After taking the natural logarithm, the Arrhenius equation becomes:

$$\ln k_0 = \ln A - \frac{E}{R}\left(\frac{1}{T}\right) \tag{5}$$

where *A*= preexponential factor or frequency factor

E= activation energy

R= gas constant

T=absolute temperature, K

The rate constant, k_0, could be represented by an Arrhenius equation and was calculated to be 5.2E+10 exp(-25348.2/RT) mol/(h · g of catalyst). The units of activation energy are calories/mole, and *T* is in Kelvin. The activation energy deduced from the slop of the curve is 25.35 kcal/mol.

Table 8.1. Effect of reaction temperature on the zero-order rate constant.

Temperature (°C)	k_0 (mol/h · g of catalyst)
220	0.19
230	0.36
240	0.53

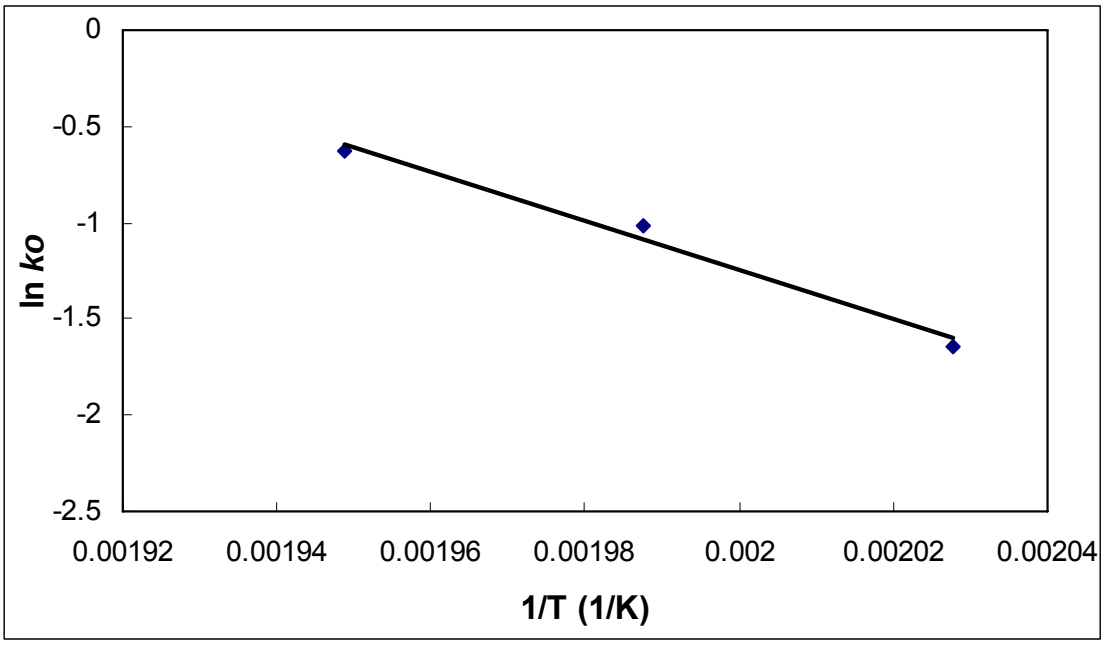

Figure 8.4. Arrhenius plot of the zero-order rate constant.

8.1.3 Conversion Profiles

Preliminary reaction kinetic studies of conversion of glycerol to propylene glycol were conducted at 220°C and 1 bar total pressure. Figure 8.5 shows the reaction profile of the reaction system at these conditions. The reaction was

found to be zero-order in glycerol conversion.

The acetol intermediate was generated during the reaction which further converts to propylene glycol. Acetol and propylene glycol were constantly produced as the reaction proceeding until it reaches equilibrium. Figure 8.6 shows the plot of glycerol conversion versus product distribution (PG to acetol mole ratio) at 220°C and 1 bar. As summarized by the reaction profiles of Figures 8.5 and Figure 8.6, the rate of second step reaction (hydrogenation of acetol) is much faster than the first step (dehydration of glycerol). In other words, for the overall reaction of converting glycerol to propylene glycol, the first step reaction is rate limited and second step reaction is equilibrium limited.

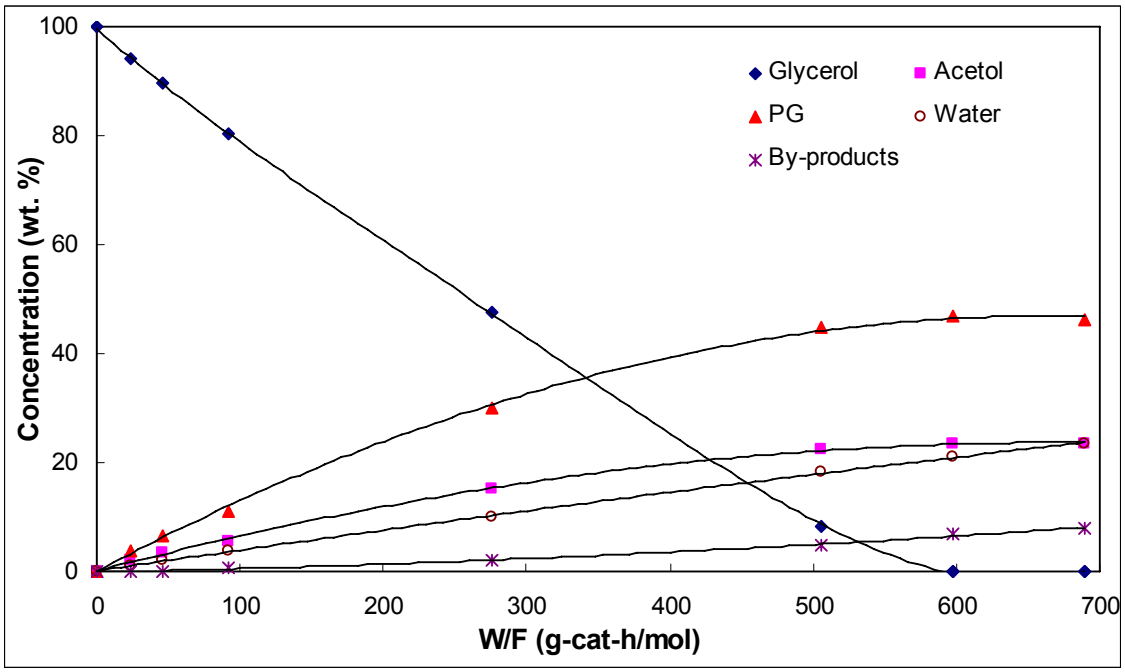

Figure 8.5. Reaction Profile for the conversion of glycerol to propylene glycol at 220°C and 1 bar.

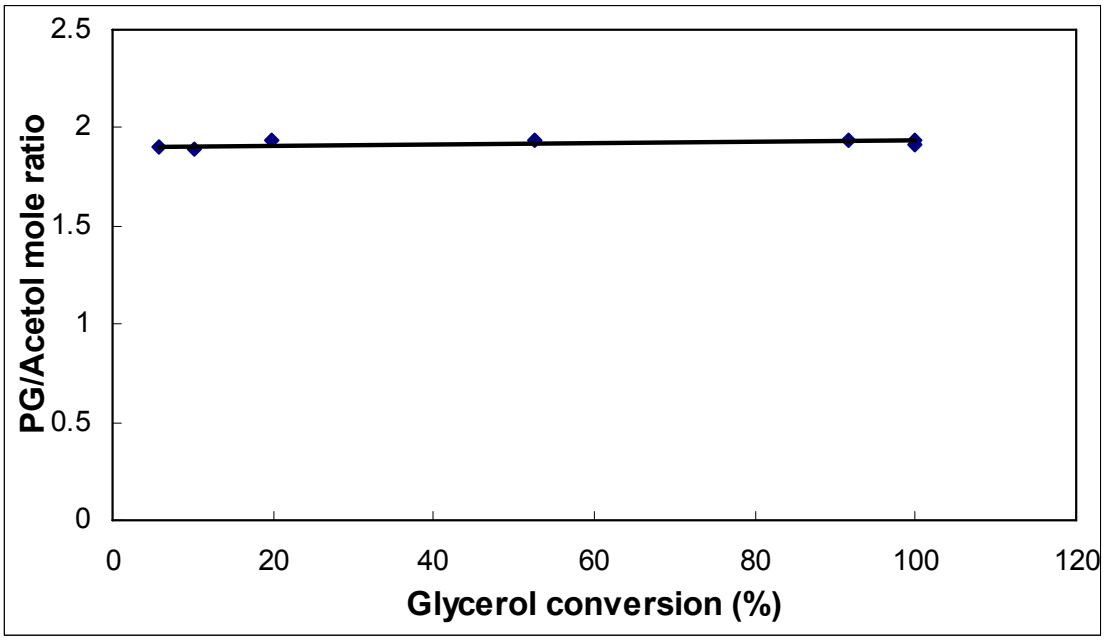

Figure 8.6. Glycerol conversion versus product distribution (PG to acetol mole ratio) at 220°C and 1 bar.

8.2 Equilibrium Studies of Converting Acetol to Propylene Glycol

Since the second step of the reaction (acetol to propylene glycol) is a reversible reaction and it is expected to be equilibrium limited, substantial amount of intermediate product (acetol) is still present when the reaction achieves equilibrium. The focus of this study is to understand, describe, and predict the reaction equilibrium of the reaction of acetol to propylene glycol. The reactions were performed at a reaction temperature from 180 to 240°C and low pressures of 1, 2, and 4 bar in a vapor-phase packed bed flow reactor.

8.2.1 Equilibrium Constant

The first step in the thermodynamic study of a chemical reaction is the determination of the equilibrium constant. The equilibrium constant is a number characteristic of a given reaction at a given temperature. For the generalized single gas-phase reaction,

$$aA + bB + ... = cC + dD + ...$$

By applying the general Mass-Action equations to homogeneous equilibrium, the equilibrium constant is represented by the equation:

$$K_{eq} = \frac{a_C^c a_D^d .....}{a_A^a a_B^b .....} = K_a \qquad (6)$$

where *a* is activity. For the case of homogeneous gaseous reactions when the standard state of each gas is one of unit fugacity, then the equation becomes:

$$K_f = \frac{\overline{f}_C^{\,c} \overline{f}_D^{\,d} .....}{\overline{f}_A^{\,a} \overline{f}_B^{\,b} .....} \qquad (7)$$

where $\overline{f}_A$, $\overline{f}_B$, etc., are the partial fugacities (or the activities, since fugacity and activity are generally made identical for a gas) of the various components in the gaseous solution represented by the equilibrium mixture. For the case of

reaction in ideal gaseous solution,

$$K_f = \frac{(y_C f_C)^c (y_D f_D)^d .....}{(y_A f_A)^a (y_B f_B)^b .....} \qquad (8)$$

where y_i is the mole fraction of component i in the mixture. By definition we also have:

$$f_i = \gamma_i P y_i \qquad (9)$$

where *P* is the total pressure. At moderate pressures, the fugacity of a gas is approximately equal to its partial pressure in atmospheres (at low pressures where all actual gases may be assumed ideal). Thus, the equilibrium constant can be written as

$$K_f = K_\gamma K_y P^{\sum_i \nu_i} \cong K_p \qquad (10)$$

K_γ is independent of the composition of the equilibrium mixture but is s function of P and T. K_γ is useful in giving a quick picture of the extent of the deviation from the simple ideal-gas case for which K_γ would have the value 1.0 at temperatures and pressures.

Of the possible methods of determining the equilibrium constant of a

reaction, the two most applicable to industrially important reactions are (1). direct experimental determination and (2). calculation by thermodynamics, where the third law of thermodynamics and the methods of statistical mechanics are utilized particularly. ΔG°_{rxn} is the Gibbs free energy change on reaction with each species in its standard state or state of unit activity, then the equilibrium condition is expressed by

$$\Delta G^{\circ}_{rxn}(T) = -RT \ln K_f \tag{11}$$

If the standard state of each component is chosen to be T= 25°C, P= 1 atm, and the state of aggregation listed in the literature, then the following equation applies:

$$\Delta G^{\circ}_{rxn}(T = 25^{\circ}C) = \sum_i \nu_i \Delta \underline{G}^{\circ}_{f,i}(T = 25^{\circ}C) \tag{12}$$

where $\Delta \underline{G}^{\circ}_{f}$ is the Gibbs free energy of formation.

8.2.2 Effect of Temperature on Equilibrium

To compute the equilibrium constant K_f at any temperature T, given the Gibbs free energies of formation at 25°C, the Van't Hoff equation is applied as follow:

$$\left(\frac{\partial \ln K_f}{\partial T}\right)_p = -\frac{1}{R}\frac{\partial}{\partial T}\left[\frac{\sum_i \nu_i \Delta \underline{G}^\circ_{f,i}}{T}\right] = \frac{1}{RT^2}\sum_i \nu_i \Delta \underline{H}^\circ_{f,i} = \frac{\Delta H^\circ_{rxn}(T)}{RT^2} \tag{13}$$

Here $\Delta H^\circ_{rxn} = \sum_i \nu_i \Delta \underline{H}^\circ_{f,i}$ is the heat of reaction in the standard state, that is, the heat of reaction if the reaction took place with each species in its standard state at the reaction temperature. If a reaction is exothermic, that is, if energy is released from reaction so that ΔH°_{rxn} is negative, the equilibrium constant and the equilibrium conversion from reactants to products decrease with increasing temperature. If energy is absorbed as the reaction proceeds, so that ΔH°_{rxn} is positive, the reaction is said to be endothermic, and both the equilibrium constant and equilibrium extent of reaction increase with increasing temperature. Equation (13) can be integrated between any two temperatures T_1 and T_2 to give,

$$\ln \frac{K_f(T_2)}{K_f(T_1)} = \int_{T_1}^{T_2} \frac{\Delta H^\circ_{rxn}(T)}{RT^2} dT \tag{14}$$

so that if K_f is known at one temperature, usually 25°C, its value at any other temperature can be computed if the standard state heat of reaction is known as a function of temperature.

If ΔH°_{rxn} is temperature independent that ΔH°_{rxn} may be assumed to be constant over the temperature range:

$$\ln \frac{K_f(T_2)}{K_f(T_1)} = -\frac{\Delta H^\circ_{rxn}}{R}\left(\frac{1}{T_2} - \frac{1}{T_1}\right) \qquad (15)$$

The assumption of constant ΔH°_{rxn} is equivalent to assuming that the total heat capacity of the products of the reaction equals that of the initial reactants. Equation (15) suggests that the logarithm of the equilibrium constant should be a linear function of the reciprocal of the absolute temperature if the heat of reaction is independent of temperature and, presumably, an almost linear function of 1/T even if ΔH°_{rxn} is a function of temperature (This behavior is compared with that of the vapor pressure of a pure substance referred to as the Clausius-Clapeyron equation). It is common practice to plot the logarithm of the equilibrium constant versus the reciprocal of temperature.

since $K_a \cong K_p$

$$\ln K_p = \frac{A}{T} + B \qquad (16)$$

Where *A* and *B* are arbitrary constant. This simple equation seems to be surprisingly accurate for correlating and extrapolating experimental data on equilibrium constants. Figure 8.7 gives the equilibrium constants for a number of reactions as a function of temperature plotted in this way.

The equilibrium constant for the reaction of converting acetol to propylene glycol as a function of temperature is shown in Figure 8.8. Figure 8.8 gives the validity of equation 16 in describing the temperature dependence of the equilibrium constant, it also shows that an exothermic reaction with ΔH°_{rxn} has a positive slope in the graph of lnK_p versus 1/T , and thus the equilibrium constant decreases with increasing temperature.

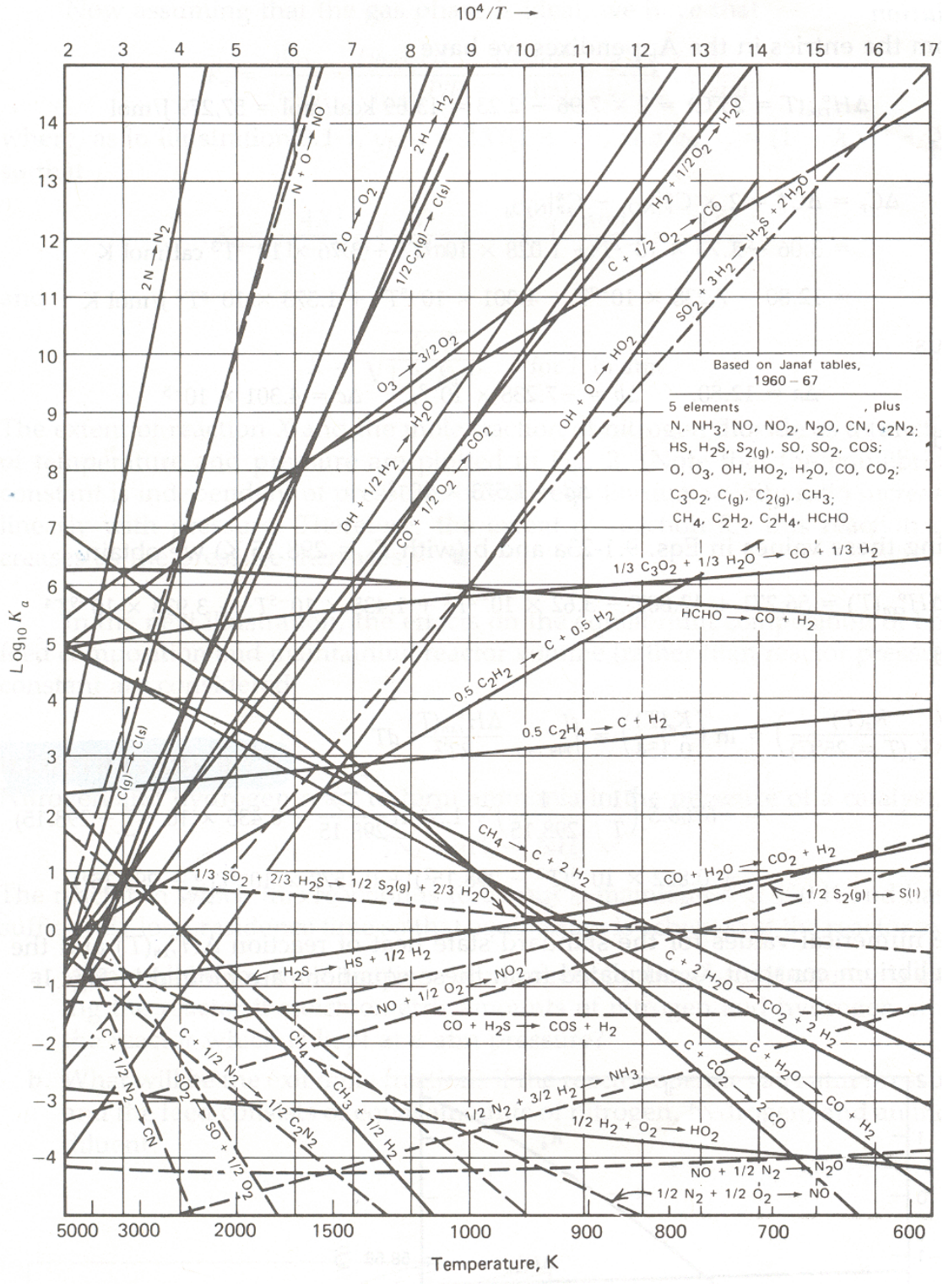

Figure 8.7. Chemical equilibrium constants as a function of temperature[56].

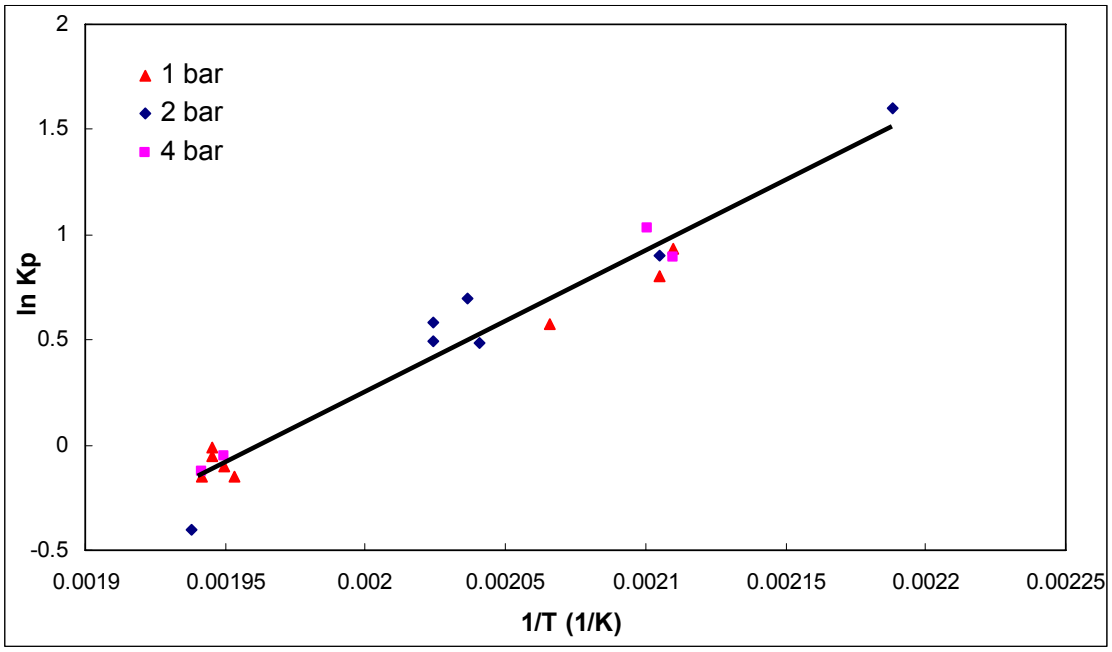

Figure 8.8. Chemical equilibrium constant as a function of temperature for the equilibrium reaction of converting acetol to propylene glycol.

8.2.3 Effect of Pressure on Equilibrium

From the general principles of equilibrium it can be deduced that increase in pressure will shift the equilibrium in the direction in which the volume of the system decreases. Reactions occurring with a decrease in volume are therefore favored by an increase in pressure. This is the basic principle behind the modern developments in high-pressure synthesis. It is important to distinguish the quantitative effect of pressure into (1). the effect of pressure on the equilibrium, and (2). the effect of pressure on the equilibrium constant.

As shown in equation (11), the equilibrium constant K_a and K_f is directly related to the change in standard state Gibbs free energy. Since ΔG°_{rxn} is a

function only of the choice of standard states for the products and reactants, it is not a function of the pressure of the system. At low pressures where gases approach to ideal state, K_p will be substantially constant and equal to K_f and K_a, so the equilibrium constant K_p can be written as:

$$K_a = K_f \cong K_p = \frac{(y_C P)^c (y_D P)^d .....}{(y_A P)^a (y_B P)^b .....} = K_\gamma K_y P^{\sum_i \nu_i} \qquad (17)$$

$K_\gamma = 1$ for ideal gas

In this study (the preferred operating pressure is less than 10 bar), it is assumed that the equilibrium reaction of acetol to propylene glycol follows that the standard state conditions are not related to the system pressure, the equilibrium constant, K_p, is independent of the pressure of the system (as see in Figure 8.8).

8.2.4 Changes in Equilibrium and Le Châtelier's Principle

Le Châtelier's principle "When a reaction at equilibrium is stressed by a change in conditions, the equilibrium will be reestablished in such a way as to counter the stress." This statement is best understood by reflection on the types of "stresses". When a reactant is added to a system at equilibrium, the reaction responds by consuming some of that added reactant as it establishes a new equilibrium. This offsets some of the stress of the increase in reactant.

Le Châtelier's principle is a useful mnemonic for predicting how we might

increase or decrease the amount of product at equilibrium by changing the conditions of the reaction. From this principle, we can predict whether the reaction should occur at high temperature or low temperature, and whether it should occur at high pressure or low pressure.

If equation (17) is applied to the reaction of converting acetol to propylene glycol, we have

$$K_{eq} = \frac{y_{PG}}{y_{Acetol} y_{H_2}} \times \frac{\gamma_{PG}}{\gamma_{Acetol} \gamma_{H_2}} \times P^{-1} = K_y K_\gamma P^{-1} \tag{18}$$

If this combined with the third law of thermodynamics and solved for y_{PG} , we have

$$y_{PG} = \frac{P}{K_\gamma} y_{Acetol} y_{H_2} e^{-\Delta H^O / RT} e^{\Delta S^O / R} \tag{19}$$

Equation 19 is a complete quantitative statement of Le Châtelier's principle for the equilibrium reaction of acetol to propylene glycol. It is clear that y_{PG}, the amount of propylene glycol present at equilibrium , increases with pressure, decreases with temperature since ΔH° is negative (exothermic reaction); all these points are in agreement with the simple Le Châtelier's principle. Figure 8.9 exhibits the dependence of K_y on pressure for the reaction of converting acetol to propylene glycol. Figure 8.10 exhibits the dependence of K_p on temperature for

the reaction of converting acetol to propylene glycol.

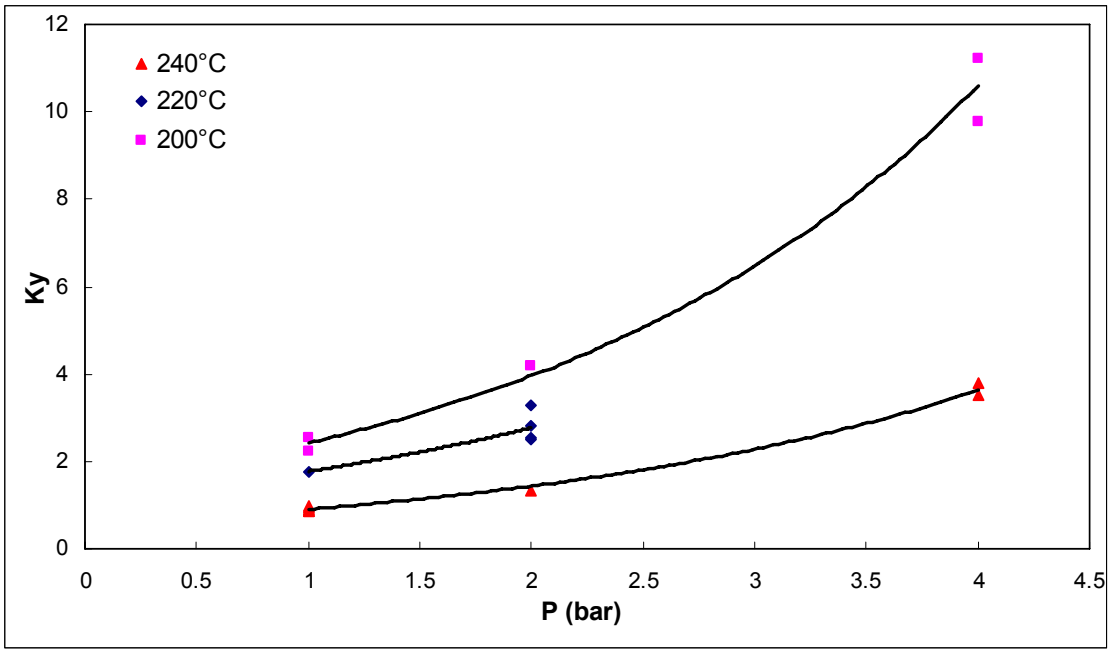

Figure 8.9. Dependence of K_y on pressure for the equilibrium reaction of converting acetol to propylene glycol.

$$K_y = \frac{Y_{PG}}{Y_{acetol} Y_{H_2}}$$

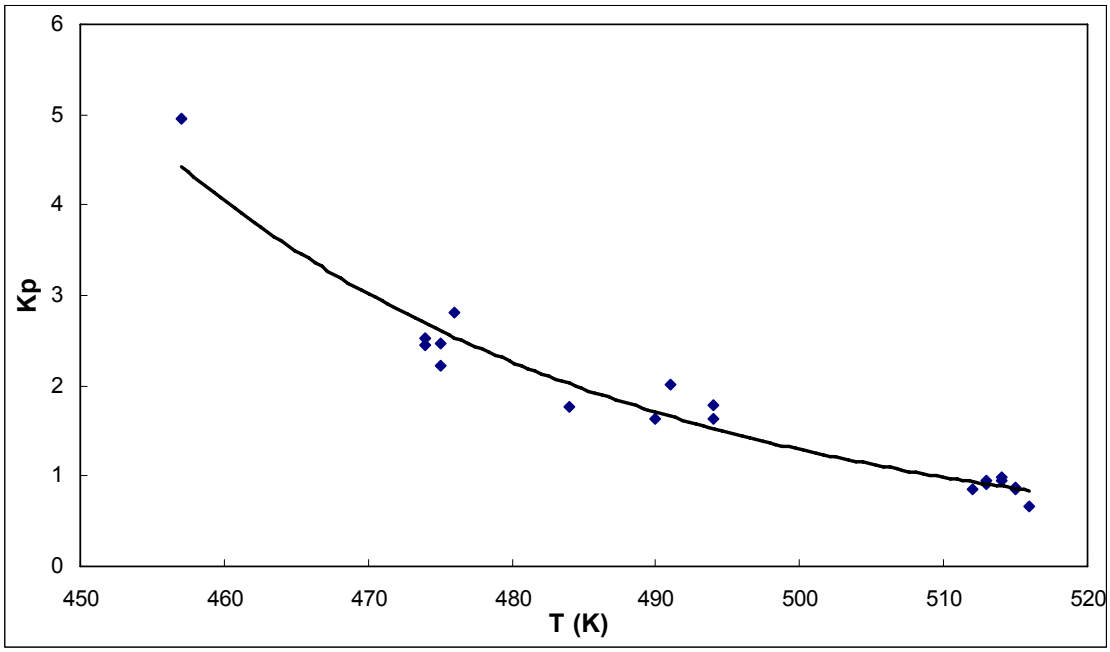

Figure 8.10. Dependence of K_p on temperature for the equilibrium reaction of converting acetol to propylene glycol.

$$K_p = \frac{Y_{PG}}{Y_{acetol} Y_{H_2}} \times \frac{1}{P}$$

CHAPTER 9

9. CONCLUSIONS AND RECOMMENDATIONS

Acetol was successfully isolated from dehydration of glycerol as the transient intermediate indicates that the reaction process for producing propylene glycerol with high selectivity can be done in two steps. Reactive distillation technology was employed to shift the equilibrium towards the right and achieve high yields. High acetol selectivity levels ($>$90%) have been achieved using copper-chromite catalyst in semi-batch reactive distillation. This catalytic process provides an alternative route for the production of propylene glycol from renewable resources.

The low-pressure vapor-phase catalytic processing using copper-chromite catalyst has been proven as feasible for producing propylene glycol from glycerol. This approach was demonstrated in a continuous process to address the concerns of scalability and suitability for large scale production. The vapor-phase reaction approach allows glycerol to be converted to propylene glycol in a single reactor. Single-pass yields in excess of 50% and with 100% conversion of glycerol have been attained. Recycle schemes can minimize any adverse impact of propylene glycol yields less than 100%. A two-step reaction process to produce propylene glycol from glycerol via an acetol intermediate was proposed and validated. A large scale process is thereby become viable.

The following conclusions can be drawn with respect to the effect of operating conditions on conversion of glycerol to propylene glycol:

- The optimal reactor temperature is between about 200 and 220°C.
- The partial pressure of glycerol should not exceed about 0.15 bar (above which the dew point is exceeded at 220°C) with an optimal total reaction pressure of 5 to 10 bar.
- To meet these pressure constraints, the glycerol should be evaporated into the hydrogen rather than boiling the glycerol under vacuum.
- To operate within these temperature and pressure constraints, undesired by-product formation will be minimal and the propylene glycol production will be maximal since the second step of reaction (acetol to propylene glycol) is equilibrium limited.
- Carbon yields of >97% to propylene glycol with a minimum yield to ethylene glycol is attainable.

The following are recommendations for process design considerations:

- The reactor should be designed for easy recovery of heat—the exothermic nature of the process allows for substantial heat integration to reduce steam costs.
- The reactor should be designed with a minimal pressure drop for the vaporous reactants—the tube-cooled packed-bed reactor design is considered crucial to the successful operation.
- A partial evaporation of glycerol followed by low-pressure flash separation is

necessary for good recovery of crude glycerol from the salts while minimizing heat input.

- Water and acetol should be recycled from a subsequent distillation process by condensing, pumping, and re-evaporating.
- Hydrogen should be first separated and recycled right after reaction vessels.
- There are four distillation processes in the preliminary separation design to produce propylene glycol product at over 99.5% purity—the first step is to remove the relative more volatile components, and the second step is to remove the most close boiling point ethylene glycol component.

The salts found in biodiesel's crude glycerol typically act as hydrogenolysis catalyst poisons, causing deactivation. The crystallization/precipitation of HAP has been demonstrated to be a cost-effective method (alternative to refining) to neutralize or remove the catalyst and/or salts from biodiesel's crude glycerol in a manner that does not lead to hydrogenolysis catalyst deactivation.

As seen by the trends of all unknown by-product formation for the reactions of glycerol to propylene glycol and acetol to propylene glycerol, the results suggest that the preferred operating conditions for converting glycerol to propylene glycol with high selectivities are lower temperatures and higher pressures. Ethylene glycol is the only by-product that follows the trend of propylene glycol production, and it is produced directly from glycerol.

The gas phase dehydration of glycerol is zero-order in glycerol

concentration over the range of conditions studied. For the overall reaction of converting glycerol to propylene glycol, the first step reaction is found to be rate limited and second step reaction is equilibrium limited. The dependence of K_y on pressure and the dependence of K_p on temperature for the reaction of converting acetol to propylene glycol are also presented.

A number of commodity chemicals can be derived from natural resources, the conversion of natural (soy-based) glycerol to propylene glycol is just an example. The fundamental understanding behind this glycerol technology paves the way for future work on exploring some more commodity chemicals that will be derived from natural resources. These can be either directly from glycerol or from some other glycerol derivatives.

One of the emphases of research is placed in advancing our understanding of reactive-separation methods toward reducing the cost of converting biomass feed stocks to chemical building blocks. This reactive-separation approach is generally applicable to a range of reactions having similar overall mechanisms where a liquid-phase reactant is converted to at least a product that has a boiling point at least 20°C lower in temperature than the reactant. Further studies are required in identifying more applications for this technology. The future work needs to be undertaken on developing materials and processing technologies to better utilize biomass as a sustainable feed stock for producing a variety of materials and chemicals.

REFERENCES

[1] Stournas, S., E. Lois, A. Serdari. Effects of Fatty Acid Derivatives on the Ignition Quality and Cold flow of Diesel Fuel. *JAOCS*, **1995**, 72(4):433-437.

[2] Suppes, G.J., Dasari, M.A., Doskocil, E.J., Mankidy, P.J., Goff, M.J. Transesterification of soybean oil with zeolite and metal catalysts. *Applied Catalysis A: General*, **2004**, 257:213-223.

[3] Canakci, M., Gerpen, J.V. Biodiesel production from oils and fats with high FFAs. *Transactions of the ASAE*, **2001**, 44(6):1429-1436.

[4] Chiu, C-W, Goff, M.J., Suppes, G.J. Distribution of methanol and catalysts between biodiesel and glycerol. *AIChE Journal*, **2005**, 51(4):1274-1278.

[5] Dasari, M.A., Goff, M.J., Suppes, G.J. Noncatalytic alcoholysis kinetics of soybean oil. *Journal of the American Oil Chemists' Society*, **2003**, 80(2):189-192.

[6] Krawezky, T., Biodiesel – Alternative fuel makes inroads but hurdles remain. *Inform*, **1996**, 7:801.

[7] Ludwig, S., Manfred, E. Preparation of 1, 2 propanediol. US Patent 5,616,817, **1997**.

[8] Tessie, C. Production of propanediols. US Patent 4,642,394, **1987**.

[9] Casale, B., Gomez, A.M. Method of hydrogenating glycerol. US Patent 5,214,219, **1993**.

[10] Casale, B., Gomez, A.M. Catalytic method of hydrogenating glycerol. US Patent 5,276,181, **1994**.

[11] Dasari, M.A., Kiatsimkul, P., Sutterlin, W.R., Suppes, G.J. Low-pressure

Hydrogenolysis of Glycerol to Propylene Glycol. *Appl. Catal. A.,* **2005**, *281*(1-2): 225.

[12] Chiu, C-W, Dasari, M.A., Sutterlin, W.R., Suppes, G.J. Dehydration of Glycerol to Acetol via Catalytic Reactive Distillation. *AIChE Journal,* **2006**, 52(10): 3543-3548.

[13] Suppes, G.J., Sutterlin, W.R., Dasari, M.A. Method of producing lower alcohols from glycerol. US Patent Application 2005244312, **2005**.

[14] Sprules, F.J., Price, D. Production of Fatty esters. U.S. Patent 2,494,366, **1950**.

[15] Runeberg, J., Baiker, A., Kijenski, J. Copper catalyzed amination of ethylene glycol. *Appl. Catal.,* **1985**, 17(2):309.

[16] Montassier, C., Giraud, D., Barbier, J. Polyol conversion by liquid phase heterogeneous catalysis over metals. *Stud. Surf. Sci. Catal.,* **1988**, 41:165.

[17] Rase, H.F. *Handbook of Commercial Catalysts Heterogeneous Catalysts*, CRC Press: New York, **2000**.

[18] Zoltek, J. Jr. Phosphorous Removal by Orthophosphate Nucleation. *J. Water Pollut. Control Fed*., **1974**, 46:2498.

[19] Hirasawa, I., Shimada, K., Osanai, M. Phosphorus removal process from wastewater by contact crystallization of calcium apatite. *Proc.-Pac. Chem. Eng. Congr*., *[Proc.]*, **1983**, 4 (3rd):259.

[20] Joko, I. Phosphorous Removal from Wastewater by the Crystallization Method. *Water Sci. Technol*., **1984**, 17(2/3):121.

[21] Van Dijk, J.C., Braakensiek, H. Phosphate Removal by Crystallization in the

Fluidized Beds. *Water. Sci. Technol*., **1984**, 17(2/3):133.

[22] Momberg, G.A., Oellermann, R.A. The Removal of Phosphate by Hydroxyapatite and Struvite Crystallization in South Africa. *Waert. Sci. Technol*., **1992**, 26(5/6):987.

[23] Boskey, A.L., Posner, A.S. Formation of Hydroxyapatite at Low Supersaturation. *J. Phys. Chem*., **1976**, 80:40.

[24] Kaneko, S., Nakajima, K. Phosphorous Removal by Crystallization Using a Granular Activated Magnesia Clinker. *J. WPCF,* **1988**, 60:1239.

[25] Song, Y. Hahn, H.H., Hoffmann, E. The effects of pH and Ca/P ratio on the precipitation of calcium phosphate. *Chemical Water and Wastewater Treatment VII*. Proceedings of the Gothenburg Symposium, 10th, Gothenburg, Sweden. **2002**, pp. 349.

[26] Garti, N., Aserin, A., Zaidman, B. Polyglycerol ester: optimization and techno economic evaluation. *J. Am. Oil Chem. Soc*., **1981**, 58:878.

[27] Nancollas, G.H., Mohan, M.S. The growth of hydroxyapatite crystals. *Arch Oral Biol*., **1970**, 15:731.

[28] Higgins, J. On the road to fueling the future. Bioenergy ’02 Proceedings Paper 2062, Pacific Regional Biomass Energy Program, Boise, ID, **2002**.

[29] Chemical Market Reporter. Sept 24, **2001**, 260(11):30.

[30] Chemical Market Reporter. April 26, **2004**, 265(17):20.

[31] Martin, A.E., Murphy, F.H. Kirk-Othmer encyclopedia of chemical technology (4th edition). New York: John Wiley & Sons, Inc., **1994**,17:715

[32] Trent, D.T. Kirk-Othmer encyclopedia of chemical technology (4th edition). New York: John Wiley & Sons, Inc., **1996**, 20:271.

[33] Gaikar, V.G., Sharma, M.M. Separations through reactions and over novel strategies. *Separation and Purification Methods*., **1989**,18(2):111-176.

[34] Doherty, M.F., Buzad, G. Reactive distillation by design. *Chemical Engineering Research and Design*., **1992**, 70(A5):448-458.

[35] DeGarmo, J.L., Parulekar, V.N., Pinjala, V. Consider reactive distillation. *Chemical Engineering Progress*., **1992**, 88(3):43-50.

[36] Clacens, J-M, Pouilloux, Y., Barrault, J. Selective etherification of glycerol to polyglycerols over impregnated basic MCM-41 type mesoporous catalysts. *Applied Catalysis A: General*., **2002**, 227(1-2):181-190.

[37] Newsome, D.S. The water-gas shift reaction. *Catalysis Reviews-Science and Engineering*., **1980**, 21(2):275-318.

[38] Ohara, T., Sato, T., Shimizu, N., Prescher, G., Schwind, H., Weiberg, O. Acrolein and Methacrolein, in Ullman's Encyclopedia of Industrial Chemistry, Fifth Edition, VCH publishers, NY, **1985**, vol A1.

[39] Ju, L.K., Chase, G.G. Improved scale-up strategies of bioreactors. *Bioprocess Engineering*., **1992**, 8:49.

[40] Baekeland, L. H. *J. Ind. Eng. Chem.*, **1916**, 8:184.

[41] Davis, G.E. *A Handbook of Chemical Engineering*. Davis Bros., Manchester, England, **1901**.

[42] Boreskov, G.K., Matros, Y.S., Klenov, O.P., Lugovskoi, V.I., Lakhmostov, V.S.

Local Nonuniformities in a Catalyst Bed. *Dokl. Akad. Nauk SSSR*., **1981**, 258:1418.

[43] Colin, P., Balakotaiah, V., Analysis of Concentration and Temperature Patterns on Catalytic Surfaces. *J. Chem. Phys.*, **1994**, 100:5338.

[44] Nguyen, D., Balakotaiah, V. Flow Mal-Distributions and Hot Spots in Down-Flow Packed-Bed Reactors. *Chem. Eng. Sci.*, **1994**, 49:5489.

[45] Benneker, A.H., Kronberg, A.E., Westerterp, K.R. Influence of Buoyancy Forces on the Flow of Gases through Packed Beds at Elevated Pressures. *AIChE J.*, **1998**, 44:263.

[46] Jaffe, S.B. Hot Spot Simulation in Commercial Hydrogenation Processes. *Ind. Eng. Chem. Proc. Des. Dev.*, **1976**, 15:410.

[47] Barkelew, C.H., Gambhir, B.S. Stability of Trickle-Bed Reactors. *ACS Symp. Ser.*, **1984**, 237:61.

[48] Mills, P.L., Harold, M.P., Lerou, J.J. Industrial heterogeneous gas-phase oxidation processes. *Catalytic Oxidation*, **1995**, 291-369.

[49] Henley, E.J., Seader, J.D. *Equilibrium-Stage Separation Operations in Chemical Engineering*. Wiley: New York, **1981**.

[50] Fenske, M.R. Fractionation of straight-run Pennsylvania gasoline. *Ind. Eng. Chem.*, **1932**, 24:482-485.

[51] Shiras, R.N., Hanson, D.N., Gibson, C.H. Calculation of Minimum Reflux Ratio in Distillation Columns. *Znd. Eng. Chem.*, **1960**, 42:871.

[52] Underwood, A.J.V. Fractional distillation of multicomponent mixtures.

Calculation of minimum reflux ratio. *J. Inst. Petrol.*, **1946**, 32:614-26.

[53] Molokanov, Y.K., Korablina, T.P., Mazurina, N.I., Nikiforov, G.A., *Int. Chem. Eng.*, **1972**, 12(2):209-212.

[54] Bowman, J.R. Interrelations between distillation curves. *J. Ind. Eng. Chem.*, **1951**, 42:2622-24.

[55] Froment, G. F. Bischoff, K. B. *Chemical Reactor Analysis and Design*. Wiley: New York, **1979**.

[56] Modell, M., Reid, R.C. *Thermodynamics and Its applications*. Reprinted by permission of Prentic-Hall, Inc., Englewood Cliffs, N.J., **1974**, pp.396.

APPENDIX

Reverse Chronological Summary of Vapor-Phase Experimental Runs

Date	Description of Experimental Run						Result			
	Reactor	Temperature (°C)	Pressure (bar)	Catalyst mass (g)	Hydrogen flow rate (L/min)	Glycerol flow rate (g/h)	Glycerol conversion (%)	Acetol (wt.%)	Propylene glycol (wt.%)	Unknowns (wt.%)
2006/08/18[a]	Lab scale D: 0.75 (in) L: 12 (ft.)	220	1	750	5	100	100	23.45	46.30	7.89
2006/08/18[a]	Lab scale D: 0.75 (in) L: 12 (ft.)	220	1	650	5	100	100	23.50	46.89	6.8
2006/08/17[a]	Lab scale D: 0.75 (in) L: 12 (ft.)	220	1	550	5	100	91.77	22.55	44.95	4.99
2006/08/16[a]	Lab scale D: 0.75 (in) L: 8 (ft.)	220	1	300	5	100	52.55	15.11	30.11	2.01
2006/08/16[b]	Lab scale D: 0.75 (in) L: 8 (ft.)	230	1	300	5	100	83.98	-	-	-
2006/08/16[c]	Lab scale D: 0.75 (in) L: 8 (ft.)	240	1	300	5	100	100	-	-	-

2006/08/11[a]	Lab scale D: 0.75 (in) L: 4 (ft.)	220	1	100	5	100	19.78	5.52	11.01	0.57
2006/08/11[b]	Lab scale D: 0.75 (in) L: 4 (ft.)	230	1	100	5	100	33.12	-	-	-
2006/08/11[c]	Lab scale D: 0.75 (in) L: 4 (ft.)	240	1	100	5	100	48.89	-	-	-
2006/08/07[a]	Lab scale D: 0.75 (in) L: 2 (ft.)	220	1	50	5	100	10.22	3.43	6.65	0.32
2006/08/07[b]	Lab scale D: 0.75 (in) L: 2 (ft.)	230	1	50	5	100	18.03	-	-	-
2006/08/07[c]	Lab scale D: 0.75 (in) L: 2 (ft.)	240	1	50	5	100	23.45	-	-	-
2006/08/03[a]	Lab scale D: 0.75 (in) L: 2 (ft.)	220	1	25	5	100	5.89	1.95	3.81	0.11
2006/08/03[b]	Lab scale D: 0.75 (in) L: 2 (ft.)	230	1	25	5	100	7.01	-	-	-
2006/08/03[c]	Lab scale D: 0.75 (in) L: 2 (ft.)	240	1	25	5	100	13.98	-	-	-

2006/06/16-2006/07/01[d]	Pilot scale TubeCooled D: 2 ID (in) L: 5 (ft.)	220	1	3600	80-100 Recycled Hydrogen	1300	Avg.95	Avg.22	Avg.45	Avg.6
2006/06/06-2006/06/14[e]	Pilot scale TubeCooled D: 2 ID (in) L: 5 (ft.)	220	1	3600	80-100 Recycled Hydrogen	1500-2000	Avg.85	Avg.18	Avg.30	Avg.15
2006/05/26-2006/05/19	Pilot scale Shell-Tube D: 1 OD (in) L: 10 (ft.)	220	1	2200	70-80 Recycled Hydrogen	1200	Avg. 100-99.5	Avg.25	Avg.47	Avg.7
2006/05/26-2006/05/09[f]	Pilot scale Shell-Tube D: 0.75 OD (in) L: 16 (ft.)	220	1	1500	70-80 Recycled Hydrogen	800	Avg. 100-99.5	Avg.25	Avg.47	Avg.7
2006/01/26-2006/04/31	Exploring different pilot-scale reactor design configurations									
2005/11/17[g]	Lab scale D: 0.75 (in) L: 16 (ft.)	220	1	1160	0.1	Batch mode	100	47.9	10.4	10.9
2005/11/17[g,h]	Lab scale D: 0.75 (in) L: 16 (ft.)	220	1	1160	2.4	Batch mode	100	44.0	28.6	5.8
2005/11/16[g,i]	Lab scale D: 0.75 (in) L: 16 (ft.)	220	1	1160	5	Batch mode	100	32.1	42.4	4.6

2005/11/16[g]	Lab scale D: 0.75 (in) L: 16 (ft.)	220	1	1160	7.1	Batch mode	100	28.0	50.1	4.0
2005/11/09[g]	Lab scale D: 0.75 (in) L: 16 (ft.)	230	1	1160	0.1	Batch mode	100	46.9	6.4	12.4
2005/11/09[g]	Lab scale D: 0.75 (in) L: 16 (ft.)	230	1	1160	2.4	Batch mode	100	43.0	25.1	7.6
2005/11/09[g, i]	Lab scale D: 0.75 (in) L: 16 (ft.)	230	1	1160	5	Batch mode	100	32.3	38.7	5.9
2005/11/03[i]	Lab scale D: 0.75 (in) L: 16 (ft.)	200	1	1160	5	Batch mode	78.1	26.1	35.3	2.3
2005/11/03[i]	Lab scale D: 0.75 (in) L: 16 (ft.)	210	1	1160	5	Batch mode	91.6	30.6	39.3	3.2
2005/11/03[i]	Lab scale D: 0.75 (in) L: 16 (ft.)	240	1	1160	5	Batch mode	100	31.4	35.1	8.3
2005/10/31[h]	Lab scale D: 0.75 (in) L: 20 (ft.)	220	1	1560	2.4	Batch mode	100	42.3	26.9	7.9
2005/10/25[h]	Lab scale D: 0.75 (in) L: 16 (ft.)	220	1	1350	2.4	Batch mode	100	43.6	27.5	6.5

2005/10/19[h]	Lab scale D: 0.75 (in) L: 16 (ft.)	220	1	760	2.4	Batch mode	84.5	41.9	23.2	2.6
2005/10/14[h]	Lab scale D: 0.75 (in) L: 1 (ft.)	230	1	150 (9-40 mesh)	0.1	Batch mode	92.9	64.1	6.4	3.6
2005/10/10[h]	Lab scale D: 0.75 (in) L: 1 (ft.)	230	1	100 (9-40 mesh)	0.1	Batch mode	63.5	44.7	2.4	3.4
2005/10/05[h]	Lab scale D: 0.75 (in) L: 1 (ft.)	230	1	50 (9-40 mesh)	0.1	Batch mode	31.9	23.1	1.7	0.6
2005/09/26[j]	Lab scale D: 0.75 (in) L: 1 (ft.)	230	1	50	Nitrogen 0.1	Batch mode	20.7	11.2	0.5	2.1
2005/09/19[j]	Lab scale D: 0.75 (in) L: 1 (ft.)	230	1	50	Hydrogen 0.1	Batch mode	25.6	18.4	1.5	0.4
2005/09/09[j,l]	Lab scale D: 0.75 (in) L: 1 (ft.)	230	0.1	50	No gas purge	Batch mode	22.1	13.7	1.1	0.8
2005/08/03-2005/09/09[k]	Exploring different vapor-phase reaction experimental setups									
2005/07/29[l]	Lab scale D: 0.75 (in) L: 1 (ft.)	230	0.1	50	No gas purge	Liquid phase 90	20.4	6.1	0.9	5.3

[a] Used to compile Figure 8.1, Figure 8.5, Figure 8.6

[b] Used to compile Figure 8.2

[c] Used to compile Figure 8.3

[d] Used to compile Table 6.1, Figure 6.3

[e] Data discarded because of liquid glycerol accumulation in the reactor (limited glycerol evaporation)

[f] Used to compile Table 6.1, Figure 6.3, Figure 6.4

[g] Used to compile Figure 4.4

[h] Used to compile Table 4.4

[i] Used to compile Table 4.5

[j] Used to compile Table 4.3

[k] Data discarded because of failure in temperature control (runaway reaction)

[l] Used to compile Table 4.2

VITA

Chuang-Wei (Roger) Chiu was born June 9, 1976 in Taichung, Taiwan. He attended private elementary school and public high school in Taichung, Taiwan. He received his Bachelor of Science degree in Chemical Engineering from the National Chung-Hsing University, Taichung, Taiwan in 1999. Since 2002 he initiated graduate studies in Chemical Engineering at the University of Missouri-Columbia and received his M.S. in May 2004 and a Doctor of Philosophy degree in October 2006.